International Journal of Engineering Science 168 (2021) 103540

Contents lists available at ScienceDirect

International Journal of Engineering Science

journal homepage: www.elsevier.com/locate/ijengsci

Dynamics of incompressible fluids with incompatible distortion rates

Roger Fosdick [a,*], Eliot Fried [b,*]

[a] Department of Aerospace Engineering and Mechanics, University of Minnesota, Minneapolis, MN 55455-0153, USA
[b] Mathematics, Mechanics and Materials Unit, Okinawa Institute of Science and Technology Graduate University, 1919-1 Tancha, Onna, Okinawa, 904-0495, Japan

ARTICLE INFO

Keywords:
Saint Venant compatibility
Incompatibility field
Incompatibility flux field
Incompatibility balance
Plane Poiseuille flow

ABSTRACT

We consider the implication of allowing the distortion rate in a fluid to be the sum of two smooth components, both incompatible in the sense that they are not gradients of vector fields. Whereas one of these components embodies a smooth distribution of slippage, the other describing the repair needed to ensure that the distortion rate is the gradient of the velocity field. Our considerations lead to a generalization of the Navier–Stokes equations for an incompressible fluid. A tensor field which characterizes incompatibility is introduced and a fundamental equation for its evolution is proposed. Properties of these equations are exemplified by revisiting the classical problem of pressure-driven flow in a plane, rectangular channel. For a sufficiently large instantaneously applied pressure drop, a novel action due to the diffusivity κ associated with the transport of incompatibility is illustrated in addition to the normal diffusive and dissipative affect of viscosity ν. The steady state of the velocity and incompatibility is governed by a system of two ordinary differential equations which are fully analyzed and the resulting fields are determined and discussed. The transient problem is solved numerically and the graphical results show how these fields are structured in time by diffusion and dissipation in the channel during the transition from rest to steady state. A precursor laminar flow persists until a particular time at which the wall shear stress becomes equal to an a priori given cut-off value that initiates incompatibility at the walls of the channel. This incompatibility diffuses inward and interacts synergistically with the viscous action present in the channel to flatten the velocity profile so as to take on a 'plug flow-like' appearance, and to redistribute the viscous dissipation and the dissipation due to incompatibility into boundary layers at the channel walls.

1. Introduction

In the kinematics of continua, the instantaneous distortion of a material filament $\mathrm{d}\boldsymbol{x}$ with unit orientation $\boldsymbol{n}$ is described by the relation

$$\overset{\cdot}{\mathrm{d}\boldsymbol{x}} = \boldsymbol{L}\,\mathrm{d}\boldsymbol{x}, \tag{1.1}$$

where, as explained in A.3, a superposed dot is used to indicate the material time derivative, and where the distortion rate tensor $\boldsymbol{L} := \operatorname{grad}\boldsymbol{v}$ is the gradient of the velocity $\boldsymbol{v}$ and is, therefore, said to be compatible. The stretch λ of the material filament is governed

* Corresponding authors.
E-mail addresses: fosdick@aem.umn.edu (R. Fosdick), eliot.fried@oist.jp (E. Fried).

https://doi.org/10.1016/j.ijengsci.2021.103540
Received 3 February 2021; Received in revised form 2 May 2021; Accepted 5 July 2021
Available online 30 July 2021

by

$$\overline{\log \lambda}^{\cdot} = \boldsymbol{n} \cdot \boldsymbol{D}\boldsymbol{n}, \tag{1.2}$$

where $\boldsymbol{D}$ is the stretching tensor defined according to

$$\boldsymbol{D} := \tfrac{1}{2}(\boldsymbol{L} + \boldsymbol{L}^{\top}) := \operatorname{sym} \boldsymbol{L}. \tag{1.3}$$

Also, the interior angle α between two material filaments with distinct unit orientations $\boldsymbol{n}_1$ and $\boldsymbol{n}_2$ emanating from the same material point is governed by the relation

$$(\sin\alpha)\dot{\alpha} = (\boldsymbol{n}_1 \cdot \boldsymbol{D}\boldsymbol{n}_1 + \boldsymbol{n}_2 \cdot \boldsymbol{D}\boldsymbol{n}_2)\boldsymbol{n}_1 \cdot \boldsymbol{n}_2 - 2\boldsymbol{n}_1 \cdot \boldsymbol{D}\boldsymbol{n}_2. \tag{1.4}$$

If at some point and some instant the magnitude $|\boldsymbol{D}|$ of the stretching tensor $\boldsymbol{D}$ is sufficiently large relative to some characteristic frequency, we expect on the basis of (1.2) and (1.4) that the rate of stretching $\dot{\lambda}$ of the material filament with orientation $\boldsymbol{n}$ at that point and the rate of shearing $\dot{\alpha}$ between the material filaments with orientations $\boldsymbol{n}_1$ and $\boldsymbol{n}_2$ will be large relative to that same frequency, thus triggering a local reformational change in the existing compatible structure of the fluid, analogous to casual observations concerning turbulent flow behavior. We consequently envision a splitting of the compatible distortion rate into an additive composition of two incompatible distortion rates, each not expressible as the gradient of a vector field. This supports the intuitive notion of smooth distributions of slippage and repair that take place sympathetically and instantaneously at the macroscopic scale.

Stimulated by the foregoing observations, we explore the implication

$$\boldsymbol{L} = \boldsymbol{\Lambda} + \bar{\boldsymbol{\Lambda}} \qquad \Longrightarrow \qquad \overline{\mathrm{d}\boldsymbol{x}}^{\cdot} = \boldsymbol{L}\,\mathrm{d}\boldsymbol{x} = \boldsymbol{\Lambda}\,\mathrm{d}\boldsymbol{x} + \bar{\boldsymbol{\Lambda}}\,\mathrm{d}\boldsymbol{x}, \tag{1.5}$$

where the two distortion rate tensor fields $\boldsymbol{\Lambda}$ and $\bar{\boldsymbol{\Lambda}}$, are smooth but their differential forms are not integrable so they cannot be expressed as the gradients of vector fields, as is $\boldsymbol{L}$. Thus, while $\boldsymbol{\Lambda}$ and $\bar{\boldsymbol{\Lambda}}$ are individually incompatible, it is evident from (1.5) that the composition $\boldsymbol{\Lambda} + \bar{\boldsymbol{\Lambda}}$ must be compatible. It is the relations (1.2) and (1.4), in conjunction with the belief that material filaments $\mathrm{d}\boldsymbol{x}$ of a fluid may respond to severe distortion rates $\boldsymbol{L}$ by undergoing a process of reformation based upon the idea of incompatibility that motivates this article. Summing-up, we envision an instantaneous splitting of the distortion rate $\boldsymbol{L}$ of a generic material filament into two complimentary, incompatible and additive distortion rates, one of which is responsible for the presence of incompatibility, the other being essential for repairing and maintaining the integrity of the fluid, which is expressed by the gradient structure of $\boldsymbol{L}$. In crystalline solids, lattice defects have been studied extensively as manifestations of incompatible deformation gradients. The notion of a primitive unit cell, distributed periodically in space, is indispensable in that setting. In fluids, which exhibit no such order, there appears to be no credible basis for pursuing analogies to the physics of defective crystals, so we shall not pursue that lead here.[1]

We begin, in Section 2, with a discussion of the main hypothesis of this work, namely that under certain flow conditions the velocity gradient distortion rate $\boldsymbol{L}$ may be decomposed additively into two smooth distortion rates, $\boldsymbol{\Lambda}$ and $\bar{\boldsymbol{\Lambda}}$ that are not gradients of vector fields, as is expressed in (1.5). By definition, we associate the distortion rate $\boldsymbol{\Lambda}$ with an incompatibility that is envisioned intuitively as a smooth distribution of local velocity slippage. The distortion rate $\bar{\boldsymbol{\Lambda}}$ is conceived to be an instantaneous response to $\boldsymbol{\Lambda}$ which repairs and preserves the local integrity of the fluid so that the compatible gradient structure of $\boldsymbol{L}$ is assured. To more clearly express this notion, we introduce via Stokes' theorem a related incompatibility tensor

$$\boldsymbol{G} := -\operatorname{curl} \boldsymbol{\Lambda} \tag{1.6}$$

as a kinematic descriptor of the incompatibility associated with the distortion rate $\boldsymbol{\Lambda}$, independent of $\boldsymbol{v}$, where the application of the 'curl' operator to a tensor field is made explicit in $(A.32)_2$ (or in its indicial counterpart $(A.62)_2$). In Section 2.1, we develop the kinematic relations and connections of $\boldsymbol{G}$ to the symmetric and skew parts, $\boldsymbol{D}_{\Lambda}$ and $\boldsymbol{W}_{\Lambda}$, of $\boldsymbol{\Lambda}$, and we determine the specific conditions that define the incompatibility of these two fields.

In Section 3, we formulate the basic laws governing the dynamics of incompressible fluids with incompatible distortion rates. After recalling, in Section 3.1, the classical balance laws for momentum and moment of momentum, we introduce, in Section 3.2, a balance law for the incompatibility $\boldsymbol{G}$. This law embodies the requirement that the generation of incompatibility in a material region is due to advective and diffusive transfer of incompatibility across the boundary of that region together with an a priori given external volumetric supply. The surfacial diffusive transfer is characterized by an incompatibility flux tensor $\boldsymbol{J}$ which is important to the subsequent development. An alternative, equivalent version of the incompatibility balance involving integration over material surfaces is presented in Section 3.3. In Sections 3.4 and 3.5, we introduce a thermodynamical setting for the balance of energy and a dissipation inequality. The incompatibility $\boldsymbol{G}$ is paired with a constant specific moment of inertia $\iota > 0$ and is included as a novel additional source of kinetic energy in expressing the balance of energy, and a tensor $\boldsymbol{\Pi}$ that serves as a chemical potential for incompatibility is introduced to ensure the correct reckoning of energy transfers associated with the diffusive surface transfer and volumetric supply of incompatibility.

[1] Working by analogy to the continuum description of defects in solids, Acharya and Fosdick (2019) recently provided formal observations on a defect Navier–Stokes system based upon the failure of compatibility. Questions related to fluid behavior which are fundamental to the underlying physics are not addressed in that brief note.

In Section 4, we turn to constitutive relations and, for the remainder of this work, we specialize not only to incompressible fluids but also to isothermal conditions. We find that constitutive relations are needed for the Cauchy stress tensor $\boldsymbol{T}$ (excepting the constitutively independent constraint reaction due to incompressibility), the incompatibility flux $\boldsymbol{J}$, and the chemical potential $\boldsymbol{\Pi}$ for incompatibility, in terms of the symmetric part $\boldsymbol{D}$ of the velocity gradient $\boldsymbol{L}$, the incompatibility $\boldsymbol{G}$, and $\operatorname{grad}\boldsymbol{G}$. We, then, concentrate on the simplest constitutive structure for $\boldsymbol{T}$, $\boldsymbol{J}$, and $\boldsymbol{\Pi}$ that expresses a nontrivial incompatibility theory and that satisfies the dissipation inequality for all possible flows. This structure involves, in addition to the specific moment of inertia constant ι, two material coefficients: the classical kinematic viscosity $\nu > 0$, and a diffusivity $\kappa > 0$ associated with the transport of incompatibility. When combined with the fundamental balance laws for momentum and incompatibility, we arrive, in Section 5, at a coupled system of governing equations for $\boldsymbol{v}$ and $\boldsymbol{G}$. If external supplies are neglected, the equation expressing momentum balance takes the form

$$\dot{\boldsymbol{v}} = -\frac{1}{\varrho}\operatorname{grad} q + \nu\Delta\boldsymbol{v} + \iota^2 \operatorname{div}(\boldsymbol{G}^{\top}\boldsymbol{G}), \tag{1.7}$$

where ϱ is the constant mass density of the fluid and q is related to the pressure p of the fluid by $q = p + \varrho\iota^2|\boldsymbol{G}|^2$, and the equation expressing incompatibility balance takes the form

$$\dot{\boldsymbol{G}} = \boldsymbol{G}\boldsymbol{L}^{\top} + \kappa\,\Delta\boldsymbol{G}. \tag{1.8}$$

These evolution equations are to be solved subject to the requirements

$$\operatorname{div}\boldsymbol{v} = 0 \qquad \text{and} \qquad \operatorname{div}\boldsymbol{G} = \boldsymbol{0}, \tag{1.9}$$

the first of which stems from the assumption that the fluid is incompressible and the second of which arises because $\boldsymbol{G}$, as defined by (1.6), is the curl of a tensor field (cf. (A.42)). The flow equation (1.7) differs from the Navier–Stokes equation for an incompressible fluid only to the extent that it contains a term arising from the added divergence of a symmetric incompatibility stress tensor $\boldsymbol{R} = \varrho\iota^2\boldsymbol{G}^{\top}\boldsymbol{G}$ which enters the constitutively determined portion of the Cauchy stress $\boldsymbol{T}$.

In Section 6, we discuss the boundary conditions at a fixed and impermeable wall. As is common, the velocity $\boldsymbol{v}$ is taken to vanish at such a boundary:

$$\boldsymbol{v} = \boldsymbol{0}. \tag{1.10}$$

To determine a suitable boundary condition for the incompatibility $\boldsymbol{G}$, we observe that if $\boldsymbol{m}$ is the unit normal, directed outward from the fluid, on such a boundary, then the incompatibility vector $\boldsymbol{G}\boldsymbol{m}$ associated with such a surface depends only on the surface gradient of $\boldsymbol{\Lambda}$. Thus, resting on the intuitive notion that incompatibility is generated at a fixed and impermeable boundary only if the tangential wall stress exceeds or meets a certain threshold value, we propose to assign $\boldsymbol{G}\boldsymbol{m}$ as zero if the threshold is not met and nonzero if otherwise. The final version of this condition takes the form

$$\boldsymbol{G}\boldsymbol{m} = \begin{cases} \boldsymbol{0}, & \text{if} \quad 2\varrho\nu|(\boldsymbol{1}-\boldsymbol{m}\otimes\boldsymbol{m})\boldsymbol{D}\boldsymbol{m}| < \tau_c, \\ \gamma\boldsymbol{m}, & \text{if} \quad 2\varrho\nu|(\boldsymbol{1}-\boldsymbol{m}\otimes\boldsymbol{m})\boldsymbol{D}\boldsymbol{m}| \geq \tau_c, \end{cases} \tag{1.11}$$

where $\tau_c > 0$ is the aforementioned threshold. Moreover, we argue that the incompatibility vector $\boldsymbol{G}\boldsymbol{t}$ associated with a surface whose oriented normal $\boldsymbol{t}$ is tangent to the wall should not take part in the generation of incompatibility at the boundary:

$$\boldsymbol{G}\boldsymbol{t}\cdot\boldsymbol{m} = 0 \qquad \text{for all} \qquad \boldsymbol{t}\perp\boldsymbol{m}. \tag{1.12}$$

In Section 7, we apply our theory to the classical problem of steady plane Poiseuille flow in a rectangular channel, and for sufficiently large pressure gradients we obtain many results reminiscent of results for laminar flows of non-Newtonian fluids and fully developed turbulence in Newtonian fluids. This is followed in Section 8 with a study of the transient effects in the associated dynamical Poiseuille problem. In Sections 8.1 and 8.2, we present an energy-like analysis which allows us to quantitatively characterize the overall transition to steady state, and then, in Section 8.3, we provide a numerical account of the transition process, together with a related discussion based on the physical effects of diffusion and dissipation.

Finally, in Section 9, we summarize and assess our theory and some implications of our analysis on fluid flows with incompatible velocity gradients.

2. Compatibility and incompatibility

In an incompatible flow, we envision that the distortion rate of the material, characterized by the velocity gradient $\boldsymbol{L}$, is such that local velocity slippage and instantaneous repair takes place as a sympathetic kinematic process. The (smooth) velocity gradient is then considered to be the instantaneous additive composition of two smooth incompatible distortion rates: $\boldsymbol{\Lambda}$, which by definition is a distortion rate due to the generation of incompatibility, and $\bar{\boldsymbol{\Lambda}}$, which reacts to repair and preserve the local integrity of the material structure so that the gradient representation, $\boldsymbol{L} = \operatorname{grad}\boldsymbol{v}$, is assured.[2] With reference to (1.5), we write[3]

$$\boldsymbol{L} := \operatorname{grad}\boldsymbol{v} = \boldsymbol{\Lambda} + \bar{\boldsymbol{\Lambda}}. \tag{2.1}$$

[2] Throughout this work, we assume that the velocity field $\boldsymbol{v}$ is spatially and temporally smooth; singularities are not considered and weak function spaces are not needed. The mention of velocity slippage in relation to the incompatible distortion rate $\boldsymbol{\Lambda}$ is meant to be phenomenologically suggestive of its meaning, but the field $\boldsymbol{\Lambda}$ itself is considered to be smooth, and may be regarded intuitively as a smooth distribution of velocity slippages. The resolution of a velocity slippage event is not of interest in this work.

[3] In classical linear elasticity theory, a similar decomposition of the local distortion tensor, characterized as a smooth displacement gradient, is proposed within the context of incipient plastic deformation. The material is supposed to maintain its integrity as it deforms, and to support this notion it is envisioned

The distortion rate $\bar{\boldsymbol{\Lambda}}$ plays no significant quantitative role in this work, the main kinematic quantities being the velocity $\boldsymbol{v}$ and the incompatible distortion rate $\boldsymbol{\Lambda}$. However, the presence of $\bar{\boldsymbol{\Lambda}}$ in (2.1) does ensure the compatibility of the velocity gradient $\boldsymbol{L}$, as is expressed by $\operatorname{curl}\bar{\boldsymbol{\Lambda}} = -\operatorname{curl}\boldsymbol{\Lambda}$, where the 'curl' operator on a tensor field is made explicit in $(A.32)_2$ (or in its indicial counterpart $(A.62)_2$). Incompatible flow may take place in subregions of the flow domain $\mathcal{B}_t$, wherein $\boldsymbol{\Lambda} \neq \boldsymbol{0}$, the remaining part undergoing compatible flow with $\boldsymbol{\Lambda} \equiv \boldsymbol{0}$ and, of course, $\bar{\boldsymbol{\Lambda}} = \boldsymbol{L}$. Otherwise, $\bar{\boldsymbol{\Lambda}}$ is determined by $\boldsymbol{v}$ and $\boldsymbol{\Lambda}$ according to $\bar{\boldsymbol{\Lambda}} = \boldsymbol{L} - \boldsymbol{\Lambda}$.

As a consequence of the notion of incompatibility, and in particular the non-integrability of the differential form $\boldsymbol{\Lambda}\,\mathrm{d}\boldsymbol{x}$ expressed in (1.5), it is natural to introduce a surfacial incompatibility vector $\boldsymbol{g_n}$ such that, for any open surface $\mathcal{S}_t \subset \mathcal{B}_t$ with boundary $\mathcal{C}_t$ and oriented unit normal $\boldsymbol{n}$ chosen so that $\boldsymbol{p} := \boldsymbol{t} \times \boldsymbol{n}$ is the outward unit tangent-normal to $\mathcal{S}_t$ on $\mathcal{C}_t$,

$$\int_{\mathcal{S}_t} \boldsymbol{g_n}\,\mathrm{d}a := -\int_{\mathcal{C}_t} \boldsymbol{\Lambda}\,\mathrm{d}\boldsymbol{x} = -\int_{\mathcal{C}_t} \boldsymbol{\Lambda}\boldsymbol{t}\,\mathrm{d}s. \tag{2.2}$$

Then, involving Stokes' theorem for second-order tensor fields,[4] we see that $\boldsymbol{g_n} = \boldsymbol{G}\boldsymbol{n}$, where $\boldsymbol{G}$, the incompatibility tensor, is defined by

$$\boldsymbol{G} := -\operatorname{curl}\boldsymbol{\Lambda}. \tag{2.3}$$

In the subregions of the flow domain $\mathcal{B}_t$ where $\boldsymbol{\Lambda} \neq \boldsymbol{0}$ and, of course, $\boldsymbol{\Lambda}$ is not the gradient of a vector field, it is evident that $\boldsymbol{G} \neq \boldsymbol{0}$. Also, in the complementary subregions of $\mathcal{B}_t$ where $\boldsymbol{\Lambda} \equiv \boldsymbol{0}$, it is evident that $\boldsymbol{G} \equiv \boldsymbol{0}$. Thus, modulo the normalization requirement that whenever $\boldsymbol{\Lambda} \neq \boldsymbol{0}$ it is not the gradient of a vector field, we see that

$$\boldsymbol{\Lambda} = \boldsymbol{0} \qquad \text{if and only if} \qquad \boldsymbol{G} = \boldsymbol{0}. \tag{2.4}$$

If $\mathcal{S}_t$ is closed in the sense that it has no boundary, namely if $\mathcal{C}_t = \varnothing$, then the integral (2.2) vanishes, with the consequence that if the region $\mathcal{B}_t$ occupied by the fluid is periphractic[5] then (2.2) vanishes on every boundary of an internally embedded hole. Since, according to (2.3) and (A.42),

$$\operatorname{div}\boldsymbol{G} = \boldsymbol{0} \tag{2.5}$$

throughout the region $\mathcal{B}_t$ occupied by the fluid, it then follows that the integral also vanishes for the external boundary $\partial\mathcal{B}_t$ of the region occupied by the fluid.[6]

2.1. The stretching and vorticity tensors

The symmetric stretching tensor $\boldsymbol{D}$ and the skew vorticity tensor $\boldsymbol{W}$, defined in terms of $\boldsymbol{L} = \operatorname{grad}\boldsymbol{v}$ through

$$\boldsymbol{D} := \tfrac{1}{2}(\boldsymbol{L} + \boldsymbol{L}^{\top}) := \operatorname{sym}\boldsymbol{L}, \quad \boldsymbol{W} := \tfrac{1}{2}(\boldsymbol{L} - \boldsymbol{L}^{\top}) := \operatorname{skw}\boldsymbol{L}, \tag{2.6}$$

are inherently compatible because they are a priori determined by the gradient of a smooth velocity $\boldsymbol{v}$. However, considered as primitive symmetric and skew tensor fields defining a distortion rate $\boldsymbol{L} = \boldsymbol{D} + \boldsymbol{W}$, the issue of the integrability of the differential form $\overset{\cdot}{\mathrm{d}\boldsymbol{x}} = \boldsymbol{L}\,\mathrm{d}\boldsymbol{x}$ and the consequent existence of a smooth velocity $\boldsymbol{v}$ becomes fundamental. While this kind of question is not broached in classical fluid mechanics,[7] it is one of great importance in linear elasticity theory and it was solved by Cesàro (1906).

---

that local displacement dislocation (nominally displacement slippage) associated with the concept of plastic deformation, together with an elastic kinematic repair process, takes place coincidently. The displacement gradient is, thus, taken to be the additive composition of two smooth distortion tensors; namely, a plastic distortion tensor, and an elastic distortion tensor, neither of which can be represented as the gradient of displacement-like vectors. The plastic distortion tensor is considered to be the source of a smooth field of defects, referred to as a dislocation density field, and it is quantified by the value of its curl, which is a measure of its incompatibility. The decomposition of the velocity gradient $\boldsymbol{L}$ advanced in (1.5) is, thus, completely analogous to that considered in classical linear elasticity theory.

[4] Given a surface $\mathcal{S}$ orientated by a unit normal field $\boldsymbol{n}$ with unit tangent $\boldsymbol{t}$ relative to $\boldsymbol{n}$ in the right-handed sense, Stokes' theorem for a second-order tensor field $\boldsymbol{J}$, namely

$$\int_{\mathcal{S}} (\operatorname{curl}\boldsymbol{J})\boldsymbol{n}\,\mathrm{d}a = \int_{\partial\mathcal{S}} \boldsymbol{J}\boldsymbol{t}\,\mathrm{d}s,$$

follows from the classical version of Stokes' theorem for a vector field $\boldsymbol{f}$, namely

$$\int_{\mathcal{S}} (\operatorname{curl}\boldsymbol{f})\cdot\boldsymbol{n}\,\mathrm{d}a = \int_{\partial\mathcal{S}} \boldsymbol{f}\cdot\boldsymbol{t}\,\mathrm{d}s.$$

To verify this assertion, let $\boldsymbol{f} = \boldsymbol{J}^{\top}\boldsymbol{a}$ for some constant vector $\boldsymbol{a}$. Then, since $(\operatorname{curl}\boldsymbol{f})\cdot\boldsymbol{n} = (\operatorname{curl}(\boldsymbol{J}^{\top}\boldsymbol{a}))\cdot\boldsymbol{n} = ((\operatorname{curl}\boldsymbol{J})^{\top}\boldsymbol{a})\cdot\boldsymbol{n} = \boldsymbol{a}\cdot((\operatorname{curl}\boldsymbol{J})\boldsymbol{n})$ by $(A.32)_2$ and since $\boldsymbol{J}^{\top}\boldsymbol{a}\cdot\boldsymbol{n} = \boldsymbol{a}\cdot\boldsymbol{J}\boldsymbol{n}$, we see that

$$\boldsymbol{a}\cdot\left(\int_{\mathcal{S}} (\operatorname{curl}\boldsymbol{J})\boldsymbol{n}\,\mathrm{d}a - \int_{\partial\mathcal{S}} \boldsymbol{J}\boldsymbol{t}\,\mathrm{d}s\right) = 0$$

for any choice of $\boldsymbol{a}$, to complete the assertion.

[5] An open, connected region in three-dimensional Euclidean point space $\mathbb{E}^3$ that has embedded holes is said to be periphractic.

[6] We remark in passing that the integrand $\boldsymbol{g_n} = \boldsymbol{G}\boldsymbol{n}$ of (2.2) satisfies the identity $\boldsymbol{G}\boldsymbol{n} = (\operatorname{grad}_{\mathcal{S}}\boldsymbol{\Lambda})[\boldsymbol{n}\times]$, where $\operatorname{grad}_{\mathcal{S}}$ denotes the surface gradient on $\mathcal{S}_t$ and the operation on the right-hand side is as described in (A.40), and so depends only on the distribution of $\boldsymbol{\Lambda}$ over the surface $\mathcal{S}_t$. See the development of (6.11) for details.

[7] See Fosdick and Royer-Carfagni (2020) for a related discussion.

In the present context, Cesàro's result implies that if the stretching tensor $\boldsymbol{D}$ is smooth throughout a simply connected region and satisfies the Saint Venant compatibility condition

$$\operatorname{curl}((\operatorname{curl}\boldsymbol{D})^{\top})=\boldsymbol{0}, \tag{2.7}$$

then the distortion rate $\boldsymbol{L}$ is given as the gradient of a velocity $\boldsymbol{v}$ of the form

$$\boldsymbol{v}(\boldsymbol{x},t)=\boldsymbol{v}_0(t)+\boldsymbol{\omega}_0(t)\times(\boldsymbol{x}-\bar{\boldsymbol{x}}(0))+\int_0^1(\boldsymbol{D}\big(\bar{\boldsymbol{x}}(\alpha),t\big)+(\boldsymbol{x}-\bar{\boldsymbol{x}}(\alpha))\times(\operatorname{curl}\boldsymbol{D}(\bar{\boldsymbol{x}}(\alpha),t))^{\top})\bar{\boldsymbol{x}}'(\alpha)\,\mathrm{d}\alpha, \tag{2.8}$$

where $\bar{\boldsymbol{x}}$ parametrizes a smooth curve connecting the arbitrarily chosen points $\bar{\boldsymbol{x}}(0)$ and $\boldsymbol{x}$ in the region $\mathcal{B}_t$ instantaneously occupied by the fluid. Here, $\boldsymbol{v}_0$ and $\boldsymbol{\omega}_0$ are arbitrary vector valued functions of time which represent, respectively, a translational velocity of $\bar{\boldsymbol{x}}(0)$ and a rigid body angular velocity about (the translating point) $\bar{\boldsymbol{x}}(0)$ of the entire body of fluid. An interesting consequence of (2.8) is that, modulo the additive rigid body angular velocity $\boldsymbol{\omega}_0$, the vorticity tensor $\boldsymbol{W}$, or its related vorticity vector $\operatorname{curl}\boldsymbol{v}$, can be calculated and, thus, is determined by $\boldsymbol{D}$ provided that the region occupied by the fluid is simply connected and that $\boldsymbol{D}$ is compatible.

Consider, now, the fundamental incompatibility questions that are directly associated with the symmetric and skew parts of the distortion rate $\boldsymbol{\Lambda}$, namely the tensors $\boldsymbol{D}_{\Lambda}:=\operatorname{sym}\boldsymbol{\Lambda}$ and $\boldsymbol{W}_{\Lambda}:=\operatorname{skw}\boldsymbol{\Lambda}$ in the decomposition $\boldsymbol{\Lambda}=\boldsymbol{D}_{\Lambda}+\boldsymbol{W}_{\Lambda}$. To facilitate the discussion, we note that $\boldsymbol{W}_{\Lambda}$ and its axial vector $\boldsymbol{\omega}_{\Lambda}$ obey the identity

$$\operatorname{curl}\boldsymbol{W}_{\Lambda}=(\operatorname{div}\boldsymbol{\omega}_{\Lambda})\boldsymbol{1}-(\operatorname{grad}\boldsymbol{\omega}_{\Lambda})^{\top}, \tag{2.9}$$

where $\operatorname{grad}\boldsymbol{\omega}_{\Lambda}$ is given by

$$\operatorname{grad}\boldsymbol{\omega}_{\Lambda}=(\operatorname{curl}\boldsymbol{D}_{\Lambda})^{\top}+\boldsymbol{G}^{\top}-\tfrac{1}{2}(\operatorname{tr}\boldsymbol{G})\boldsymbol{1}. \tag{2.10}$$

Since $\operatorname{tr}(\operatorname{curl}\boldsymbol{D}_{\Lambda})=0$ due to (A.52) and the symmetry of $\boldsymbol{D}_{\Lambda}$, we thus find that $\operatorname{div}\boldsymbol{\omega}_{\Lambda}$ is given by

$$\operatorname{div}\boldsymbol{\omega}_{\Lambda}=-\tfrac{1}{2}\operatorname{tr}\boldsymbol{G}. \tag{2.11}$$

Additionally, we see that $\boldsymbol{D}_{\Lambda}$ obeys the identity

$$\operatorname{curl}((\operatorname{curl}\boldsymbol{D}_{\Lambda})^{\top})=\operatorname{curl}(\tfrac{1}{2}(\operatorname{tr}\boldsymbol{G})\boldsymbol{1}-\boldsymbol{G}^{\top}), \tag{2.12}$$

In view of (A.54), the left-hand side of (2.12) is symmetric and, consequently, the skew part of the right-hand side of (2.12) must vanish identically. Using (2.3) and (2.11), while noting from (A.34) that $\operatorname{curl}((\operatorname{tr}\boldsymbol{G})\boldsymbol{1})$ is skew, we find that

$$\operatorname{skw}(\operatorname{curl}(\tfrac{1}{2}(\operatorname{tr}\boldsymbol{G})\boldsymbol{1}-\boldsymbol{G}^{\top}))=\operatorname{curl}((\tfrac{1}{2}\operatorname{tr}\boldsymbol{G}+\operatorname{div}\boldsymbol{\omega}_{\Lambda})\boldsymbol{1})=\boldsymbol{0}, \tag{2.13}$$

and, thus, that the right-hand side of (2.12) may be written equivalently as

$$\operatorname{curl}(\tfrac{1}{2}(\operatorname{tr}\boldsymbol{G})\boldsymbol{1}-\boldsymbol{G}^{\top})=-\operatorname{sym}(\operatorname{curl}(\boldsymbol{G}^{\top})). \tag{2.14}$$

2.2. Alternative representations for the incompatible distortion rate $\boldsymbol{\Lambda}$

Recalling the normalization requirement (2.4), we see that (2.9)–(2.11) are identically satisfied in subregions where $\boldsymbol{G}\equiv\boldsymbol{0}$. In complimentary subregions of incompatibility, where $\boldsymbol{G}\neq\boldsymbol{0}$, while (2.3) determines $\boldsymbol{\Lambda}$, the conditions (2.9)–(2.11) place restrictions on the forms of $\boldsymbol{D}_{\Lambda}$ and $\boldsymbol{\omega}_{\Lambda}$ (or equivalently $\boldsymbol{W}_{\Lambda}$) with the understanding that $\boldsymbol{\Lambda}$ is not the gradient of a smooth vector field. For this situation, there are several possible scenarios to consider and, for definiteness in the following descriptions, we suppose that the region occupied by the fluid is simply connected. First, we observe that the right-hand side of (2.12) can vanish even though $\boldsymbol{G}\neq\boldsymbol{0}$. In this case, according to (2.8) with $\boldsymbol{D}$ replaced by $\boldsymbol{D}_{\Lambda}$, there is a smooth vector field $\boldsymbol{u}$ such that

$$\boldsymbol{D}_{\Lambda}=\operatorname{sym}(\operatorname{grad}\boldsymbol{u}). \tag{2.15}$$

In addition, even if $\boldsymbol{G}\neq\boldsymbol{0}$ it may happen that $\operatorname{tr}\boldsymbol{G}=0$ or $\operatorname{tr}\boldsymbol{G}\neq0$. These alternatives have the following ramifications:

(A) If $\operatorname{tr}\boldsymbol{G}=0$, then according to (2.11) and Stokes' theorem there is a smooth vector field $\boldsymbol{w}$ such that

$$\boldsymbol{\omega}_{\Lambda}=\tfrac{1}{2}\operatorname{curl}\boldsymbol{w},\qquad\operatorname{div}\boldsymbol{w}=0, \tag{2.16}$$

with the consequence that $\boldsymbol{W}_{\Lambda}=\operatorname{skw}(\operatorname{grad}\boldsymbol{w})$. We thus see that if $\boldsymbol{G}\neq\boldsymbol{0}$ but $\operatorname{tr}\boldsymbol{G}=0$, then the distortion rate $\boldsymbol{\Lambda}$ admits a representation of the form

$$\boldsymbol{\Lambda}=\underbrace{\operatorname{sym}(\operatorname{grad}\boldsymbol{u})}_{\boldsymbol{D}_{\Lambda}}+\underbrace{\operatorname{skw}(\operatorname{grad}\boldsymbol{w})}_{\boldsymbol{W}_{\Lambda}}, \tag{2.17}$$

subject to $(2.16)_2$. While $\boldsymbol{\Lambda}$ is not the gradient of a smooth vector field, we infer from (2.17) that the symmetric and skew parts of $\boldsymbol{\Lambda}$ involve symmetric and skew gradients of vector fields, respectively.

(B) If $\operatorname{tr} \boldsymbol{G} \neq 0$, then according to (2.11) and the Helmholtz representation theorem, there are smooth scalar and vector fields φ and $\boldsymbol{w}$ such that

$$\boldsymbol{\omega}_{\Lambda} = \operatorname{grad} \varphi + \tfrac{1}{2} \operatorname{curl} \boldsymbol{w}, \qquad \operatorname{div} \boldsymbol{w} = 0, \tag{2.18}$$

with the consequence that $\boldsymbol{W}_{\Lambda} = \operatorname{skw}(\operatorname{grad} \boldsymbol{w}) + (\operatorname{grad} \varphi)\times$, where, as explained in Appendix A.1, $(\operatorname{grad} \varphi)\times$ is the skew tensor with axial vector $\operatorname{grad} \varphi$, and, thus, that

$$\operatorname{div} \boldsymbol{\omega}_{\Lambda} = \Delta \varphi, \tag{2.19}$$

where Δ is the Laplacian. Using (2.19) in (2.11), we find that φ is determined by

$$\Delta \varphi = -\tfrac{1}{2} \operatorname{tr} \boldsymbol{G}. \tag{2.20}$$

From (2.15) and $(2.18)_1$, if $\boldsymbol{G} \neq \boldsymbol{0}$ and $\operatorname{tr} \boldsymbol{G} \neq 0$, then we find, subject to $(2.18)_2$, that the distortion rate $\boldsymbol{\Lambda}$ admits a representation of the form

$$\boldsymbol{\Lambda} = \underbrace{\operatorname{sym}(\operatorname{grad} \boldsymbol{u})}_{\boldsymbol{D}_{\Lambda}} + \underbrace{\operatorname{skw}(\operatorname{grad} \boldsymbol{w}) + (\operatorname{grad} \varphi)\times}_{\boldsymbol{W}_{\Lambda}}. \tag{2.21}$$

Finally, if the right-hand side of (2.12) does not vanish, we observe that due to a well-known representation theorem for symmetric second order-tensor fields,[8] there are smooth symmetric tensor and vector fields $\boldsymbol{\Phi}$ and $\boldsymbol{u}$ such that

$$\boldsymbol{D}_{\Lambda} = \operatorname{curl}((\operatorname{curl} \boldsymbol{\Phi})^{\top}) + \operatorname{sym}(\operatorname{grad} \boldsymbol{u}), \qquad \operatorname{div} \boldsymbol{\Phi} = \boldsymbol{0}, \tag{2.22}$$

with the consequence that

$$\operatorname{curl}((\operatorname{curl} \boldsymbol{D}_{\Lambda})^{\top}) = \Delta^2 \boldsymbol{\Phi}, \tag{2.23}$$

where Δ^2 is the biharmonic operator. Using (2.22) and (2.23) in (2.12), we find that $\boldsymbol{\Phi}$ is determined by

$$\Delta^2 \boldsymbol{\Phi} = \operatorname{curl}(\tfrac{1}{2}(\operatorname{tr} \boldsymbol{G})\boldsymbol{1} - \boldsymbol{G}^{\top}). \tag{2.24}$$

The two cases $\operatorname{tr} \boldsymbol{G} = 0$ and $\operatorname{tr} \boldsymbol{G} \neq 0$ considered above are again possible and, correspondingly, we infer that:

(A′) If $\operatorname{tr} \boldsymbol{G} = 0$, then (2.16), (2.22), and (2.24) hold and we find, subject to $(2.18)_2$ and $(2.22)_2$, that the distortion rate $\boldsymbol{\Lambda}$ admits a representation of the form

$$\boldsymbol{\Lambda} = \underbrace{\operatorname{curl}((\operatorname{curl} \boldsymbol{\Phi})^{\top}) + \operatorname{sym}(\operatorname{grad} \boldsymbol{u})}_{\boldsymbol{D}_{\Lambda}} + \underbrace{\operatorname{skw}(\operatorname{grad} \boldsymbol{w})}_{\boldsymbol{W}_{\Lambda}}. \tag{2.25}$$

(B′) If $\operatorname{tr} \boldsymbol{G} \neq 0$, then (2.18), (2.20), (2.22), and (2.24) hold and we find, subject to $(2.18)_2$ and $(2.22)_2$, that the distortion rate $\boldsymbol{\Lambda}$ admits a representation of the form

$$\boldsymbol{\Lambda} = \underbrace{\operatorname{curl}((\operatorname{curl} \boldsymbol{\Phi})^{\top}) + \operatorname{sym}(\operatorname{grad} \boldsymbol{u})}_{\boldsymbol{D}_{\Lambda}} + \underbrace{\operatorname{skw}(\operatorname{grad} \boldsymbol{w}) + (\operatorname{grad} \varphi)\times}_{\boldsymbol{W}_{\Lambda}}. \tag{2.26}$$

In summary: Within subregions of incompatibility where $\boldsymbol{G} \neq \boldsymbol{0}$, the distortion rate $\boldsymbol{\Lambda}$ has the general representation as shown in case (B′) above. If the right-hand side of (2.12) vanishes in those subregions, then $\boldsymbol{\Phi}$ can be eliminated; otherwise $\boldsymbol{\Phi}$ is governed by $(2.22)_2$ and (2.24). If, alternatively, the right-hand side of (2.11) vanishes in those subregions, then φ can be eliminated; otherwise φ is governed by (2.20).

3. Basic laws

This section is devoted to formulating the basic laws underlying the dynamics of a homogeneous and incompressible fluid with velocity gradient $\boldsymbol{L}$ which supports incompatibility as introduced in (2.1) and (2.3), with non-zero incompatibility $\boldsymbol{G} = -\operatorname{curl} \boldsymbol{\Lambda} \neq \boldsymbol{0}$. We first express the basic laws in integral form, working with a material region $\mathcal{P}_t$ the boundary $\partial \mathcal{P}_t$ of which is smooth and orientable, with unit normal $\boldsymbol{n}$ directed outward from $\mathcal{P}_t$, and subsequently localize to obtain their equivalent pointwise versions.

Since $\boldsymbol{v}$ and $\boldsymbol{G}$ are independent kinematical descriptors, it is necessary to supplement the familiar balance laws for momentum and moment of momentum by an additional evolutionary balance law for incompatibility and to augment the balance law for energy to incorporate transfers of energy that accompany a flux or supply of incompatibility. The second law of thermodynamics is imposed in the form of the Clausius–Duhem inequality. To emphasize the mechanical aspects of this theory and to promote simplicity, we opt to specialize and thereafter confine our attention to isothermal processes, in which case the energy balance and Clausius–Duhem inequality combine to yield a dissipation inequality.

[8] See Fosdick and Royer-Carfagni (2005).

3.1. Momentum balance. Moment of momentum balance

To begin, we introduce the mass density ϱ, Cauchy stress tensor $\boldsymbol{T}$, and specific body force $\boldsymbol{b}$. Since we consider only fluids that are both homogeneous and incompressible, mass balance simplifies to the requirement that the velocity $\boldsymbol{v}$ be solenoidal:

$$\operatorname{div} \boldsymbol{v} = 0. \tag{3.1}$$

For a material region $\mathcal{P}_t$ with boundary $\partial\mathcal{P}_t$ and outward unit normal $\boldsymbol{n}$, momentum balance has the conventional form

$$\frac{\mathrm{d}}{\mathrm{d}t}\int_{\mathcal{P}_t} \varrho \boldsymbol{v}\, \mathrm{d}v = \int_{\partial\mathcal{P}_t} \boldsymbol{T}\boldsymbol{n}\, \mathrm{d}a + \int_{\mathcal{P}_t} \varrho\, \boldsymbol{b}\, \mathrm{d}v. \tag{3.2}$$

Also, given a point $\boldsymbol{x}_0$ about which moments are computed and defining $\boldsymbol{r}$ by $\boldsymbol{r}(\boldsymbol{x}) = \boldsymbol{x} - \boldsymbol{x}_0$, the moment of momentum balance for $\mathcal{P}_t$ has the conventional form

$$\frac{\mathrm{d}}{\mathrm{d}t}\int_{\mathcal{P}_t} \boldsymbol{r}\times\varrho \boldsymbol{v}\, \mathrm{d}v = \int_{\partial\mathcal{P}_t} \boldsymbol{r}\times\boldsymbol{T}\boldsymbol{n}\, \mathrm{d}a + \int_{\mathcal{P}_t} \boldsymbol{r}\times\varrho\, \boldsymbol{b}\, \mathrm{d}v. \tag{3.3}$$

Applying the transport and divergence theorems to (3.2) and (3.3) and localizing the resulting identities, we obtain their familiar pointwise counterparts

$$\varrho\dot{\boldsymbol{v}} = \operatorname{div}\boldsymbol{T} + \varrho\, \boldsymbol{b} \qquad \text{and} \qquad \boldsymbol{T} = \boldsymbol{T}^{\top}. \tag{3.4}$$

3.2. Incompatibility balance

In formulating a balance law for incompatibility, we account for the possibility that the incompatibility of a material region $\mathcal{P}_t$ may be influenced by advective and diffusive transfer across its boundary $\partial\mathcal{P}_t$ and by the action of an external volumetric supply. Whereas advective transfer of incompatibility involves the surfacial incompatibility vector $\boldsymbol{g}_{\boldsymbol{n}} = \boldsymbol{G}\boldsymbol{n}$ and is measured by the integral of $\boldsymbol{G}\boldsymbol{n}\otimes\boldsymbol{v}$ over $\partial\mathcal{P}_t$, additional fields are required to incorporate diffusive transfer and external supply of incompatibility. We therefore introduce a second-order tensor $\boldsymbol{J}_{\boldsymbol{n}}$, the surfacial incompatibility flux, depending on the surface normal $\boldsymbol{n}$, and a second-order tensor $\boldsymbol{H}$, the incompatibility supply per unit volume, and express the balance of incompatibility for $\mathcal{P}_t$ as

$$\frac{\mathrm{d}}{\mathrm{d}t}\int_{\mathcal{P}_t} \boldsymbol{G}\, \mathrm{d}v = \int_{\partial\mathcal{P}_t} \boldsymbol{G}\boldsymbol{n}\otimes\boldsymbol{v}\, \mathrm{d}a - \int_{\partial\mathcal{P}_t} \boldsymbol{J}_{\boldsymbol{n}}\, \mathrm{d}a + \int_{\mathcal{P}_t} \boldsymbol{H}\, \mathrm{d}v, \tag{3.5}$$

Applying the transport theorem to the left-hand side of (3.5) and the divergence theorem to the first term on the right-hand side of (3.5), we obtain the condition

$$\int_{\mathcal{P}_t} (\dot{\boldsymbol{G}} - \boldsymbol{G}\boldsymbol{L}^{\top})\, \mathrm{d}v = -\int_{\partial\mathcal{P}_t} \boldsymbol{J}_{\boldsymbol{n}}\, \mathrm{d}a + \int_{\mathcal{P}_t} \boldsymbol{H}\, \mathrm{d}v, \tag{3.6}$$

which, by a standard localization argument, implies that $\boldsymbol{J}_{\boldsymbol{n}}$ must depend linearly on $\boldsymbol{n}$ and is given in terms of a third-order tensor $\boldsymbol{J}$, the incompatibility diffusion flux, with the property that $\boldsymbol{J}_{\boldsymbol{n}} = \boldsymbol{J}\boldsymbol{n}$. In turn, by applying the divergence theorem and the arbitrariness of $\mathcal{P}_t$ to the resulting integral equation we obtain the pointwise incompatibility balance

$$\dot{\boldsymbol{G}} = \boldsymbol{G}\boldsymbol{L}^{\top} - \operatorname{div}\boldsymbol{J} + \boldsymbol{H}. \tag{3.7}$$

Taking into consideration the requirements (3.1) and (2.5) that $\boldsymbol{v}$ and $\boldsymbol{G}$ be solenoidal, we find with reference to (A.44) that

$$(\operatorname{grad}\boldsymbol{G})\boldsymbol{v} - \boldsymbol{G}\boldsymbol{L}^{\top} = \operatorname{curl}(\boldsymbol{G}\times\boldsymbol{v}). \tag{3.8}$$

Thus, using the definition $(\mathrm{A}.56)_2$ of the material time derivative of a second-order tensor field, we see that the pointwise incompatibility balance (3.7) can be written alternatively as

$$\frac{\partial\boldsymbol{G}}{\partial t} + \operatorname{curl}(\boldsymbol{G}\times\boldsymbol{v}) = -\operatorname{div}\boldsymbol{J} + \boldsymbol{H}. \tag{3.9}$$

Applying the divergence to both sides of (3.9) and invoking the requirement (2.5) that $\boldsymbol{G}$ must be solenoidal, we find that $\boldsymbol{J}$ and $\boldsymbol{H}$ must satisfy the consistency condition

$$\operatorname{div}(\operatorname{div}\boldsymbol{J}) = \operatorname{div}\boldsymbol{H}. \tag{3.10}$$

Thus, the specification of an external supply $\boldsymbol{H}$ of incompatibility cannot be completely arbitrary. If, in particular, $\boldsymbol{J}$ is skew in the sense that $\boldsymbol{J}^t = -\boldsymbol{J}$, where $\boldsymbol{J}^t$ is the third-order tensor such that $(\boldsymbol{J}^t\boldsymbol{b})\boldsymbol{a} = (\boldsymbol{J}\boldsymbol{a})\boldsymbol{b}$, as defined in (A.13), for any choice of vectors $\boldsymbol{a}$ and $\boldsymbol{b}$, then the consistency condition (3.10) reduces to the requirement that $\operatorname{div}\boldsymbol{H} = \boldsymbol{0}$.

3.3. Equivalent surfacial incompatibility balance

In (2.2), we related the integral of $\boldsymbol{g}_{\boldsymbol{n}} = \boldsymbol{G}\boldsymbol{n}$ over a material surface $\mathcal{S}_t$ with unit surface orientation $\boldsymbol{n}$ and boundary $\partial\mathcal{S}_t := \mathcal{C}_t$ with unit tangent $\boldsymbol{t}$ relative to $\boldsymbol{n}$ directly to the incompatibility condition (2.3). It, thus, seems reasonable that the volumetric incompatibility balance (3.5) for any sufficiently smooth material region $\mathcal{P}_t$ should be equivalent to a surfacial incompatibility balance that applies on any sufficiently smooth material surface $\mathcal{S}_t$. To see this, suppose that we are given a material surface $\mathcal{S}_t$ with unit orientation $\boldsymbol{n}$ and boundary $\partial\mathcal{S}_t$ with unit tangent $\boldsymbol{t}$ relative to $\boldsymbol{n}$, and we apply each side of (3.9) to $\boldsymbol{n}$, integrate the resulting identity over $\mathcal{S}_t$, and invoke the transport identity[9]

$$\frac{\mathrm{d}}{\mathrm{d}t}\int_{\mathcal{S}_t}\boldsymbol{G}\boldsymbol{n}\,\mathrm{d}a = \int_{\mathcal{S}_t}\Big(\frac{\partial\boldsymbol{G}}{\partial t} + \operatorname{curl}(\boldsymbol{G}\times\boldsymbol{v})\Big)\boldsymbol{n}\,\mathrm{d}a \tag{3.11}$$

in tandem with the consequence

$$\int_{\mathcal{S}_t}(\operatorname{div}\boldsymbol{J})\boldsymbol{n}\,\mathrm{d}a = \int_{\partial\mathcal{S}_t}(\boldsymbol{J}^t\boldsymbol{n})\boldsymbol{p}\,\mathrm{d}s + \int_{\mathcal{S}_t}((\operatorname{grad}\boldsymbol{J})[\boldsymbol{n}\otimes\boldsymbol{n}\otimes\boldsymbol{n}] + \boldsymbol{J}[\boldsymbol{K}-2H\boldsymbol{n}\otimes\boldsymbol{n}])\,\mathrm{d}a \tag{3.12}$$

of the surface divergence theorem, where $\boldsymbol{p}$ is the outward tangent-normal to the edge $\partial\mathcal{S}_t$ of $\mathcal{S}_t$, $(\operatorname{grad}\boldsymbol{J})[\boldsymbol{n}\otimes\boldsymbol{n}\otimes\boldsymbol{n}]$ and $\boldsymbol{J}[\boldsymbol{K}-2H\boldsymbol{n}\otimes\boldsymbol{n}]$ are the vector fields defined, according to (A.11)–(A.14), such that $((\operatorname{grad}\boldsymbol{J})[\boldsymbol{n}\otimes\boldsymbol{n}\otimes\boldsymbol{n}])\cdot\boldsymbol{a} = (\operatorname{grad}\boldsymbol{J})\cdot(\boldsymbol{a}\otimes\boldsymbol{n}\otimes\boldsymbol{n}\otimes\boldsymbol{n})$ and $\boldsymbol{a}\cdot\boldsymbol{J}[\boldsymbol{K}-2H\boldsymbol{n}\otimes\boldsymbol{n}] = \boldsymbol{J}\cdot(\boldsymbol{a}\otimes\boldsymbol{K}-2H\boldsymbol{a}\otimes\boldsymbol{n}\otimes\boldsymbol{n})$ for any vector $\boldsymbol{a}$, $\boldsymbol{K} := -\operatorname{grad}_S\boldsymbol{n}$ is the curvature tensor of $\mathcal{S}_t$, and $H := \frac{1}{2}\operatorname{tr}\boldsymbol{K} = -\frac{1}{2}\operatorname{div}_S\boldsymbol{n}$ is the mean curvature of $\mathcal{S}_t$.[10] This yields a surfacial balance of incompatibility of the form

$$\frac{\mathrm{d}}{\mathrm{d}t}\int_{\mathcal{S}_t}\boldsymbol{G}\boldsymbol{n}\,\mathrm{d}a = -\int_{\partial\mathcal{S}_t}(\boldsymbol{J}^t\boldsymbol{n})\boldsymbol{p}\,\mathrm{d}s + \int_{\mathcal{S}_t}(\boldsymbol{H}\boldsymbol{n} - (\operatorname{grad}\boldsymbol{J})[\boldsymbol{n}\otimes\boldsymbol{n}\otimes\boldsymbol{n}] - \boldsymbol{J}[\boldsymbol{K}-2H\boldsymbol{n}\otimes\boldsymbol{n}])\,\mathrm{d}a, \tag{3.13}$$

which, for $\boldsymbol{J}^t = -\boldsymbol{J}$, (3.13) reduces to

$$\frac{\mathrm{d}}{\mathrm{d}t}\int_{\mathcal{S}_t}\boldsymbol{G}\boldsymbol{n}\,\mathrm{d}a = \int_{\partial\mathcal{S}_t}(\boldsymbol{J}\boldsymbol{n})\boldsymbol{p}\,\mathrm{d}a + \int_{\mathcal{S}_t}\boldsymbol{H}\boldsymbol{n}\,\mathrm{d}a, \tag{3.14}$$

where, in keeping with the comment immediately after the consistency condition (3.10), $\boldsymbol{H}$ must satisfy $\operatorname{div}\boldsymbol{H} = \boldsymbol{0}$. The specialization (3.14) of (3.13) is solely for illustrative purposes, as our further developments do not require that the incompatibility flux $\boldsymbol{J}$ satisfy $\boldsymbol{J}^t = -\boldsymbol{J}$.

By Stokes' theorem and the condition (2.5), we note that (3.11) can be recast as

$$\frac{\mathrm{d}}{\mathrm{d}t}\int_{\mathcal{S}_t}\boldsymbol{G}\boldsymbol{n}\,\mathrm{d}a = \int_{\mathcal{S}_t}\frac{\partial\boldsymbol{G}}{\partial t}\boldsymbol{n}\,\mathrm{d}a + \int_{\partial\mathcal{S}_t}\boldsymbol{G}(\boldsymbol{v}\times\boldsymbol{t})\,\mathrm{d}s, \tag{3.15}$$

Whereas the first of the two integrals on the right-hand side of (3.15) represents the total rate of change of the incompatibility within the region instantaneously occupied by the surface $\mathcal{S}_t$, the remaining integral represents the total advective rate of transfer of incompatibility through the edge $\partial\mathcal{S}_t$. According to the expression $\boldsymbol{G}(\boldsymbol{v}\times\boldsymbol{t})$ of the integrand, at each point on the edge $\partial\mathcal{S}_t$ the surfacial incompatibility $\boldsymbol{g}_{\boldsymbol{m}} = \boldsymbol{G}\boldsymbol{m}$ on the oriented surface whose unit normal $\boldsymbol{m}$ is parallel to $\boldsymbol{v}\times\boldsymbol{t}$ is advected onto $\mathcal{S}_t$ with the speed $|\boldsymbol{v}|$. There is another interpretation of this advection that may help to understand the process. Suppose we introduce the positively-oriented orthonormal basis $\{\boldsymbol{t},\boldsymbol{n},\boldsymbol{p}\}$ on $\partial\mathcal{S}_t$, and observe that, on substituting the consequence

$$\boldsymbol{v}\times\boldsymbol{t} = (\boldsymbol{v}\cdot\boldsymbol{p})\boldsymbol{n} - (\boldsymbol{v}\cdot\boldsymbol{n})\boldsymbol{p} \tag{3.16}$$

---

[9] See Bowen (1989, eqn. (2.2.15)).

[10] To explain briefly the origin of (3.12), we begin with the surface divergence theorem in the form

$$\int_{\mathcal{S}_t}\operatorname{div}_S(\boldsymbol{J}^t\boldsymbol{n})^{\tan}\,\mathrm{d}a = \int_{\partial\mathcal{S}_t}(\boldsymbol{J}^t\boldsymbol{n})\boldsymbol{p}\,\mathrm{d}s,$$

where $(\boldsymbol{J}^t\boldsymbol{n})^{\tan}$ is the projection of $\boldsymbol{J}^t\boldsymbol{n}$ onto the tangent space of the surface $\mathcal{S}_t$ and is given by

$$(\boldsymbol{J}^t\boldsymbol{n})^{\tan} = \boldsymbol{J}^t\boldsymbol{n}(\boldsymbol{1}-\boldsymbol{n}\otimes\boldsymbol{n}) = \boldsymbol{J}^t\boldsymbol{n} - (\boldsymbol{J}^t\boldsymbol{n})\boldsymbol{n}\otimes\boldsymbol{n}.$$

For the surface divergence in the integrand on the left-hand side above, we thus have the identity

$$\operatorname{div}_S(\boldsymbol{J}^t\boldsymbol{n})^{\tan} = (\operatorname{div}_S\boldsymbol{J})\boldsymbol{n} + \boldsymbol{J}^t[\operatorname{grad}_S\boldsymbol{n}] - (\boldsymbol{J}^t\boldsymbol{n})\boldsymbol{n}\operatorname{div}_S\boldsymbol{n} - \operatorname{grad}_S(((\boldsymbol{J}^t\boldsymbol{n})\boldsymbol{n}))\boldsymbol{n},$$

the last term of which vanishes because the surface gradient is annihilated by the operation on $\boldsymbol{n}$. Moreover, the surface divergence $\operatorname{div}_S\boldsymbol{J}$ of $\boldsymbol{J}$ is defined by

$$\operatorname{div}_S\boldsymbol{J} := \operatorname{div}\boldsymbol{J} - ((\operatorname{grad}\boldsymbol{J})\boldsymbol{n})\boldsymbol{n},$$

where $\operatorname{grad}\boldsymbol{J}$ is evaluated on $\mathcal{S}$. Thus, we find that

$$\operatorname{div}_S(\boldsymbol{J}^t\boldsymbol{n})^{\tan} = (\operatorname{div}\boldsymbol{J})\boldsymbol{n} - \big(((\operatorname{grad}\boldsymbol{J})\boldsymbol{n})\boldsymbol{n}\big)\boldsymbol{n} + \boldsymbol{J}^t[\operatorname{grad}_S\boldsymbol{n}] - (\boldsymbol{J}^t\boldsymbol{n})\boldsymbol{n}\operatorname{div}_S\boldsymbol{n},$$

and consequently that the surface divergence theorem may be written as

$$\int_{\mathcal{S}_t}\big((\operatorname{div}\boldsymbol{J})\boldsymbol{n} - (\operatorname{grad}\boldsymbol{J})[\boldsymbol{n}\otimes\boldsymbol{n}\otimes\boldsymbol{n}] + \boldsymbol{J}^t[\operatorname{grad}_S\boldsymbol{n} - (\operatorname{div}_S\boldsymbol{n})(\boldsymbol{n}\otimes\boldsymbol{n})]\big)\,\mathrm{d}a = \int_{\partial\mathcal{S}_t}(\boldsymbol{J}^t\boldsymbol{n})\boldsymbol{p}\,\mathrm{d}s.$$

Finally, using the provided definitions of the curvature tensor $\boldsymbol{K}$, which is necessarily symmetric, and the mean curvature H, while observing that $\boldsymbol{n}\otimes\boldsymbol{n}$ is symmetric, we see that this last result may be rewritten as in (3.12).

of the resolution $\boldsymbol{v} = (\boldsymbol{v}\cdot\boldsymbol{t})\boldsymbol{t} + (\boldsymbol{v}\cdot\boldsymbol{n})\boldsymbol{n} + (\boldsymbol{v}\cdot\boldsymbol{p})\boldsymbol{p}$ of $\boldsymbol{v}$ relative to $\{\boldsymbol{t},\boldsymbol{n},\boldsymbol{p}\}$ in the second term on the right-hand side of (3.11), we obtain the identity

$$\frac{\mathrm{d}}{\mathrm{d}t}\int_{\mathcal{S}_t}\boldsymbol{G}\boldsymbol{n}\,\mathrm{d}a = \int_{\mathcal{S}_t}\frac{\partial\boldsymbol{G}}{\partial t}\boldsymbol{n}\,\mathrm{d}a + \int_{\partial\mathcal{S}_t}((\boldsymbol{v}\cdot\boldsymbol{p})\boldsymbol{G}\boldsymbol{n} - (\boldsymbol{v}\cdot\boldsymbol{n})\boldsymbol{G}\boldsymbol{p})\,\mathrm{d}s. \tag{3.17}$$

The advective transport through its edge $\partial\mathcal{S}_t$ of $\mathcal{S}_t$ can thus be interpreted as the total excess of a component $(\boldsymbol{v}\cdot\boldsymbol{p})\boldsymbol{G}\boldsymbol{n} = (\boldsymbol{G}\boldsymbol{n}\otimes\boldsymbol{v})\boldsymbol{p}$ that 'glides' in the direction of $\boldsymbol{p}$ of the tangent-normal of $\partial\mathcal{S}_t$ relative to a component $(\boldsymbol{v}\cdot\boldsymbol{n})\boldsymbol{G}\boldsymbol{p} = (\boldsymbol{G}\boldsymbol{p}\otimes\boldsymbol{v})\boldsymbol{n}$ that 'climbs' in the direction of the restriction to $\partial\mathcal{S}_t$ of the normal $\boldsymbol{n}$ to $\mathcal{S}_t$. Notice, furthermore, that with the aid of (A.13) we may write (3.17) as

$$\frac{\mathrm{d}}{\mathrm{d}t}\int_{\mathcal{S}_t}\boldsymbol{G}\boldsymbol{n}\,\mathrm{d}a = \int_{\mathcal{S}_t}\frac{\partial\boldsymbol{G}}{\partial t}\boldsymbol{n}\,\mathrm{d}a + \int_{\partial\mathcal{S}_t}(\boldsymbol{K}\boldsymbol{n})\boldsymbol{p}\,\mathrm{d}s, \tag{3.18}$$

where $\boldsymbol{K} := -(\boldsymbol{G}\otimes\boldsymbol{v} - (\boldsymbol{G}\otimes\boldsymbol{v})^t) = -\boldsymbol{K}^t$, which shows that the edge advective transport juxtaposes nicely with the edge diffusive transport in the first term on the right-hand sides of either (3.13) or (3.14).

Suppose, finally, that we consider a surfacial balance of incompatibility as primitive and propose, as is natural, that

$$\frac{\mathrm{d}}{\mathrm{d}t}\int_{\mathcal{S}_t}\boldsymbol{G}\boldsymbol{n}\,\mathrm{d}a = \int_{\mathcal{S}_t}\boldsymbol{f}_{(\boldsymbol{n},\boldsymbol{K})}\,\mathrm{d}a + \int_{\partial\mathcal{S}_t}\boldsymbol{q}_{(\boldsymbol{n},\boldsymbol{p})}\,\mathrm{d}s + \int_{\mathcal{S}_t}\boldsymbol{H}\boldsymbol{n}\,\mathrm{d}a, \tag{3.19}$$

where, recalling (2.2), $\boldsymbol{g}_{\boldsymbol{n}} = \boldsymbol{G}\boldsymbol{n}$ is the surfacial incompatibility vector on $\mathcal{S}_t$ with unit orientation $\boldsymbol{n}$, $\boldsymbol{f}_{(\boldsymbol{n},\boldsymbol{K})}$ denotes the surfacial incompatibility flux vector on $\mathcal{S}_t$ which depends on $\boldsymbol{n}$ and the curvature tensor $\boldsymbol{K} = -\operatorname{grad}_{\mathcal{S}}\boldsymbol{n}$, $\boldsymbol{q}_{(\boldsymbol{n},\boldsymbol{p})}$ is the edge incompatibility diffusion flux vector which depends on the edge orientation through $\boldsymbol{n}$ and $\boldsymbol{p}$, and, in accordance with (3.5), $\boldsymbol{H}\boldsymbol{n}$ is the incompatibility supply vector to $\mathcal{S}_t$. Then, substituting (3.11) into the left-hand side of (3.19) we see that the resulting equation may be reorganized as the sum of a surface integral over $\mathcal{S}_t$ and an edge integral over $\partial\mathcal{S}_t$ which must vanish for all $\mathcal{S}_t$, a condition equivalent to that studied by Fosdick (2016, §3.1, pp. 281–285). Thus, we may conclude that $\boldsymbol{q}_{(\boldsymbol{n},\boldsymbol{p})}$ must depend bilinearly on $\boldsymbol{n}$ and $\boldsymbol{p}$ and be given in terms of a third order tensor $\boldsymbol{Q}$, an incompatibility diffusion flux, such that $\boldsymbol{q}_{(\boldsymbol{n},\boldsymbol{p})} = (\boldsymbol{Q}\boldsymbol{n})\boldsymbol{p}$. Moreover, by comparing (3.13) and (3.19) we see that on setting

$$\boldsymbol{Q} = -\boldsymbol{J}^t, \qquad \boldsymbol{f}_{(\boldsymbol{n},\boldsymbol{K})} = -(\operatorname{grad}\boldsymbol{J})[\boldsymbol{n}\otimes\boldsymbol{n}\otimes\boldsymbol{n}] - \boldsymbol{J}[\boldsymbol{K} - 2H\boldsymbol{n}\otimes\boldsymbol{n}], \tag{3.20}$$

the volumetric balance of incompatibility for $\mathcal{P}_t$ expressed in (3.5) and the surfacial balance of incompatibility for $\mathcal{S}_t$ expressed in (3.19) are equivalent.

3.4. Energy balance

If $\boldsymbol{\Lambda} = \boldsymbol{0}$, so that the flow is compatible, then the principle of energy balance requires that the rate at which the sum of the internal and kinetic energies of a material region $\mathcal{P}_t$ be equal to the power expended on $\mathcal{P}_t$ by external agencies plus the rate at which the energy of $\mathcal{P}_t$ changes due to the flow of heat through $\partial\mathcal{P}_t$ and external radiative heating within $\mathcal{P}_t$. If, however, $\boldsymbol{\Lambda} \neq \boldsymbol{0}$ and the flow is incompatible, then exchanges of energy that accompany the flux and supply of incompatibility also occur and must also be taken into consideration when balancing energy. To accomplish this, we introduce a tensor $\boldsymbol{\Pi}$ that serves as a chemical potential for incompatibility. Additionally, we introduce a constant specific moment of inertia $\iota > 0$ to account explicitly for the kinetic energy of the additional kinematical descriptor $\boldsymbol{G}$.[11] Using ε, $\boldsymbol{q}$, and r to respectively denote the specific internal energy,

[11] Based upon an idea of Ostwald within his development of energetics during the 1890's and early 20th century, we consider the constant $\rho\iota^2$ to be the "capacity" for the kinetic energy of incompatibility — incompatibility being considered as a distinct developing system. Accordingly, its "intensity" is measured by the quantity $\frac{1}{2}|\boldsymbol{G}|^2$ in (3.21). According to Deltete (2008), Ostwald sought in his development of energetics to "construct a world view exclusively from energetic material without using the concept of matter". He promoted the point of view that every object or system is identified as energy of different, distinct forms, and that each form is resolved into factors, one indicating the "intensity" of the energy and the other being its "capacity". He conceived of the capacity factor of a given energetic system as "the amount of energy which, with a given intensity, is present in a system" and he offered a few elementary examples.

Deltete (2008) remarks that Ostwald should not be considered among the pioneers of energetics, because many of the basic approaches and principles of that enterprise had already been set forth by Georg Helm in his thesis (see Deltete Deltete (1999) for an English translation of this work), together with a few others. However, none of the earlier formulations of energetics drew much attention, and their authors, with few exceptions, were not widely known. On the other hand, when Ostwald turned his attention to the theory of energetics he was already a scientist with an international reputation and, together with Arrhenius and van't Hoff, he was recognized as a founder of physical chemistry and was widely considered its most articulate and forceful spokesman. Thus, almost immediately he became the central figure in the subsequent development of energetics.

Like Helm, Ostwald emphasized the 'capacity-intensity' characterization of systems and proposed a *Factorization Principle*, as basic to energetics calling it "the foundation of modern energetics". As an example interpretation of this principle, Jammer (1961, p. 108) observes that in early 1900 Ostwald entered the debate about the concept of 'mass' and with his developing theory of energetics supported the notion that 'mass' should be defined in terms of energy. He conceived of 'mass' as merely an embodiment of the capacity that a system has for kinetic energy, with its associated intensity being $\frac{1}{2}|\boldsymbol{v}|^2$, just as specific heat is a capacity for the system of thermal energy, its intensity being temperature.

It is interesting to learn from Deltete (2008) how energetics is thought to have emerged at the end of the 19th century. He writes that, for more than 200 years until the end of the 19th century physicists generally had a clear fixed goal: to seek a mechanical explanation for natural phenomena. But, when Heinrich Hertz wrote in 1894 that "all physicists agree that the problem of physics consists in tracing the phenomena of nature back to the simple laws of mechanics", the physics community did not agree, and many doubted that mechanics was the most basic science. Thermodynamics and electromagnetic theory were mentioned as alternatives and energetics, which was vigorously debated by Ostwald and others throughout the 1890's and the early 1900's, was another. Interestingly, the law of conservation of energy, which traces back to Robert Mayer, and the thermodynamic writings of Rudolf Clausius, William Thomson (First Baron Kelvin), and Josiah Willard Gibbs, seems to have played a fundamental role in stimulating the early development of energetics as an attempt to unify all of natural science by means of the concept of energy and of laws describing energy in its various forms.

In the end, Ostwald's energetic theory was not followed as it was thought to be of little predictive value and it never fully emerged from metaphysics to gain a physical status outside of ontological belief without philosophical overtones.

heat flux vector, and specific external heat supply, we thus express the energy balance for $\mathcal{P}_t$ as

$$\frac{\mathrm{d}}{\mathrm{d}t}\int_{\mathcal{P}_t}\rho(\varepsilon+\tfrac{1}{2}|\boldsymbol{v}|^2+\tfrac{1}{2}\iota^2|\boldsymbol{G}|^2)\,\mathrm{d}v=\int_{\partial\mathcal{P}_t}\boldsymbol{T}\boldsymbol{n}\cdot\boldsymbol{v}\,\mathrm{d}a+\int_{\mathcal{P}_t}\rho\,\boldsymbol{b}\cdot\boldsymbol{v}\,\mathrm{d}v-\int_{\partial\mathcal{P}_t}\boldsymbol{q}\cdot\boldsymbol{n}\,\mathrm{d}a+\int_{\mathcal{P}_t}\rho r\,\mathrm{d}v-\int_{\partial\mathcal{P}_t}\boldsymbol{\Pi}\cdot\boldsymbol{J}\boldsymbol{n}\,\mathrm{d}a+\int_{\mathcal{P}_t}\boldsymbol{\Pi}\cdot\boldsymbol{H}\,\mathrm{d}v. \tag{3.21}$$

Applying the transport theorem and the divergence theorem to (3.21) and invoking the pointwise momentum and incompatibility balances $(3.4)_1$ and (3.7), we obtain the internal energy balance

$$\rho\dot{\varepsilon}=(\boldsymbol{T}-\boldsymbol{\Pi}^{\top}\boldsymbol{G})\cdot\boldsymbol{L}+(\boldsymbol{\Pi}-\rho\iota^2\boldsymbol{G})\cdot\dot{\boldsymbol{G}}-\boldsymbol{J}\cdot\operatorname{grad}\boldsymbol{\Pi}-\operatorname{div}\boldsymbol{q}+\rho r. \tag{3.22}$$

3.5. Dissipation inequality

Introducing the specific entropy η and the absolute temperature $\theta>0$, we impose the second law of thermodynamics through the conventional Clausius–Duhem inequality

$$\frac{\mathrm{d}}{\mathrm{d}t}\int_{\mathcal{P}_t}\rho\eta\,\mathrm{d}v\geq-\int_{\partial\mathcal{P}_t}\frac{\boldsymbol{q}\cdot\boldsymbol{n}}{\theta}\,\mathrm{d}a+\int_{\mathcal{P}_r}\frac{\rho r}{\theta}\,\mathrm{d}v. \tag{3.23}$$

Applying the transport and divergence theorems to (3.23), introducing the specific Helmholtz free energy

$$\psi=\varepsilon-\theta\eta, \tag{3.24}$$

and using the pointwise internal energy balance (3.22) to eliminate the specific external heat supply r, we arrive at the inequality

$$\rho\delta:=(\boldsymbol{T}-\boldsymbol{\Pi}^{\top}\boldsymbol{G})\cdot\boldsymbol{L}+(\boldsymbol{\Pi}-\rho\iota^2\boldsymbol{G})\cdot\dot{\boldsymbol{G}}-\boldsymbol{J}\cdot\operatorname{grad}\boldsymbol{\Pi}-\rho(\dot{\psi}+\eta\dot{\theta})-\frac{\boldsymbol{q}}{\theta}\cdot\operatorname{grad}\theta\geq 0, \tag{3.25}$$

where δ denotes the specific dissipation.

4. Constitutive relations for incompressible fluids under isothermal conditions

We focus hereafter on isothermal processes, so that the absolute temperature θ is constant:

$$\theta=\text{constant}. \tag{4.1}$$

In line with the assumption that the fluid is homogeneous and incompressible, which requires that the mass density ρ be constant, it follows that the specific free-energy ψ, which nominally depends on θ and ρ, must be constant:

$$\psi=\text{constant}. \tag{4.2}$$

Moreover, taking into consideration the constraint (3.1) of incompressibility, we may without loss of generality take the Cauchy stress $\boldsymbol{T}$ to be of the form

$$\boldsymbol{T}=-q\boldsymbol{1}+\boldsymbol{S}+\boldsymbol{\Pi}^{\top}\boldsymbol{G}, \tag{4.3}$$

where q is a constitutively indeterminate scalar field that does not affect the internal power, $\boldsymbol{S}$ is a corresponding extra stress which we take to satisfy

$$\operatorname{tr}\boldsymbol{S}=0, \tag{4.4}$$

and $\boldsymbol{\Pi}^{\top}\boldsymbol{G}$ is an incompatibility stress. We observe from the moment of momentum balance $(3.4)_2$ that $\boldsymbol{S}$ and $\boldsymbol{\Pi}$ must satisfy

$$\operatorname{skw}(\boldsymbol{S}+\boldsymbol{\Pi}^{\top}\boldsymbol{G})=0\qquad\text{or, equivalently,}\qquad\operatorname{skw}\boldsymbol{S}=-\operatorname{skw}(\boldsymbol{\Pi}^{\top}\boldsymbol{G}). \tag{4.5}$$

For later reference, it is important to notice that the pressure p corresponding to the stress $\boldsymbol{T}$ is given by

$$p:=-\tfrac{1}{3}\operatorname{tr}\boldsymbol{T}=q-\tfrac{1}{3}\operatorname{tr}(\boldsymbol{\Pi}^{\top}\boldsymbol{G}). \tag{4.6}$$

With the aid of the incompressibility condition (3.1) and using (4.1)–(4.3) in the dissipation inequality (3.25), we now find that

$$\rho\delta=\boldsymbol{S}\cdot\boldsymbol{L}+(\boldsymbol{\Pi}-\rho\iota^2\boldsymbol{G})\cdot\dot{\boldsymbol{G}}-\boldsymbol{J}\cdot\operatorname{grad}\boldsymbol{\Pi}\geq 0. \tag{4.7}$$

On the basis of (4.7) and respecting (4.4), it is natural to consider constitutive relations that provide $\boldsymbol{S}$, $\boldsymbol{\Pi}$, and $\boldsymbol{J}$ in terms of $\boldsymbol{D}$, $\boldsymbol{G}$, and $\operatorname{grad}\boldsymbol{G}$. Instead of determining the most general class of such relations that are consistent with (4.7) in all possible processes, we consider the particular subclass of constitutive relations for which $\boldsymbol{S}$, $\boldsymbol{\Pi}$, and $\boldsymbol{J}$ are linear functions of $\boldsymbol{D}$, $\boldsymbol{G}$, and $\operatorname{grad}\boldsymbol{G}$, respectively. Specifically, complying with (4.5), we assume that

$$\boldsymbol{S}=2\rho\nu\boldsymbol{D}, \tag{4.8}$$

where $\nu>0$ is the kinematic viscosity,

$$\boldsymbol{\Pi}=\rho\iota^2\boldsymbol{G}, \tag{4.9}$$

and that

$$\boldsymbol{J} = -\frac{\kappa}{\varrho \iota^2} \operatorname{grad} \boldsymbol{\Pi} = -\kappa \operatorname{grad} \boldsymbol{G}, \tag{4.10}$$

where $\kappa > 0$ is a diffusivity associated with incompatibility transport. Using (4.8) and (4.9) in (4.11), we next find that the Cauchy stress tensor $\boldsymbol{T}$ takes the form

$$\boldsymbol{T} = -q\boldsymbol{1} + \varrho(2\nu \boldsymbol{D} + \iota^2 \boldsymbol{G}^\top \boldsymbol{G}), \tag{4.11}$$

where, according to (4.6), the pressure is given by

$$p = q - \tfrac{1}{3}\varrho \iota^2 \operatorname{tr}(\boldsymbol{G}^\top \boldsymbol{G}) = q - \tfrac{1}{3}\varrho \iota^2 |\boldsymbol{G}|^2, \top \tag{4.12}$$

and, thus, $\boldsymbol{T}$ differs from the conventional expression $-p\boldsymbol{1} + 2\varrho\nu \boldsymbol{D}$ for the stress in an incompressible linearly viscous fluid with mass density ϱ and kinematic viscosity ν by a residual contribution due to

$$\boldsymbol{R} := \varrho \iota^2 \boldsymbol{G}^\top \boldsymbol{G}, \tag{4.13}$$

which we refer to as the 'incompatibility stress tensor'. It is interesting to observe from (4.12) that the kinetic energy due to incompatibility, namely $\frac{1}{2} \operatorname{tr} \boldsymbol{R} = \frac{1}{2}\varrho \iota^2 |\boldsymbol{G}|^2$, plays a specific role in determining the pressure p.

Using (4.9)–(4.10) in (4.7), we find in addition that the specific dissipation δ reduces to

$$\delta = 2\nu |\boldsymbol{D}|^2 + \iota^2 \kappa |\operatorname{grad} \boldsymbol{G}|^2 \geq 0 \tag{4.14}$$

and, thus, apart from the conventional contribution $2\nu|\boldsymbol{D}|^2$ stemming from viscous dissipation, accounts also for dissipation due to the transport of incompatibility through the term $\iota^2 \kappa |\operatorname{grad} \boldsymbol{G}|^2$.

5. Final governing equations

Augmenting the pointwise momentum balance $(3.4)_1$ with (4.11), we arrive at a slight modification,

$$\dot{\boldsymbol{v}} = -\frac{1}{\varrho} \operatorname{grad} q + \nu \Delta \boldsymbol{v} + \iota^2 \operatorname{div}(\boldsymbol{G}^\top \boldsymbol{G}) + \boldsymbol{b}, \tag{5.1}$$

of the classical equation for an incompressible and linearly viscous fluid with constant mass density ϱ and constant kinematic viscosity ν. Furthermore, using (4.10) in the pointwise incompatibility balance (3.7), we obtain an evolution equation for $\boldsymbol{G}$:

$$\dot{\boldsymbol{G}} = \boldsymbol{G}\boldsymbol{L}^\top + \kappa \Delta \boldsymbol{G} + \boldsymbol{H}. \tag{5.2}$$

In conjunction with the constraint (3.1) of incompressibility and the condition (2.5) arising from the definition (2.3) of $\boldsymbol{G}$ and (A.42), the system (5.1)–(5.2) provides a complete set of evolution equations for the velocity $\boldsymbol{v}$, pressure p, and the incompatibility $\boldsymbol{G}$. Incorporating the identity (3.8) along with the definition $(A.56)_2$ of the material time derivative of a second-order tensor field, we see from the consistency condition (5.2) that the external supply $\boldsymbol{H}$ of incompatibility must also be solenoidal:

$$\operatorname{div} \boldsymbol{H} = \boldsymbol{0}. \tag{5.3}$$

Although, as remarked earlier after (3.10), (5.3) follows if $\boldsymbol{J} = -\boldsymbol{J}^t$, the constitutive relation (4.10) determining $\boldsymbol{J}$ need not yield this asymmetry. Instead (5.3) follows from the consequence $\operatorname{div}(\operatorname{div} \boldsymbol{J}) = \boldsymbol{0}$ of (4.10), which holds regardless of whether or not $\boldsymbol{J} = -\boldsymbol{J}^t$. Hence, none of our developments hinge on assuming that $\boldsymbol{J} = -\boldsymbol{J}^t$.

6. Boundary conditions at a rigid, fixed, impermeable wall

Consider a fixed, rigid, impermeable wall with unit normal $\boldsymbol{m}$ directed inward toward the region containing the fluid. Consistent with the assumption that the wall is impermeable, the normal component $\boldsymbol{v} \cdot \boldsymbol{m}$ of the velocity $\boldsymbol{v}$ must satisfy the impenetrability condition

$$\boldsymbol{v} \cdot \boldsymbol{m} = 0. \tag{6.1}$$

For the incompatibility vector $\boldsymbol{g}_m = \boldsymbol{G}\boldsymbol{m}$ associated with the wall surface, we propose, in contrast a condition depending on the magnitude $|(\boldsymbol{1} - \boldsymbol{m} \otimes \boldsymbol{m})\boldsymbol{T}\boldsymbol{m}|$ of the shear stress evaluated at the wall. If that magnitude is sufficiently small, we require that $\boldsymbol{g}_m = \boldsymbol{G}\boldsymbol{m} = \boldsymbol{0}$. Otherwise, we allow for incompatibility associated with the wall to be generated and directed normal to the wall surface. Specifically, we suppose that there exists a threshold value τ_c of $|(\boldsymbol{1} - \boldsymbol{m} \otimes \boldsymbol{m})\boldsymbol{T}\boldsymbol{m}|$ such that

$$\boldsymbol{g}_m = \boldsymbol{G}\boldsymbol{m} = \begin{cases} \boldsymbol{0}, & \text{if} \quad |(\boldsymbol{1} - \boldsymbol{m} \otimes \boldsymbol{m})\boldsymbol{T}\boldsymbol{m}| < \tau_c, \\ \gamma \boldsymbol{m}, & \text{if} \quad |(\boldsymbol{1} - \boldsymbol{m} \otimes \boldsymbol{m})\boldsymbol{T}\boldsymbol{m}| \geq \tau_c, \end{cases} \tag{6.2}$$

where $\gamma = |\boldsymbol{G}\boldsymbol{m}|$ is a given scalar measure of incompatibility induced by the shedding of vortices at the wall.

Supplemental to (6.1), we require that $\boldsymbol{v}$ satisfy the conventional no-slip boundary condition

$$(\boldsymbol{1} - \boldsymbol{m} \otimes \boldsymbol{m})\boldsymbol{v} = \boldsymbol{0}. \tag{6.3}$$

Additionally, since surfaces in the flow domain that intersect the wall, and are oriented by any unit tangent vector $\boldsymbol{t}$ perpendicular to $\boldsymbol{m}$, are not associated with the wall, they cannot be a source of generation of incompatibility into or out of the flow domain. Thus, the incompatibility vector $\boldsymbol{g}_t = \boldsymbol{G}\boldsymbol{t}$ associated with such a surface and evaluated at the wall is required to satisfy the boundary condition

$$\boldsymbol{g}_t \cdot \boldsymbol{m} = \boldsymbol{G}\boldsymbol{t} \cdot \boldsymbol{m} = 0 \qquad \text{for all} \qquad \boldsymbol{t} \perp \boldsymbol{m}. \tag{6.4}$$

Observing from (6.2) and (6.4) that

$$(\boldsymbol{1} - \boldsymbol{m} \otimes \boldsymbol{m})\boldsymbol{G}^{\top}\boldsymbol{G}\boldsymbol{m} = \boldsymbol{0} \tag{6.5}$$

at the wall, we see with reference to the expression (4.11) for $\boldsymbol{T}$ that

$$(\boldsymbol{1} - \boldsymbol{m} \otimes \boldsymbol{m})\boldsymbol{T}\boldsymbol{m} = 2\varrho\nu(\boldsymbol{1} - \boldsymbol{m} \otimes \boldsymbol{m})\boldsymbol{D}\boldsymbol{m}. \tag{6.6}$$

The alternative involving the threshold value τ_c, as expressed in (6.2), thus depends only on the magnitude $2\varrho\nu|(\boldsymbol{1} - \boldsymbol{m} \otimes \boldsymbol{m})\boldsymbol{D}\boldsymbol{m}|$ of the viscous contribution to the total shear stress evaluated at the wall and (6.2) can be written more explicitly as

$$\boldsymbol{g}_m = \boldsymbol{G}\boldsymbol{m} = \begin{cases} \boldsymbol{0}, & \text{if} \quad 2\varrho\nu|(\boldsymbol{1} - \boldsymbol{m} \otimes \boldsymbol{m})\boldsymbol{D}\boldsymbol{m}| < \tau_c, \\ \gamma\boldsymbol{m}, & \text{if} \quad 2\varrho\nu|(\boldsymbol{1} - \boldsymbol{m} \otimes \boldsymbol{m})\boldsymbol{D}\boldsymbol{m}| \geq \tau_c, \end{cases} \tag{6.7}$$

If, in addition, $2\varrho\nu|(\boldsymbol{1} - \boldsymbol{m} \otimes \boldsymbol{m})\boldsymbol{D}\boldsymbol{m}| \geq \tau_c$, so that the condition $\boldsymbol{G}\boldsymbol{m} = \gamma\boldsymbol{m}$ applies at the wall, then

$$(\boldsymbol{1} - \boldsymbol{m} \otimes \boldsymbol{m})\boldsymbol{G}^{\top}\boldsymbol{G}\boldsymbol{m} = \gamma(\boldsymbol{G}^{\top}\boldsymbol{m} - \gamma\boldsymbol{m}), \tag{6.8}$$

and, referring to (6.5), we find that

$$\boldsymbol{G}\boldsymbol{m} = \gamma\boldsymbol{m} \quad \text{at the wall} \qquad \Longrightarrow \qquad \boldsymbol{G}^{\top}\boldsymbol{m} = \gamma\boldsymbol{m} \quad \text{at the wall}. \tag{6.9}$$

Since the orientation $\boldsymbol{e}$ of any surface that intersects the wall may be written as $\boldsymbol{e} = (\boldsymbol{e} \cdot \boldsymbol{m})\boldsymbol{m} + (\boldsymbol{e} \cdot \boldsymbol{t})\boldsymbol{t}$ for some $\boldsymbol{t}$ perpendicular to $\boldsymbol{m}$, we infer from (6.4) and (6.7) that the incompatibility vector $\boldsymbol{g}_e = \boldsymbol{G}\boldsymbol{e}$ associated with such a surface satisfies $\boldsymbol{g}_e \cdot \boldsymbol{m} = \boldsymbol{G}\boldsymbol{e} \cdot \boldsymbol{m} = (\boldsymbol{e} \cdot \boldsymbol{m})\gamma$ and $\boldsymbol{g}_e \cdot \boldsymbol{t} = (\boldsymbol{e} \cdot \boldsymbol{t})\boldsymbol{G}\boldsymbol{t} \cdot \boldsymbol{t}$.

Finally, using the consequence $\boldsymbol{G}\boldsymbol{m} = -(\operatorname{curl}\boldsymbol{\Lambda})\boldsymbol{m} = (\operatorname{grad}\boldsymbol{\Lambda})[\boldsymbol{m}\times]$ of (A.40) in conjunction with the decomposition

$$\operatorname{grad}\boldsymbol{\Lambda} = \operatorname{grad}_S\boldsymbol{\Lambda} + ((\operatorname{grad}\boldsymbol{\Lambda})\boldsymbol{m}) \otimes \boldsymbol{m} \tag{6.10}$$

of the gradient $\operatorname{grad}\boldsymbol{\Lambda}$ of $\boldsymbol{\Lambda}$ on the wall into a tangential component and a normal component $((\operatorname{grad}\boldsymbol{\Lambda})\boldsymbol{m}) \otimes \boldsymbol{m}$, we observe that $\boldsymbol{g}_m$ can be expressed as

$$\boldsymbol{g}_m = \boldsymbol{G}\boldsymbol{m} = (\operatorname{grad}_S\boldsymbol{\Lambda})[\boldsymbol{m}\times]. \tag{6.11}$$

We hence conclude that the proposed boundary condition (6.7) encompasses the notion that incompatibility at a wall is associated with heterogeneity of the surface gradient of the incompatible distortion rate $\boldsymbol{\Lambda}$.

7. Compatible and incompatible solutions in steady plane Poiseuille flow

7.1. Preliminaries

Given a right-handed orthonormal basis $\{\boldsymbol{\imath}_1, \boldsymbol{\imath}_2, \boldsymbol{\imath}_3\}$ and a choice $\boldsymbol{o}$ of origin, let $x_i = (\boldsymbol{x} - \boldsymbol{o}) \cdot \boldsymbol{\imath}_i$, $i = 1, 2, 3$, denote the associated rectangular Cartesian coordinates. We consider a steady two-dimensional flow within an infinite rectangular channel in the $x_3 = 0$ plane with walls parallel to $\boldsymbol{\imath}_1$ and located at $x_2 = -h$ and $x_2 = h$, as driven by a negative pressure gradient with uniform streamwise component satisfying

$$\boldsymbol{\imath}_1 \cdot \operatorname{grad} p = -\frac{P}{\ell}, \qquad P > 0, \tag{7.1}$$

with $\ell > 0$ being a characteristic length in the streamwise direction. The flow domain is defined by $-\infty < x_1 < \infty$, $-h \leq x_2 \leq h$, $-\infty < x_3 < \infty$. To ensure that the velocity $\boldsymbol{v}$ and the incompatibility $\boldsymbol{G}$ are solenoidal per the requirements (2.5) and (3.1), we assume that they are given by

$$\boldsymbol{v} = v\boldsymbol{\imath}_1 \qquad \text{and} \qquad \boldsymbol{G} = G\boldsymbol{\imath}_2 \otimes \boldsymbol{\imath}_1 + \Gamma\,\boldsymbol{\imath}_2 \otimes \boldsymbol{\imath}_2, \tag{7.2}$$

where v and G depend at most on x_2 and Γ is a constant. As an immediate consequence of $(7.2)_2$, we see that

$$\operatorname{tr}\boldsymbol{G} = \Gamma = \text{constant}. \tag{7.3}$$

Moreover, we see with reference to (A.36) that

$$\operatorname{curl}(\boldsymbol{G}^{\top}) = \operatorname{curl}(G\boldsymbol{\imath}_1 \otimes \boldsymbol{\imath}_2) = ((\operatorname{grad} G)\times)\boldsymbol{\imath}_2 \otimes \boldsymbol{\imath}_1 = G'(\boldsymbol{\imath}_2 \times \boldsymbol{\imath}_2) \otimes \boldsymbol{\imath}_1 = \boldsymbol{0}, \tag{7.4}$$

where a prime denotes differentiation with respect to x_2. For $\boldsymbol{G}$ as defined in $(7.2)_2$, we also see that

$$\operatorname{curl}(\tfrac{1}{2}(\operatorname{tr}\boldsymbol{G})\boldsymbol{1} - \boldsymbol{G}^{\top}) = \boldsymbol{0}. \tag{7.5}$$

If $\Gamma \neq 0$, then alternative (B) of Section 2.1 applies. Thus, (2.15) holds and there exists a vector field $\boldsymbol{u}$ such that $\boldsymbol{D}_\Lambda$ is given by

$$\boldsymbol{D}_\Lambda = \operatorname{sym}(\operatorname{grad}\boldsymbol{u}). \tag{7.6}$$

Moreover, (2.18) holds and there exist scalar and vector fields φ and $\boldsymbol{w}$ such that $\boldsymbol{\omega}_\Lambda$ is given by

$$\boldsymbol{\omega}_\Lambda = \operatorname{grad}\varphi + \tfrac{1}{2}\operatorname{curl}\boldsymbol{w}, \qquad \operatorname{div}\boldsymbol{w} = 0, \tag{7.7}$$

and, recalling (7.3), (2.20) simplifies to

$$\Delta\varphi = -\tfrac{1}{2}\Gamma = \text{constant}. \tag{7.8}$$

Additionally, noting (A.6), $\boldsymbol{\Lambda}$ admits the representation

$$\boldsymbol{\Lambda} = \operatorname{sym}(\operatorname{grad}\boldsymbol{u}) + \operatorname{skw}(\operatorname{grad}\boldsymbol{w}) + (\operatorname{grad}\varphi)\times. \tag{7.9}$$

In particular, however, $(7.2)_2$ ensures that $\boldsymbol{\Lambda}$ is determined by the scalar quantities G and Γ through

$$\boldsymbol{\Lambda}(\boldsymbol{x}) = \Big(\Gamma x_1 - \int_{-h}^{x_2} G(\bar{x}_2)\,\mathrm{d}\bar{x}_2\Big)\boldsymbol{\iota}_2 \otimes \boldsymbol{\iota}_3, \tag{7.10}$$

and, of course, since (2.3) is satisfied, $\boldsymbol{\Lambda}$ cannot be the gradient of a vector field within the channel.

The dependence of $\boldsymbol{\Lambda}$ on x_1 may seem puzzling and somewhat ponderous. However it can be shown that

$$\int_{C_t} \boldsymbol{\Lambda}\boldsymbol{t}\,\mathrm{d}s = -\Big(\int_{S_t} (\Gamma\boldsymbol{\iota}_2 + G(x_2)\boldsymbol{\iota}_1)\cdot\boldsymbol{n}\,\mathrm{d}a\Big)\boldsymbol{\iota}_2 \tag{7.11}$$

for any circuit C_t spanned by the surface S_t in the flow domain. Thus, for any $\boldsymbol{\iota}_1$-translate of C_t to $C_t(c) := \{\boldsymbol{y} \in \mathbb{E}^3 \mid \boldsymbol{y} = \boldsymbol{x}+c\boldsymbol{\iota}_1, \boldsymbol{x} \in C_t\}$, where c = constant, it follows that the integral is $\boldsymbol{\iota}_1$-translation invariant:

$$\int_{C_t(c)} \boldsymbol{\Lambda}\boldsymbol{t}\,\mathrm{d}s = \int_{C_t} \boldsymbol{\Lambda}\boldsymbol{t}\,\mathrm{d}s. \tag{7.12}$$

Clearly, there are many circuits C_t for which the integral (7.11) does not vanish, for example for any circuit lying in an x_1 = constant or x_2 = constant plane for which $\boldsymbol{n} = \boldsymbol{\iota}_1$ or $\boldsymbol{n} = \boldsymbol{\iota}_2$, respectively. And there are some circuits for which (7.11) vanishes, for example for any circuit lying in an x_3 = constant surface for which $\boldsymbol{n} = \boldsymbol{\iota}_3$. In any case, the x_1 dependence in (7.10), while being present in the incompatible distortion rate $\boldsymbol{\Lambda}$, is not present in the incompatibility $\boldsymbol{G}$ or any physical field directly dependent upon it.

7.2. Governing equations and boundary conditions

From (7.2), we find that

$$\left.\begin{aligned} \boldsymbol{L} = v'\boldsymbol{\iota}_1 \otimes \boldsymbol{\iota}_2, \qquad \boldsymbol{\Delta v} = v''\boldsymbol{\iota}_1, \qquad \operatorname{div}(\boldsymbol{G}^\top\boldsymbol{G}) = \Gamma G'\boldsymbol{\iota}_1, \\ \boldsymbol{G}\boldsymbol{L}^\top = \Gamma v'\boldsymbol{\iota}_2 \otimes \boldsymbol{\iota}_1, \qquad \operatorname{grad}\boldsymbol{G} = G'\boldsymbol{\iota}_2 \otimes \boldsymbol{\iota}_1 \otimes \boldsymbol{\iota}_2, \qquad \boldsymbol{\Delta G} = G''\boldsymbol{\iota}_2 \otimes \boldsymbol{\iota}_1, \end{aligned}\right\} \tag{7.13}$$

and, moreover, from the definition (4.13) of the incompatibility stress tensor $\boldsymbol{R}$, that

$$\boldsymbol{R} = \varrho\iota^2 G^2 \boldsymbol{\iota}_1 \otimes \boldsymbol{\iota}_1 + \varrho\iota^2\Gamma G(\boldsymbol{\iota}_1 \otimes \boldsymbol{\iota}_2 + \boldsymbol{\iota}_2 \otimes \boldsymbol{\iota}_1) + \varrho\iota^2\Gamma^2\boldsymbol{\iota}_2 \otimes \boldsymbol{\iota}_2. \tag{7.14}$$

According to (4.12), we thus have the relation

$$p = q - \tfrac{1}{3}\varrho\iota^2(G^2 + \Gamma^2), \tag{7.15}$$

and it follows that

$$\boldsymbol{\iota}_1 \cdot \operatorname{grad} p = \boldsymbol{\iota}_1 \cdot \operatorname{grad} q. \tag{7.16}$$

Using (7.1) and (7.13) in (5.1)–(5.2) while recalling that Γ is constant, we then find that

$$\operatorname{grad} q = -\frac{P}{\ell}\boldsymbol{\iota}_1, \tag{7.17}$$

and we obtain a system of two second-order ordinary-differential equations for v and G:

$$\Big(v' + \frac{\iota^2\Gamma}{\nu}G\Big)' = -\frac{P}{\varrho\nu\ell}, \qquad \Big(G' + \frac{\Gamma}{\kappa}v\Big)' = 0. \tag{7.18}$$

Applying the boundary conditions (6.1) and (6.3) to $(7.2)_1$, we find that v must satisfy

$$v(\pm h) = 0. \tag{7.19}$$

Additionally, applying the boundary conditions (6.2) and (6.4) to $(7.2)_2$, we find that Γ is determined according to

$$\Gamma = \begin{cases} 0, & \text{if} \quad \varrho\nu|v'(\pm h)| < \tau_c, \\ \gamma, & \text{if} \quad \varrho\nu|v'(\pm h)| \geq \tau_c, \end{cases} \tag{7.20}$$

and that G must satisfy

$$G(\pm h) = 0. \tag{7.21}$$

We consider the alternatives $\varrho\nu|v'(\pm h)| < \tau_c$ and $\varrho\nu|v'(\pm h)| \geq \tau_c$ in sequence, starting with $\varrho\nu|v'(\pm h)| < \tau_c$.

7.3. Compatible solutions

For $\varrho\nu|v'(\pm h)| < \tau_c$, (7.20) gives $\Gamma = 0$, $(7.18)_2$, (7.20), and (7.21) require also that $G = 0$, whereby $(7.2)_2$ and (7.10) reduce to

$$\boldsymbol{G} = \boldsymbol{0} \qquad \text{and} \qquad \boldsymbol{\Lambda} = \boldsymbol{0}. \tag{7.22}$$

Hence, the distortion rate $\boldsymbol{L}$ has no incompatible component $\boldsymbol{\Lambda}$ if $\varrho\nu|v'(\pm h)| < \tau_c$. Moreover, $(7.18)_1$ and (7.19) simplify to the boundary-value problem for conventional Poiseuille flow and the streamwise velocity, which, reserving the symbol v for use in the alternative case $\varrho\nu|v'(\pm h)| \geq \tau_c$ of incompatible solutions, we denote by V, with the familiar quadratic expression

$$V(x_2) = \frac{Ph^2}{2\varrho\nu\ell}\Big(1 - \frac{x_2^2}{h^2}\Big), \qquad -h \leq x_2 \leq h. \tag{7.23}$$

7.4. Incompatible solutions

For the alternative $\varrho\nu|v'(\pm h)| \geq \tau_c$, (7.20) yields $\Gamma = \gamma$ and we may solve (7.18) subject to (7.19) and (7.21), with the outcome that v and G are given by

$$\left.\begin{aligned} v(x_2) &= \frac{Ph^2}{\varrho\nu\ell}\frac{\coth\Omega h}{\Omega h}\Big(1 - \frac{\cosh\Omega x_2}{\cosh\Omega h}\Big), \\ G(x_2) &= \frac{Ph}{\varrho\iota^2\gamma\ell}\Big(\frac{\sinh\Omega x_2}{\sinh\Omega h} - \frac{x_2}{h}\Big), \end{aligned}\right\} \quad -h \leq x_2 \leq h, \tag{7.24}$$

where we have introduced a wavenumber Ω defined by

$$\Omega := \sqrt{\frac{\iota^2\gamma^2}{\nu\kappa}}. \tag{7.25}$$

In this case, the distortion rate $\boldsymbol{L}$ has a nontrivial incompatible component $\boldsymbol{\Lambda}$ and we may use the relation $\Gamma = \gamma$ and the expression $(7.24)_2$ for G in (7.10) to find that

$$\boldsymbol{\Lambda} = \Lambda\boldsymbol{\imath}_2 \otimes \boldsymbol{\imath}_3, \tag{7.26}$$

where Λ is given by

$$\Lambda(x_1, x_2) = \gamma x_1 + \frac{\gamma}{\kappa\Omega^2}(v(x_2) - V(x_2)), \qquad -\infty < x_1 < \infty, \quad -h \leq x_2 \leq h, \tag{7.27}$$

with V and v as provided in (7.23) and $(7.24)_1$. Thus, we see that

$$\boldsymbol{D}_\Lambda = \operatorname{sym}(\operatorname{grad}\boldsymbol{u}) = \tfrac{1}{2}\Lambda(\boldsymbol{\imath}_2 \otimes \boldsymbol{\imath}_3 + \boldsymbol{\imath}_3 \otimes \boldsymbol{\imath}_2), \tag{7.28}$$

which, in accord with (2.8), (2.12), and (7.5), having replaced $\boldsymbol{D}$ by $\boldsymbol{D}_\Lambda$, we may integrate to find $\boldsymbol{u}$. Up to added unimportant (and dropped) constant translational and angular velocities, we find that $\boldsymbol{u}$ is of the form

$$\boldsymbol{u} = u_i\boldsymbol{\imath}_i, \tag{7.29}$$

where u_i, $i = 1, 2, 3$, are given by

$$\left.\begin{aligned} u_1(\boldsymbol{x}) &= -\tfrac{1}{2}\gamma x_2 x_3, \\ u_2(\boldsymbol{x}) &= \tfrac{1}{2}\gamma x_1 x_3, \\ u_3(\boldsymbol{x}) &= \tfrac{1}{2}\gamma h x_1 + \int_{-h}^{x_2}(\Lambda(x_1, \bar{x}_2) - \tfrac{1}{2}\gamma x_1)\,\mathrm{d}\bar{x}_2, \end{aligned}\right\} \quad -\infty < x_1 < \infty, \qquad -h \leq x_2 \leq h. \tag{7.30}$$

From (7.26), we also find that

$$\boldsymbol{W}_\Lambda = \operatorname{skw}(\operatorname{grad}\boldsymbol{w}) + (\operatorname{grad}\varphi)\times = \tfrac{1}{2}\Lambda(\boldsymbol{\imath}_2 \otimes \boldsymbol{\imath}_3 - \boldsymbol{\imath}_3 \otimes \boldsymbol{\imath}_2), \tag{7.31}$$

or, equivalently, by (A.7), that

$$\boldsymbol{\omega}_\Lambda = \tfrac{1}{2}\operatorname{curl}\boldsymbol{w} + \operatorname{grad}\varphi = -\tfrac{1}{2}\Lambda\boldsymbol{\imath}_1, \tag{7.32}$$

where $\boldsymbol{w}$ and φ must obey

$$\operatorname{div}\boldsymbol{w} = 0 \qquad \text{and} \qquad \Delta\varphi = -\tfrac{1}{2}\gamma. \tag{7.33}$$

Up to added unimportant (and dropped) constant translational and angular velocities, we thus find that $\boldsymbol{w}$ is given by

$$\boldsymbol{w}(\boldsymbol{x}) = \Big(\gamma x_1(x_2+h) - \int_{-h}^{x_2} \Lambda(x_1,\bar{x}_2)\,\mathrm{d}\bar{x}_2\Big)\boldsymbol{\imath}_3, \qquad -\infty < x_1 < \infty, \quad -h \le x_2 \le h, \tag{7.34}$$

and, correspondingly, up to an added (and dropped) constant, that φ is given by

$$\varphi(\boldsymbol{x}) = -\tfrac{1}{4}\gamma x_1^2. \qquad -\infty < x_1 < \infty. \tag{7.35}$$

In view of (4.11) and $(7.18)_1$, the total shear stress $T_{12} = \boldsymbol{\imath}_1 \cdot \boldsymbol{T}\boldsymbol{\imath}_2 = \varrho(\nu v' + \imath^2\gamma G)$ must be a linear function of the spanwise coordinate x_2, as is known to be so in conventional Poiseuille flow. Indeed, from (7.24), we see that it has the standard form

$$T_{12}(\boldsymbol{x}) = -\frac{P x_2}{\ell}, \qquad -h \le x_2 \le h. \tag{7.36}$$

We will nevertheless show in Section 7.6 that the contributions $\varrho\nu v'$ and $\varrho\imath^2\gamma G$ to T_{12} due, respectively, to ordinary viscous effects and the incompatible distortion rate $\boldsymbol{\Lambda}$ are considerably more interesting. From (7.13), (7.14), (7.20), and (7.24), we see that the normal stresses $T_{\alpha\alpha} = \boldsymbol{\imath}_\alpha \cdot \boldsymbol{T}\boldsymbol{\imath}_\alpha$, $\alpha = 1,2$, are given by

$$\left.\begin{aligned} T_{11}(\boldsymbol{x}) &= R_{11}(\boldsymbol{x}) = \varrho\imath^2 G^2(x_2),\\ T_{22}(\boldsymbol{x}) &= R_{22}(\boldsymbol{x}) = \varrho\imath^2\gamma^2, \end{aligned}\right\} \qquad -h \le x_2 \le h, \tag{7.37}$$

with G as defined in $(7.24)_2$. Thus, in contrast to conventional Poiseuille flow, incompatibility gives rise to nontrivial normal stresses and an associated first normal stress difference

$$T_{11}(\boldsymbol{x}) - T_{22}(\boldsymbol{x}) = R_{11}(\boldsymbol{x}) - R_{22}(\boldsymbol{x}) = \varrho\imath^2(G^2(x_2) - \gamma^2), \qquad -h \le x_2 \le h. \tag{7.38}$$

7.5. Asymptotic results for small values of the dimensionless wavenumber

For $\varrho\nu|v'(\pm h)| \ge \tau_c$, we may use the Taylor expansions of the hyperbolic sine and cosine in (7.24) to find that

$$v(x_2) \sim V(x_2) \qquad \text{and} \qquad G(x_2) \sim 0 \qquad \text{for} \qquad \Omega h \ll 1. \tag{7.39}$$

Thus, granted that the dimensionless wavenumber Ωh satisfies $\Omega h \ll 1$, the classical quadratic velocity profile (7.23) is recovered and the contribution G to the incompatibility $\boldsymbol{G}$ vanishes.

To put one physical interpretation on what governs the size of the dimensionless wave number Ωh, suppose we return to (7.25) and write

$$\Omega h = \sqrt{\frac{\imath^2\gamma^2/\nu^2}{\kappa/\nu}}\,h. \tag{7.40}$$

Now, for a given mass density ϱ, we observe that $(7.2)_2$, (7.20), and (7.21) require the kinetic energy of incompatibility that enters the region occupied by the fluid though the boundary to be given by

$$\tfrac{1}{2}\varrho\imath^2|\boldsymbol{G}|^2 = \tfrac{1}{2}\varrho\imath^2\gamma^2. \tag{7.41}$$

Thus, suppose that for a fluid with fixed density ϱ and kinematic viscosity ν this boundary input of kinetic energy of incompatibility is specified. Then, if $\kappa \gg \nu$ so that the fluid efficiently diffuses the transport of incompatibility relative to the viscous diffusive effect of viscosity, we see that for a given channel width $2h$, Ωh is small and we may conclude that incompatibility plays a minor role in the flow behavior of the fluid. In this scenario, it is when the diffusivity κ of incompatibility transport is small relative to the kinematic viscosity ν that a significant presence of incompatibility becomes an important element of the flow behavior, and, of course Ωh is large.

7.6. Dimensionless results

Fig. 1(a) contains plots of the dimensionless velocity v_* defined by

$$v_*(y) := \frac{v(hy)}{v(0)} = 1 - \frac{1-\cosh\Omega h y}{1-\cosh\Omega h}, \qquad -1 \le y \le 1, \tag{7.42}$$

for representative values of the dimensionless wavenumber Ωh. For the smallest value $\Omega h = 0.01$ of Ωh considered, the plot of v_* is difficult to distinguish from the classical quadratic expression. This is consistent with the asymptotic result $(7.39)_1$. The plots of v_* become progressively more blunted as Ωh increases.[12] To further explore the influence of the dimensionless parameter Ωh on

[12] Similarly blunted velocity profiles are common to steady laminar channel flows of incompressible non-Newtonian fluids and fully developed turbulent channel flows of incompressible Newtonian fluids. In the former context, they are captured by power-law (Saramito, 2016; Schechter, 1961), pseudoplastic (Matsuhisa & Bird, 1965; Rotem & Shinnar, 1961), viscoelastic (Griffiths, 2020; Oliveira, 2002; Oliveira & Pinho, 1999; Siline & Leonov, 2001; Yoo & Choi, 1989), and viscoelastic–plastic (White, 1981) models. In the latter context, they are captured by direct numerical simulations (Abe, Kawamura, & Choi, 2004; Abe, Kawamura, & Matsuo, 2001; Bernardini, Pirozzoli, & Orlandi, 2014; Hoyas & Jiménez, 2003; Kim, Moin, & Moser, 1987; Lee & Moser, 2015; Lozano-Durán & Jiménez, 2014; Monty & Chong, 2009).

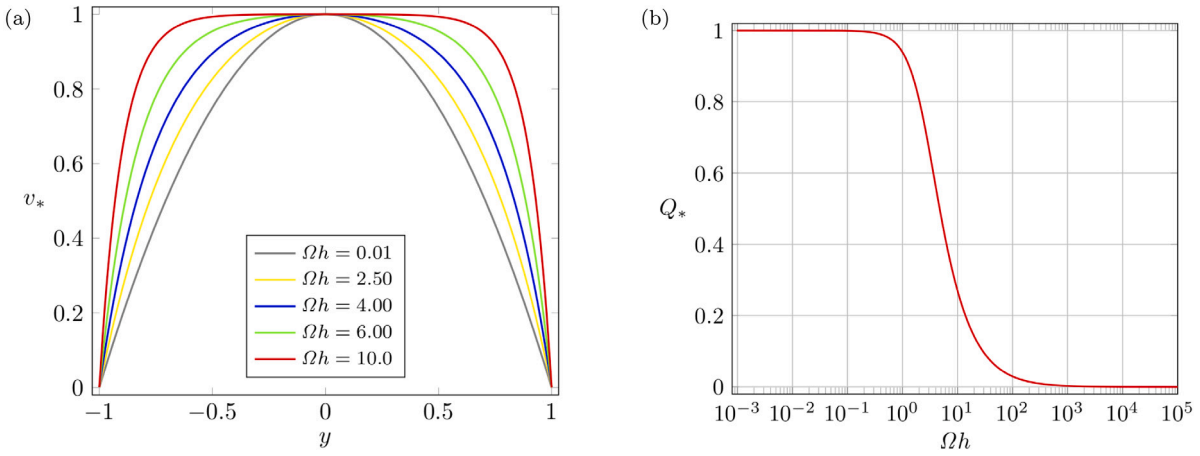

Fig. 1. (a) Plots of the dimensionless downstream velocity v_* defined in (7.42) versus the dimensionless spanwise coordinate $y = x_2/h$ for select values of the dimensionless counterpart Ωh of the wavenumber from (7.25). (b) Plot of the dimensionless flow rate Q_* defined in (7.43) versus Ωh.

the solution to the incompatible flow problem, we integrate v spanwise and divide by the flow rate $\int_{-h}^{h} V(x_2)\,\mathrm{d}x_2 = 2Ph^3/3\varrho\nu\ell$ corresponding to the classical quadratic profile V in (7.23), yielding the dimensionless flow rate

$$Q_* := \frac{3\coth\Omega h}{\Omega h}\Big(1 - \frac{\tanh\Omega h}{\Omega h}\Big). \tag{7.43}$$

The decay of Q_* as Ωh increases that is depicted in Fig. 1(b) is consistent with the blunting of the velocity profile shown in Fig. 1(a). Consequently, a larger pressure drop P/l is needed to maintain a given flow rate as Ωh increases.

Fig. 2 contains plots of the dimensionless viscous shear stress τ_* defined by

$$\tau_*(y) := \frac{\varrho\nu v'(hy)}{\varrho\nu v'(-h)} = -\frac{\sinh\Omega hy}{\sinh\Omega h}, \qquad -1 \le y \le 1, \tag{7.44}$$

and the dimensionless incompatibility shear stress σ_* defined by

$$\sigma_*(y) := \frac{\varrho\iota^2\gamma G(hy)}{\varrho\nu v'(-h)} = \frac{\sinh\Omega hy}{\sinh\Omega h} - y, \qquad -1 \le y \le 1, \tag{7.45}$$

for representative values of Ωh.[13] Consistent with the asymptotic result (7.36) for T_{12}, we see that τ_* does not deviate substantially from $-y$ for $\Omega h = 1.50$. However, as Ωh becomes large, we see that τ_* vanishes outside boundary layers near the walls. Within those layers, the magnitude of τ_* increases monotonically as Ωh increases. Consistent with the asymptotic result $(7.39)_2$ for G, we see that $\sigma_* \approx 0$ for $\Omega h = 0.01$. For larger values of Ωh, σ_* is odd about the midline $x_2 = 0$ of the channel, like τ_*. For non-negligible values of Ωh, $|\sigma_*|$ is maximized near the channel walls, respectively, and those maxima are connected by a nearly straight line of negative slope with monotonically increasing magnitude. In line with the previous observation that, as a consequence of the balance $(7.18)_1$, the total shear stress T_{12} must be a linear function of the spanwise coordinate, from (7.44) and (7.45) we see that the dimensionless shear stresses compensate one another to ensure that $\tau_*(y) + \sigma_*(y) = -y$ for $-1 \le y \le 1$. Less obvious, however, is a cross-over between conventional viscous effects and incompatibility evident from Fig. 2: Although the viscous contribution to the total shear stress T_{12} dominates for $\Omega h \ll 1$, it becomes increasingly less significant as Ωh increases and is completely overwhelmed by the incompatibility shear stress contribution for $\Omega h \gg 1$.

Recalling from $(7.37)_2$ that the spanwise normal stress T_{22} is constant, we next consider the dimensionless streamwise normal stress N_* defined in terms of $T_{11} = \varrho\iota G^2$ by

$$N_*(y) = \frac{\varrho\iota^2\kappa G^2(hy)}{\frac{1}{2}\varrho\nu v^2(0)} = 2\Big(\frac{\sinh\Omega h}{\cosh\Omega h - 1}\Big)^2\sigma_*^2(y) = 2\Big(\frac{\sinh\Omega hy - (\sinh\Omega h)y}{\cosh\Omega h - 1}\Big)^2. \tag{7.46}$$

Fig. 3 contains plots of N_* for representative values of Ωh.[14] Apart from showing that N_* vanishes along the walls and midline of the channel walls but is otherwise positive, these plots show that the peak values of N_*, which necessarily coincide with the maxima and minima of the dimensionless incompatibility shear stress σ_*, increase monotonically with Ωh. Determining $\boldsymbol{D}$ from $(7.24)_1$ and

[13] The plots of σ_* resemble the experimentally determined Reynolds shear stress profiles presented in Figure 12 of Schultz and Flack (2013), whose results for friction Reynolds numbers $\mathrm{Re}_\tau = 944$ and $\mathrm{Re}_\tau = 2000$ closely match results from direct numerical simulations performed by Del Alamo, Jiménez, Zandonade, and Moser (2004) and Hoyas and Jiménez (2003), respectively.

[14] The plots of Fig. 3 share the qualitative features of experimentally determined streamwise Reynolds normal stress profiles presented in Figure 8 of Schultz and Flack (2013), whose measurements are closely matched by results from the direct numerical simulations of Hoyas and Jiménez (2003), the plots of N_* show that the streamwise normal stress peaks near the channel walls.

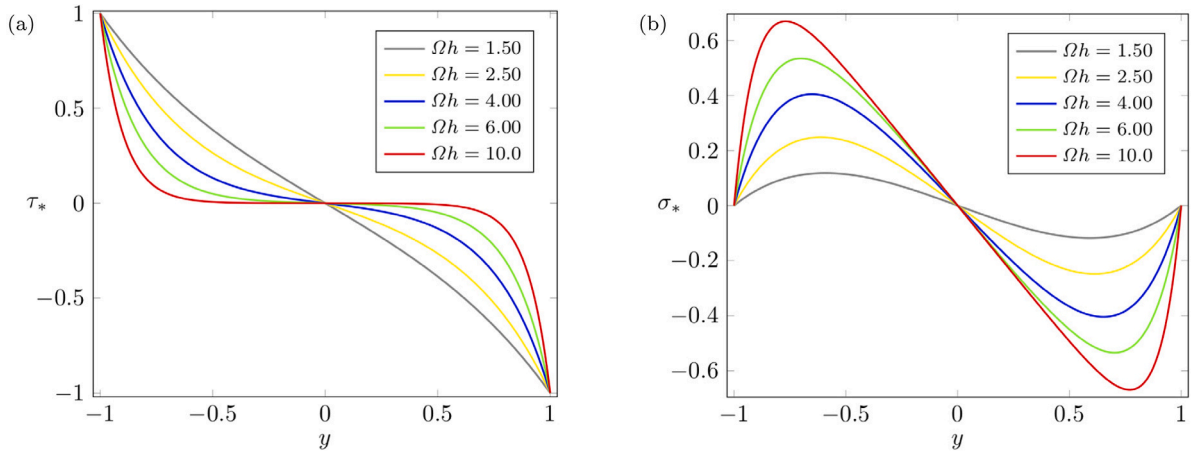

Fig. 2. Plots of (a) the dimensionless viscous shear stress τ_* defined in (7.44) and (b) the dimensionless incompatibility shear stress σ_* defined in (7.45) versus the dimensionless spanwise coordinate $y = x_2/h$ for select values of the dimensionless counterpart Ωh of the wavenumber from (7.25).

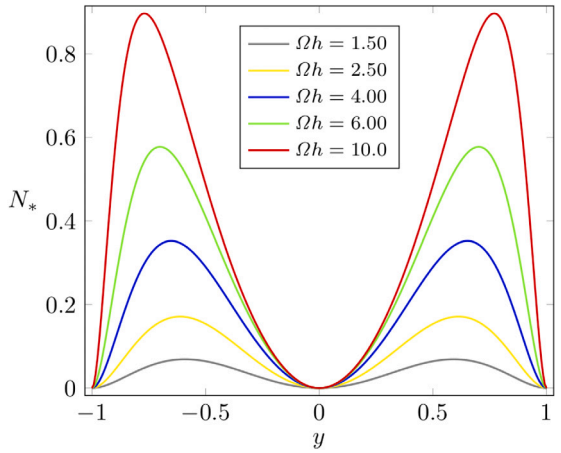

Fig. 3. Plots of the dimensionless streamwise normal stress N_* defined in (7.46) versus the dimensionless spanwise coordinate $y = x_2/h$ for select values of the dimensionless counterpart Ωh of the wavenumber from (7.25).

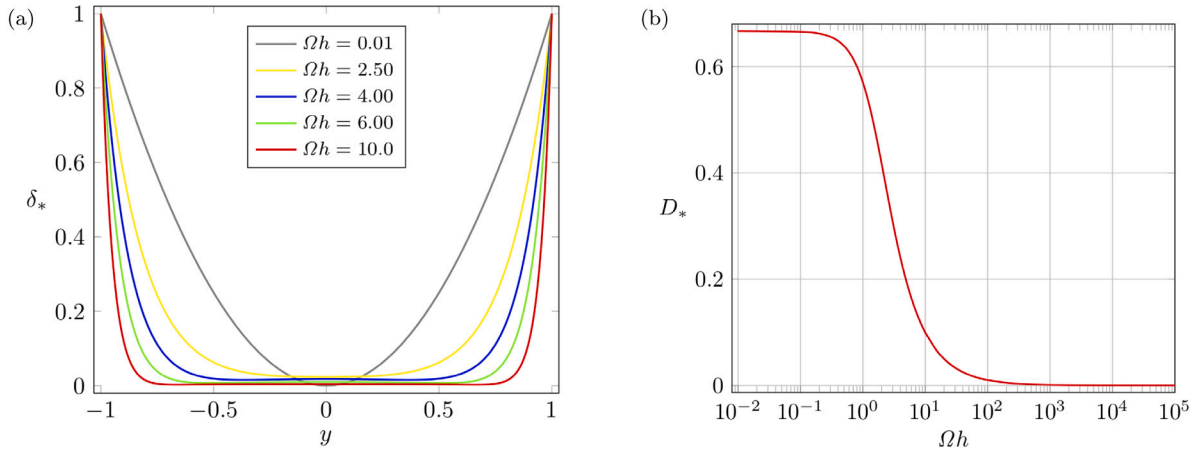

Fig. 4. (a) Plots of the dimensionless specific dissipation δ_* defined in (7.47) versus the dimensionless spanwise coordinate $y = x_2/h$ for select values of the dimensionless counterpart Ωh of the wavenumber Ω from (7.25). (b) Plot of the total dimensionless dissipation D_* defined in (7.48) versus Ωh.

curl $\boldsymbol{G}$ from (7.2)$_2$ and (7.24)$_2$, we next construct the dimensionless specific dissipation δ_* defined by

$$\delta_*(y) = \frac{\delta(hy)}{\delta(\pm h)} = \frac{\Omega^2 h^2 \sinh^2 \Omega h y + (\Omega h \cosh \Omega h y - \sinh \Omega h)^2}{\Omega^2 h^2 \sinh^2 \Omega h + (\Omega h \cosh \Omega h - \sinh \Omega h)^2}, \qquad -1 \le y \le 1. \tag{7.47}$$

Plots of δ_* for representative values of Ωh provided in Fig. 4(a) show that the dissipation is generally concentrated near the channel walls and becomes more so as Ωh increases. From Fig. 4(b), we see that the total dimensionless dissipation, as defined by

$$D_* = \int_{-1}^{1} \delta_*(y)\, \mathrm{d}y = \frac{\Omega h \coth \Omega h - 1}{\Omega^2 h^2 + (\Omega h \coth \Omega h - 1)^2}, \tag{7.48}$$

decays monotonically as Ωh increases. As $\Omega h \to 0$, $D_* \to 2/3$, which is the dimensionless dissipation for the classical quadratic expression V defined by (7.23). The ratio of the dimensional version of the total specific dissipation (7.48) to the dimensional version of the flow rate (7.43) scales with P/ℓ and, thus, the dissipation associated with applying the pressure drop needed to induce a certain flow rate would increase linearly with that pressure drop, when measured relative to the flow rate.

8. Transient effects in plane Poiseuille flow

We now consider the transient version of the plane channel flow problem considered in Section 7 with the purpose of exploring the transition to steady state from compatible to incompatible flow. We thus take the velocity $\boldsymbol{v}$ and the incompatibility $\boldsymbol{G}$ to be of the form (7.2) and the pressure gradient $\operatorname{grad} p$ to satisfy (7.1), while allowing the streamwise velocity $v = \boldsymbol{v} \cdot \boldsymbol{\imath}_1$ and the shear contribution $G = \boldsymbol{\imath}_1 \cdot \boldsymbol{G}\boldsymbol{\imath}_2$ to the incompatibility to depend not only on the spanwise coordinate x_2 but also on time t and allowing Γ and P to depend on t, the latter being given as a Heaviside step function

$$P(t) = \begin{cases} 0, & \text{if} \quad t \le 0, \\ P, & \text{if} \quad t > 0. \end{cases} \tag{8.1}$$

Following the same procedure as in the development of the system (7.18) of ordinary-differential equations governing steady channel flow, we thus find that Γ = constant and that v and G must evolve according to

$$\frac{\partial v}{\partial t} = \nu \frac{\partial^2 v}{\partial x_2^2} + \imath^2 \Gamma \frac{\partial G}{\partial x_2} + \frac{P}{\rho \ell} \qquad \text{and} \qquad \frac{\partial G}{\partial t} = \Gamma \frac{\partial v}{\partial x_2} + \kappa \frac{\partial^2 G}{\partial x_2^2}. \tag{8.2}$$

We consider the parabolic system (8.2) for all (x_2, t) in $(-h, h) \times (0, \infty)$ subject to the boundary conditions

$$v(\pm h, t) = 0, \qquad G(\pm h, t) = 0, \qquad t \ge 0, \tag{8.3}$$

and the initial condition

$$v(x_2, 0) = 0, \qquad G(x_2, 0) = 0, \qquad -h \le x_2 \le h, \tag{8.4}$$

in conjunction with the following alternative criteria:

(C1) $\rho\nu \left| \dfrac{\partial v(x_2, t)}{\partial x_2} \right|_{x_2 = \pm h} < \tau_c$ for all $t \ge 0$;

(C2) $\rho\nu \left| \dfrac{\partial v(x_2, t)}{\partial x_2} \right|_{x_2 = \pm h} < \tau_c$ for $t < t^*$ and $\rho\nu \left| \dfrac{\partial v(x_2, t)}{\partial x_2} \right|_{x_2 = \pm h} \ge \tau_c$ for $t \ge t^*$.

8.1. Compatible solutions

If (C1) holds, then the flow is compatible and $G = \Gamma = 0$. In this event, only one equation in (8.2) survives, namely

$$\frac{\partial v}{\partial t} = \nu \frac{\partial^2 v}{\partial x_2^2} + \frac{P}{\rho \ell}, \tag{8.5}$$

along with corresponding reductions

$$v(\pm h, t) = 0, \qquad t \ge 0, \tag{8.6}$$

and

$$v(x_2, 0) = 0, \qquad -h \le x_2 \le h, \tag{8.7}$$

of the boundary and initial conditions.

To analyze the asymptotic behavior of the solution of the problem (8.5)–(8.7), we introduce the difference velocity field

$$v_d := v - v_0, \tag{8.8}$$

where v_0 satisfies $\nu v_0'' + P/\rho\ell = 0$ subject to the boundary conditions $v_0(\pm h) = 0$ and is therefore given by V defined in (7.23). Then, v_d satisfies the partial differential equation

$$\frac{\partial v_d}{\partial t} = \nu \frac{\partial^2 v_d}{\partial x_2^2}, \tag{8.9}$$

the boundary conditions

$$v_d(\pm h, t) = 0, \qquad t \geq 0, \tag{8.10}$$

and the initial condition

$$v_d(x_2, 0) = -V(x_2), \qquad -h \leq x_2 \leq h. \tag{8.11}$$

Multiplying (8.9) by v_d, integrating by parts, using the boundary conditions (8.10), and invoking the Poincaré inequality

$$\int_{-h}^{h} |v_d(x_2,t)|^2 \, \mathrm{d}x_2 \leq C \int_{-h}^{h} \Big| \frac{\partial v_d(x_2,t)}{\partial x_2} \Big|^2 \, \mathrm{d}x_2, \tag{8.12}$$

where $C > 0$ is a constant with the dimensions of length, we find that

$$\frac{\mathrm{d}}{\mathrm{d}t} \int_{-h}^{h} |v_d(x_2,t)|^2 \, \mathrm{d}x_2 = -2\nu \int_{-h}^{h} \Big| \frac{\partial v_d(x_2,t)}{\partial x_2} \Big|^2 \, \mathrm{d}x_2 \leq -\frac{2\nu}{C} \int_{-h}^{h} |v_d(x_2,t)|^2 \, \mathrm{d}x_2. \tag{8.13}$$

Thus,

$$\frac{\mathrm{d}}{\mathrm{d}t} \Big(\exp\Big(-\frac{2\nu t}{C}\Big) \int_{-h}^{h} |v_d(x_2,t)|^2 \, \mathrm{d}x_2 \Big) \leq 0, \tag{8.14}$$

and integrating over the interval $[0, t]$, and using the initial condition (8.11), we arrive at the inequality

$$\int_{-h}^{h} |v_d(x_2,t)|^2 \, \mathrm{d}x_2 \leq \exp\Big(-\frac{2\nu t}{C}\Big) \int_{-h}^{h} V^2(x_2) \, \mathrm{d}x_2, \tag{8.15}$$

which implies that $|v_d(x_2,t)| = |v(x_2,t) - V(x_2)| \to 0$ as $t \to \infty$ for all x_2 in $(-h, h)$ in the sense of the L^2 norm.

Nominally, we conclude that the transition of v to fully developed steady laminar flow $v_0 = V$ increases monotonically with time t. However, if the assigned pressure P is too large, there will be a critical transition time t^* at which

$$\rho\nu \Big| \frac{\partial v(x_2,t^*)}{\partial x_2} \Big|_{x_2=\pm h} = \tau_c \tag{8.16}$$

and this solution no longer applies for $t > t^*$. We next address that possibility.

8.2. Transition to incompatible solutions

If (C2) holds then both of (8.2) are relevant with the understanding that only (8.5) applies for $t < t^*$ and that Γ is determined through the boundary condition $(7.21)_1$ by

$$\Gamma = \begin{cases} 0, & 0 \leq t < t^*, \\ \gamma, & t^* \leq t \leq \infty. \end{cases} \tag{8.17}$$

To analyze the asymptotic behavior of the solution of this problem, we introduce difference fields

$$v_d := v - v_0 \qquad \text{and} \qquad G_d := G - G_0, \tag{8.18}$$

where v_0 and G_0 satisfy

$$\nu \frac{\mathrm{d}^2 v_0}{\mathrm{d}x_2^2} + t^2 \gamma \frac{\mathrm{d}G_0}{\mathrm{d}x_2} + \frac{P}{\rho \ell} = 0 \qquad \text{and} \qquad \kappa \frac{\mathrm{d}^2 G_0}{\mathrm{d}x_2^2} + \gamma \frac{\mathrm{d}v_0}{\mathrm{d}x_2} = 0 \tag{8.19}$$

subject to the boundary conditions

$$v_0(\pm h) = 0 \qquad \text{and} \qquad G_0(\pm h) = 0. \tag{8.20}$$

Consequently, the fields v_0 and G_0 are equivalent to the fully developed steady fields given in (7.24). Following this, the difference fields satisfy

$$\frac{\partial v_d}{\partial t} = \nu \frac{\partial^2 v_d}{\partial x_2^2} + t^2 \gamma \frac{\partial G_d}{\partial x_2} \qquad \text{and} \qquad \frac{\partial G_d}{\partial t} = \kappa \frac{\partial^2 G_d}{\partial x_2^2} + \gamma \frac{\partial v_d}{\partial x_2}. \tag{8.21}$$

subject to boundary conditions

$$v_d(\pm h, t) = 0 \qquad \text{and} \qquad G_d(\pm h, t) = 0, \qquad t \geq t^*, \tag{8.22}$$

along with conditions

$$v_d(x_2, t^*) = v(x_2, t^*) - v_0(x_2) \qquad \text{and} \qquad G_d(x_2, t^*) = -G_0(x_2), \qquad -h \leq x_2 \leq h, \tag{8.23}$$

that apply at the transition time $t = t^*$, namely when, according to (8.16),

$$\rho\nu \Big| \frac{\partial v(x_2,t^*)}{\partial x_2} \Big|_{x_2=\pm h} = \tau_c. \tag{8.24}$$

Multiplying $(8.21)_1$ through by v_d, integrating by parts, and using the homogeneous boundary conditions (8.22) for v_d and G_d, we find that

$$\frac{1}{2}\frac{\mathrm{d}}{\mathrm{d}t}\int_{-h}^{h}|v_d(x_2,t)|^2\,\mathrm{d}x_2 = -\nu\int_{-h}^{h}\Big|\frac{\partial v_d(x_2,t)}{\partial x_2}\Big|^2\,\mathrm{d}x_2 - \iota^2\gamma\int_{-h}^{h}G_d(x_2,t)\frac{\partial v_d(x_2,t)}{\partial x_2}\,\mathrm{d}x_2. \tag{8.25}$$

Similarly, multiplying $(8.21)_2$ through by G_d, integrating by parts, and using the homogeneous boundary conditions $(8.22)_2$ for G_d, we find that

$$\frac{1}{2}\frac{\mathrm{d}}{\mathrm{d}t}\int_{-h}^{h}|G_d(x_2,t)|^2\,\mathrm{d}x_2 = \gamma\int_{-h}^{h}G_d(x_2,t)\frac{\partial v_d(x_2,t)}{\partial x_2}\,\mathrm{d}x_2 - \kappa\int_{-h}^{h}\Big|\frac{\partial G_d(x_2,t)}{\partial x_2}\Big|^2\,\mathrm{d}x_2. \tag{8.26}$$

Thus, multiplying (8.26) by ι^2 and adding the resulting equation to (8.25), we obtain the identity

$$\frac{1}{2}\frac{\mathrm{d}}{\mathrm{d}t}\int_{-h}^{h}(|v_d(x_2,t)|^2+\iota^2|G_d(x_2,t)|^2)\,\mathrm{d}x_2 = -\nu\int_{-h}^{h}\Big|\frac{\partial v_d(x_2,t)}{\partial x_2}\Big|^2\,\mathrm{d}x_2 - \iota^2\kappa\int_{-h}^{h}\Big|\frac{\partial G_d(x_2,t)}{\partial x_2}\Big|^2\,\mathrm{d}x_2. \tag{8.27}$$

Applying the Poincaré inequality to both terms on the right-hand side of (8.27), we next see that

$$\begin{aligned}\frac{\mathrm{d}}{\mathrm{d}t}\int_{-h}^{h}(|v_d(x_2,t)|^2+\iota^2|G_d(x_2,t)|^2)\,\mathrm{d}x_2 &\le -\frac{2\nu}{C}\int_{-h}^{h}\Big|\frac{\partial v_d(x_2,t)}{\partial x_2}\Big|^2\,\mathrm{d}x_2 - \frac{2\kappa}{C}\int_{-h}^{h}\iota^2\Big|\frac{\partial G_d(x_2,t)}{\partial x_2}\Big|^2\,\mathrm{d}x_2\\ &\le -\frac{2\lambda\nu}{C}\int_{-h}^{h}(|v_d(x_2,t)|^2+\iota^2|G_d(x_2,t)|^2)\,\mathrm{d}x_2,\end{aligned} \tag{8.28}$$

where λ is defined by

$$\lambda := \min\Big(1,\frac{\kappa}{\nu}\Big) > 0. \tag{8.29}$$

Finally, multiplying by the integrating factor $2\nu\lambda/C$ on both sides of (8.28), integrating the resulting inequality from the transition time t^* to a generic time $t > t^*$, and applying the transition conditions (8.23) for v_d and G_d, we obtain the inequality

$$\int_{-h}^{h}(|v_d(x_2,t)|^2+\iota^2|G_d(x_2,t)|^2)\,\mathrm{d}x_2 \le \exp\Big(-\frac{2\lambda\nu(t-t^*)}{C}\Big)\int_{-h}^{h}(|v_0(x_2)|^2+\iota^2|G_0(x_2)|^2)\,\mathrm{d}x_2, \tag{8.30}$$

which applies for each $t \ge t^*$ and implies that $|v_d(x_2,t)| = |v(x_2,t)-v_0(x_2)| \to 0$ and $|G_d(x_2,t)| = |G(x_2,t)-G_0(x_2)| \to 0$ as $t\to\infty$ for all x_2 in $(-h,h)$ in the sense of the L^2 norm.

Nominally, we conclude that during the time interval $(0,t^*)$, the spanwise velocity v is laminar and the flow is compatible, meaning that the field $G = 0$. At time t^*, the velocity field satisfies the condition

$$\rho\nu\Big|\frac{\partial v(x_2,t^*)}{\partial x_2}\Big|_{x_2=\pm h} = \tau_c \tag{8.31}$$

and from that time onward the flow is incompatible with $G \neq 0$. As time t progresses, the streamwise velocity v and shear contribution G to the incompatibility field tend monotonically to the steady fully developed expressions given in (7.24).

8.3. Numerical results

For a sufficiently large pressure P the boundary–initial-value problem arising from (8.2)–(8.4) with the pressure given by (8.1) and the condition (8.17) on Γ, there will be a critical transition time t^*, at which (8.16) holds. Thereafter, the solution will change its structure from compatible to incompatible and the criterion (C2) will be in place. We describe the nature of this transition and the settling to a steady state in the following two subsections.

8.3.1. Precursor compatible flow

Here, we consider the solution for $t \in (0,t^*]$, and determine the velocity profile $v(x_2,t^*)$ and the time t^* from

$$\rho\nu\Big|\frac{\partial v(x_2,t^*)}{\partial x_2}\Big|_{x_2=\pm h} = \tau_c, \tag{8.32}$$

both of which will serve as initial conditions for the subsequent incompatible flow that follows.

To render the problem dimensionless, we scale the spanwise coordinate x_2 by the half-width h of the channel and scale the time t by the ratio of h^2 to the kinematic viscosity ν. In parallel with these choices, we scale the streamwise velocity v by

$$\bar v := \frac{\cosh\Omega h - 1}{\Omega h\sinh\Omega h}\frac{Ph^2}{\rho\nu\ell}, \tag{8.33}$$

the maximum value of the dimensionless steady solution $(7.24)_1$, which is natural considering that this precursor flow will be matched to an incompatible flow that will be scaled equivalently. Thus, introducing

$$v^*(y,s) := \frac{v(x_2,t)}{\bar v}, \qquad y := \frac{x_2}{h}, \qquad \text{and} \qquad s := \frac{\nu t}{h^2}, \tag{8.34}$$

we find from (8.2) and (8.17) that $v^\star$ evolves according to

$$\frac{\partial v^*}{\partial s} = \frac{\partial^2 v^*}{\partial y^2} + \frac{\Omega h\sinh\Omega h}{\cosh\Omega h - 1} \tag{8.35}$$

on $-1 < y < 1$ and $s > 0$ subject to the boundary conditions

$$v^*(\pm 1, s) = 0, \qquad s \geq 0, \tag{8.36}$$

and the initial condition

$$v^*(y, 0) = 0, \qquad -1 \leq y \leq 1. \tag{8.37}$$

Taking v^* to be of the form

$$v^*(y, s) = u(y, s) + \frac{1}{2}\frac{\Omega h \sinh \Omega h}{\cosh \Omega h - 1}(1 - y^2), \tag{8.38}$$

we find from (8.35)–(8.37) that u must satisfy the homogeneous partial-differential equation

$$\frac{\partial u}{\partial s} = \frac{\partial^2 u}{\partial y^2} \tag{8.39}$$

for $-1 < y < 1$ and $s > 0$, the boundary conditions

$$u(\pm 1, s) = 0, \qquad s \geq 0, \tag{8.40}$$

and the initial condition

$$u(y, 0) = -\frac{1}{2}\frac{\Omega h \sinh \Omega h}{\cosh \Omega h - 1}(1 - y^2), \qquad -1 \leq y \leq 1. \tag{8.41}$$

Using standard techniques from Fourier analysis, we find that the solution u of (8.39)–(8.41) admits a representation of the form

$$u(y, s) = \frac{4\Omega h \sinh \Omega h}{\cosh \Omega h - 1} \sum_{n=1}^{\infty} \frac{2(\cos n\pi - 1) + n\pi \sin n\pi}{n^3 \pi^3} \sin\Big(\frac{n\pi(1 + y)}{2}\Big) \exp\Big(-\frac{n^2 \pi^2 s}{4}\Big) \tag{8.42}$$

for $-1 \leq y \leq 1$ and $s \geq 0$. However, by virtue of the identity

$$2(\cos n\pi - 1) + n\pi \sin n\pi = \begin{cases} -4, & \text{if } n \text{ is odd,} \\ 0, & \text{if } n \text{ is even,} \end{cases} \tag{8.43}$$

we see that (8.42) simplifies to

$$u(y, s) = -\frac{\Omega h \sinh \Omega h}{\cosh \Omega h - 1} \sum_{n=1}^{\infty} \frac{16}{(2n - 1)^3 \pi^3} \sin\Big(\frac{(2n - 1)\pi(1 + y)}{2}\Big) \exp\Big(-\frac{(2n - 1)^2 \pi^2 s}{4}\Big). \tag{8.44}$$

Thus, by (8.38), v^* is given by

$$v^*(y, s) = \frac{\Omega h \sinh \Omega h}{\cosh \Omega h - 1}\Big(\frac{1 - y^2}{2} - \sum_{n=1}^{\infty} \frac{16}{(2n - 1)^3 \pi^3} \sin\Big(\frac{(2n - 1)\pi(1 + y)}{2}\Big) \exp\Big(-\frac{(2n - 1)^2 \pi^2 s}{4}\Big)\Big), \tag{8.45}$$

for $-1 \leq y \leq 1$ and $s \geq 0$. Hence, it follows that

$$\frac{\partial v^*(y, s)}{\partial y} = -\frac{\Omega h \sinh \Omega h}{\cosh \Omega h - 1}\Big(y + \sum_{n=1}^{\infty} \frac{8}{(2n - 1)^2 \pi^2} \cos\Big(\frac{(2n - 1)\pi(1 + y)}{2}\Big) \exp\Big(-\frac{(2n - 1)^2 \pi^2 s}{4}\Big)\Big), \tag{8.46}$$

for $-1 \leq y \leq 1$ and $s \geq 0$, from which we determine

$$\Big|\frac{\partial v^*(y, s)}{\partial y}\Big|_{y=\pm 1} = \frac{\Omega h \sinh \Omega h}{\cosh \Omega h - 1}\Big(1 - \sum_{n=1}^{\infty} \frac{8}{(2n - 1)^2 \pi^2} \exp\Big(-\frac{(2n - 1)^2 \pi^2 s}{4}\Big)\Big), \tag{8.47}$$

for $s \geq 0$.

Now, using (8.33) and (8.34) we see that

$$\Big|\frac{\partial v^*(y, s)}{\partial y}\Big| = \Big|\frac{\partial v(x_2, t)}{\partial x_2}\Big| \frac{\Omega h \sinh \Omega h}{\cosh \Omega h - 1} \frac{\varrho v \ell}{Ph}, \tag{8.48}$$

and we find from (8.32) that

$$\Big|\frac{\partial v^*(y, s^*)}{\partial y}\Big|_{y=\pm 1} = \frac{\Omega h \sinh \Omega h}{\cosh \Omega h - 1} \frac{\tau_c \ell}{Ph}, \tag{8.49}$$

where $s^* := vt^*/h^2$. So, to determine the dimensionless critical time s^* (and, thus, its dimensional counterpart $t^* = h^2 s^*/v$), we see from (8.47) that

$$\frac{8}{\pi^2} \sum_{n=1}^{\infty} \frac{1}{(2n - 1)^2} \exp\Big(-\frac{(2n - 1)^2 \pi^2 s^*}{4}\Big) = 1 - \frac{\tau_c \ell}{Ph}, \tag{8.50}$$

where the dimensionless quantity $\tau_c \ell / Ph$ is to be specified and must be less than unity.

It is convenient, and also representative of the general character of this solution, to set

$$\frac{\tau_c \ell}{Ph} = \frac{2(\cosh \Omega h - 1)}{\Omega h \sinh \Omega h}, \tag{8.51}$$

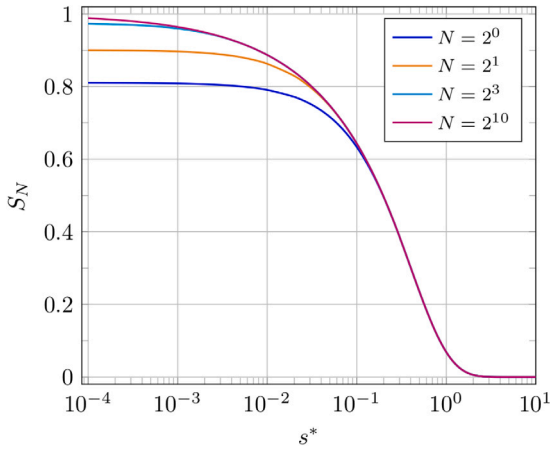

Fig. 5. Plots of the partial sum S_N defined in (8.53) for $N = 1$, $N = 2$, $N = 8$, and $N = 1024$.

Table 1
Values of the dimensionless critical time s^* determined from solving $S_8 = 1 - \tau_c \ell / Ph$, S_N being defined by (8.53), for the Ωh used in Figs. 1 and 4.

Ωh	s^*
0.01	4.66×10^{1}
1.50	6.80×10^{0}
2.50	3.75×10^{-1}
4.00	1.83×10^{-1}
6.00	8.64×10^{-2}
10.0	3.14×10^{-2}

in which case the right-hand side is less than unity for representative values of the dimensionless number Ωh, as we shall see. Referring to the expressions (7.23) and $(7.24)_1$, we observe that, along the midline $x_2 = 0$ of the channel, the ratio of the steady-state velocity $v(0)$ to the corresponding compatible quantity $V(0) = Ph^2/2\rho\nu\ell$ obeys

$$\frac{v(0)}{V(0)} = \frac{2(\cosh \Omega h - 1)}{\Omega h \sinh \Omega h}. \tag{8.52}$$

Given a value of $\tau_c \ell / Ph$ satisfying $\tau_c \ell / Ph < 1$, we hence determine from (8.50) both Ωh and the foregoing ratio. From plots of the partial sum

$$S_N = \frac{8}{\pi^2} \sum_{n=1}^{N} \frac{1}{(2n-1)^2} \exp\Big(-\frac{(2n-1)^2 \pi^2 s^*}{4}\Big) \tag{8.53}$$

versus s^* for select choices of N in Fig. 5, we see that S_8 provides an excellent approximation for the left-hand side of (8.50) for $s^* > 1.50 \cdot 10^{-3}$. Select values of s^* determined from solving $S_8 = 1 - \tau_c \ell / Ph$ are given in Table 1.

8.3.2. *Incompatible flow and transition to steady state*

We next consider the boundary–initial-value problem arising from (8.2)–(8.4) for $t > t^*$ with the initial instant t^* determined in terms of Ωh by (8.50) and (8.51) with $t^* = h^2 s^*/\nu$, the pressure given by (8.1), and criterion (C2) in place. Again, to render the problem dimensionless, we scale the spanwise coordinate x_2 by the half-width h of the channel, as we did above, and scale the time t by the ratio of h^2 to the kinematic viscosity ν, while, for the purposes of this subsection, shifting time forward by the critical transition time t^*. In parallel with these choices, we scale the streamwise velocity v the same as in Section 8.3.1 and we scale the shear contribution G to the incompatibility tensor according to

$$\bar{v} := \frac{\cosh \Omega h - 1}{\Omega h \sinh \Omega h} \frac{Ph^2}{\rho \nu \ell} \qquad \text{and} \qquad \bar{G} := \frac{\cosh \Omega h - 1}{\Omega h \sinh \Omega h} \frac{Ph}{\rho \ell^2 \gamma \ell}, \tag{8.54}$$

respectively. As in Section 8.3.1, $\bar{v}$ is the maximum value of the dimensionless steady solution $(7.24)_1$ and is thus natural, and we choose $\bar{G}$ to simplify the final governing equations. Thus, in this subsection we introduce

$$v^*(y,s) := \frac{v(x_2,t)}{\bar{v}}, \qquad G^*(y,s) := \frac{G(x_2,t)}{\bar{G}}, \qquad \text{for } y := \frac{x_2}{h} \text{ and } s := \frac{\nu(t-t^*)}{h^2}, \tag{8.55}$$

and we find from (8.2) and (8.17) that v^* and G^* evolve according to

$$\frac{\partial v^*}{\partial s} = \frac{\partial^2 v^*}{\partial y^2} + \frac{\partial G^*}{\partial y} + \frac{\Omega h \sinh \Omega h}{\cosh \Omega h - 1} \qquad \text{and} \qquad \frac{\partial G^*}{\partial s} = \frac{\kappa}{\nu}\Big(\frac{\partial^2 G^*}{\partial y^2} + \Omega^2 h^2 \frac{\partial v^*}{\partial y}\Big) \tag{8.56}$$

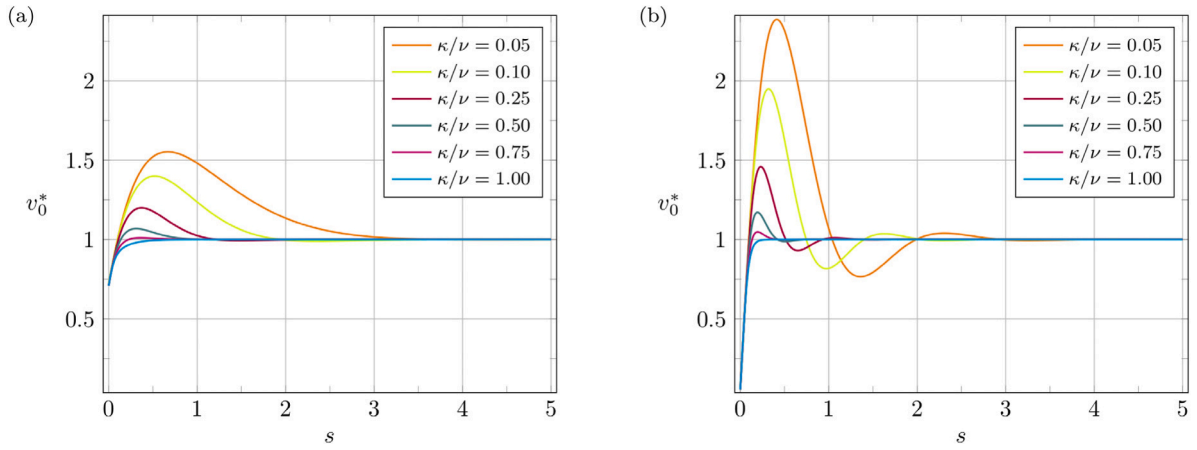

Fig. 6. Plots of the restriction v_0^* of the dimensionless velocity defined in (8.63) for two representative values, (a) $\Omega h = 4.00$ and (b) $\Omega h = 10.0$, of the dimensionless wavenumber Ωh and six representative values, $\kappa/\nu = 0.05$, $\kappa/\nu = 0.10$, $\kappa/\nu = 0.25$, $\kappa/\nu = 0.50$, $\kappa/\nu = 0.75$, and $\kappa/\nu = 1.00$, of the ratio of diffusivity κ to the kinematic viscosity ν.

for $s > 0$. We emphasize that the appropriate initial condition at $s = 0$ for determining the solution v^* is given by (8.45) evaluated at $s = s^*$, where s^* is determined in terms of Ωh from (8.50) and (8.51). Thus, in line with (8.3) and (8.4), we solve the system (8.56) numerically for $-1 < y < 1$ and $s > 0$ subject to the homogeneous boundary conditions

$$v^*(\pm 1, s) = 0 \qquad \text{and} \qquad G^*(\pm 1, s) = 0, \qquad s \geq 0, \tag{8.57}$$

along with the initial conditions

$$v^*(y, 0) = \frac{\Omega h \sinh \Omega h}{\cosh \Omega h - 1}\Big(\frac{1 - y^2}{2} - \sum_{n=1}^{\infty} \frac{16}{(2n-1)^3 \pi^3} \sin\Big(\frac{(2n-1)\pi(1+y)}{2}\Big) \exp\Big(-\frac{(2n-1)^2 \pi^2 s^*}{4}\Big)\Big) \tag{8.58a}$$

and

$$G^*(y, 0) = 0, \qquad -1 \leq y \leq 1, \tag{8.58b}$$

where s^* is determined in terms of Ωh from (8.50) and (8.51). In view of the results of Section 8.2 and the scaling (8.54)–(8.55), v^* and G^* must approach the corresponding dimensionless quantities from the solution to the steady-state problem as $s \to \infty$:

$$\left.\begin{aligned} \lim_{s\to\infty} v^*(y, s) &= 1 - \frac{1 - \cosh \Omega h y}{1 - \cosh \Omega h}, \\ \lim_{s\to\infty} G^*(y, s) &= \frac{\Omega h \sinh \Omega h}{\cosh \Omega h - 1}\Big(\frac{\sinh \Omega h y}{\sinh \Omega h} - y\Big). \end{aligned}\right\} \tag{8.59}$$

Thus, in particular, we have that

$$\lim_{s\to\infty} v^*(0, s) = 1, \tag{8.60}$$

or, equivalently, in terms of dimensional quantities and consistent with the relation (8.52) determining the ratio of the steady-state velocity $v(0)$ to the corresponding compatible quantity $V(0) = Ph^2/2\rho\nu\ell$,

$$\lim_{t\to\infty} \frac{v(0, t)}{V(0)} = \frac{2(\cosh \Omega h - 1)}{\Omega h \sinh \Omega h}. \tag{8.61}$$

The boundary–initial-value problem (8.56)–(8.58) involves two dimensionless parameters: the ratio κ/ν of the diffusivity associated with incompatibility transport to the kinematic viscosity ν and the dimensionless wavenumber Ωh. If $\kappa < \nu$, it follows from the decay relation (8.30) that the dimensionless time required for the system to reach steady state must decrease monotonically with increasing κ/ν. Otherwise, if $\kappa > \nu$, it follows from (8.30) that conventional viscous effects dominate the evolution toward steady state. To explore the competition between such effects and the transport of incompatibility, we therefore restrict attention to situations in which κ and ν satisfy

$$0 < \frac{\kappa}{\nu} \leq 1. \tag{8.62}$$

Details of the scheme used to construct approximate numerical solutions of (8.56)–(8.58) are provided as Supplementary Information.

Fig. 6 contains plots of the dimensionless midline velocity v_0^*, as defined by

$$v_0^*(s) := v^*(0, s), \qquad s \geq 0, \tag{8.63}$$

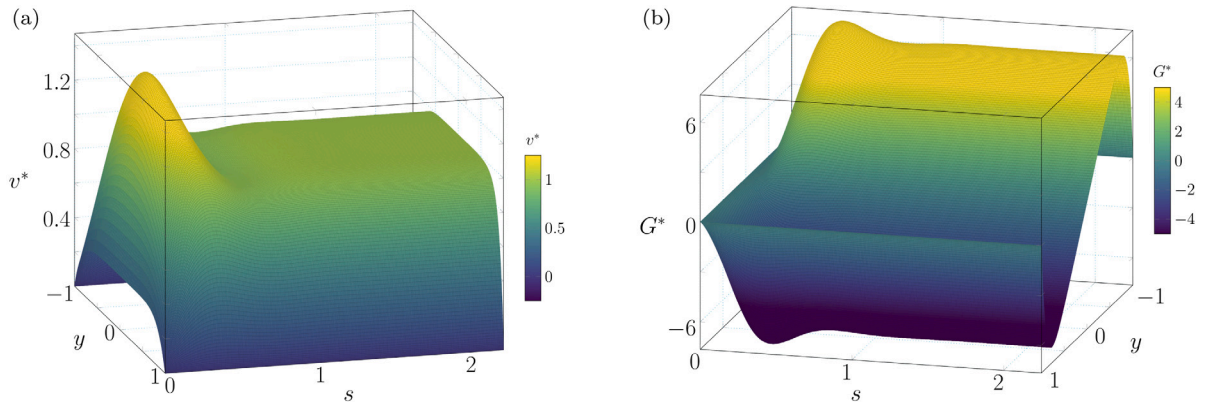

Fig. 7. Plots of (a) the dimensionless velocity v^* and (b) the dimensionless shear contribution G^* to the incompatibility tensor for $\kappa/\nu = 0.25$ and $\Omega h = 10.0$.

for $0 \leq s \leq 2.5$ and representative choices of κ/ν and Ωh. In each plot, v_0^* grows initially from its initial value $v_0^*(0) = v^*(0,0)$, as determined from the first of (8.58) in response to the initially imposed pressure for the precursor compatible flow. The effects shown in these plots hinge upon the coupling between v^* and G^* in the system (8.56). After reaching a maximum value, v_0^* eventually achieves the value $v_0^* = 1$ corresponding to setting $y = 0$ in the dimensionless steady state solution (7.42). For both choices of Ωh presented here and κ/ν sufficiently small, v_0^* decreases from its maximum to a minimum value below the asymptotic limit $v_0^* = 1$ and this mildly oscillatory pattern repeats at least once more before steady state is achieved.[15] If κ/ν is sufficiently large, however, v_0^* decreases monotonically from its maximum value to unity without oscillating. Consistent with the decay relation (8.30), the dimensionless time elapsed toward reaching steady state decreases as κ/ν increases and simulations performed for other choices of κ/ν show that this trend is monotonic. Comparing the plots for $\Omega h = 4.0$ and $\Omega h = 10.0$, we see that the maxima of v_0^* increase with Ωh and an analogous comment applies to the minima that are exhibited during the oscillations that occur for sufficiently small values of κ/ν. Moreover, simulations performed for other choices of Ωh show that these trends are monotonic.

Fig. 7 shows the dimensionless velocity v^* and the dimensionless shear contribution to the incompatibility field G^* for $\kappa/\nu = 0.25$ and $\Omega h = 10.0$ up to $s = 2.25$, at which steady state appears to have been attained. The plot of v^* starts at $s = 0$ with the initial values given by the first of (8.58), which is flat-looking except near the channel walls at which it must be zero. The precursor surface is not shown, but in terms of the dimensionless time s, consistent with the entry of Table 1 corresponding to $\Omega h = 10.0$, that surface begins on this figure at $s \approx -3.14 \cdot 10^{-2}$. As the dimensionless velocity v^* begins to grow with the dimensionless time s, it rapidly changes to a more parabolic-like character with the central portion losing its bluntness while it is peaking, followed by a smooth drop as a growing central portion of relative bluntness spreads outward toward the channel walls with increasing s. The initial parabolic-like growth in the central portion appears to be driven by the effects of viscosity as if incompatibility was not present and this must be due to the low value of diffusivity κ relative to viscosity ν. As s increases further, these formative effects result in a steady shape at $s = 2.5$ which, consistent with the steady solution $(7.24)_1$ and the velocity profile for $\Omega h = 10.0$ shown in Fig. 1(a), resembles a plug-like flow that smoothly attaches to the channel walls. The surface undergoes local structural changes that accompany this process and that are related to the kinematic viscosity and the diffusivity associated with the transport of incompatibility, both of which contribute coincidently and interactively to the dissipation of energy. These are manifested in the oscillating, undulating and blunting features that appear during the recovery that takes place following the initial burst to peak level.

The plot of G^*, shown in Fig. 7, also exhibits the early growth of initial peaks and subsequent oscillations before steady state is achieved consistent with $(7.24)_2$. This plot illustrates that as s increases the growth of incompatibility is mostly concentrated in narrow zones near the channel walls, with the two peaks in G^* appearing somewhat later than the peak in v^*. This gives evidence that for the choice $\kappa/\nu = 0.25$ the initial response of the system is dominated by viscous action and the rapid growth of the dimensionless velocity profile is momentarily unabated as if no incompatibility were present in the flow. However, as the incompatibility G^* grows and diffuses and is realized through its contribution to the changing stress field, it has the effect to draw down and to flatten the profile v^*, perhaps too quickly, which results in a slight undulation and oscillation of the surface as it reaches its steady form. Of course, the size of the diffusivity κ relative to the kinematic viscosity ν plays a central role in the details of this process.

Additional plots of v^* and G^* for the choices $\Omega h = 4.00$ and $\Omega h = 10.0$ of the dimensionless wavenumber Ωh and the values, $\kappa/\nu = 0.05$, $\kappa/\nu = 0.10$, $\kappa/\nu = 0.25$, $\kappa/\nu = 0.50$, $\kappa/\nu = 0.75$, and $\kappa/\nu = 1.00$, of the ratio κ/ν used in Fig. 6 are included in the Supplementary Information. From these plots, it is evident that for small values of Ωh the precursor laminar flow is well developed and almost parabolic before incompatibilities begin to have an effect and, consistent with Fig. 2 of the manuscript, the plug-like steady state is not as noticeable. As the diffusivity κ associated with incompatibility increases relative to the kinematic viscosity ν,

[15] Viscoelastic models for polymeric fluids predict initial bursts, followed by damped oscillations, a quiescent polymeric fluid in a channel or pipe that is suddenly subjected to a constant pressure drop, as predicted by viscoelastic models (Akyildiz & Jones, 1993; Chong & Franks, 1970a, 1970b; Fielder & Thomas, 1967; Fong, 1972; Waters & King, 1970).

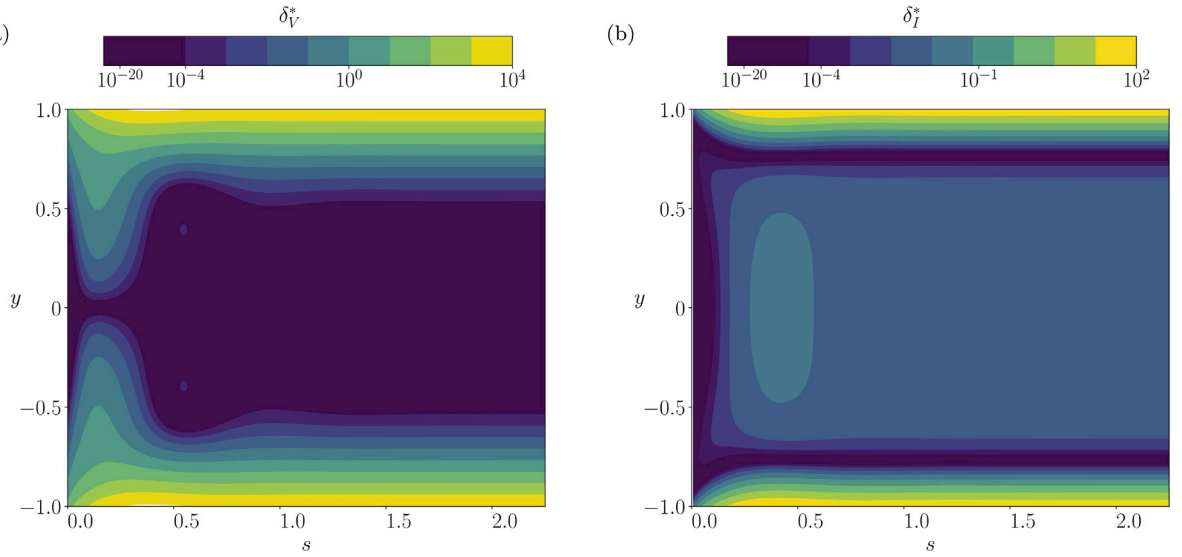

Fig. 8. Plots of the isoclines of (a) the dimensionless specific viscous dissipation δ_V^* and (b) the dimensionless specific incompatibility dissipation δ_I^*, defined in (8.66), for $\kappa/\nu = 0.25$ and $\Omega h = 10.0$.

the initial peaks and undulations of v^* and G^* in these plots diminish, consistent with a previous observation. The incompatibility in the boundary layers evidenced in the plots of G^* tends to concentrate closer to the walls as κ/ν increases. For sufficiently small values of Ωh, the tendency for incompatibility to concentrate near the walls appears to diminish the blunting of the velocity profiles seen in the plots of v^*. However, the decreasing thickness of the boundary layers and enhanced blunting of the velocity profiles that occurs as Ωh increases becomes compatible with the enhanced concentration of incompatibility near the walls as κ/ν increases.

The effects of kinematic viscous dissipation and the dissipation due to incompatibility appear to play a synergistic role in structuring the dimensionless velocity profile. To support this conjecture quantitatively, we first note, from (4.14) and the transient version of the Poiseuille flow problem as formulated at the beginning of Section 8, that the specific dissipation δ is given by

$$\delta(x_2,t) = \nu\Big|\frac{\partial v(x_2,t)}{\partial x_2}\Big|^2 + \iota^2\kappa\Big|\frac{\partial G(x_2,t)}{\partial x_2}\Big|^2. \tag{8.64}$$

Using the definitions of y, s, $v^\star$, and G^* in (8.55), we then find that

$$\delta(x_2,t)\Big|_{(x_2,t)=(hy,vs/h^2)} = \frac{\nu\bar{v}^2}{h^2}\Big(\Big|\frac{\partial v^\star(t,s)}{\partial y}\Big|^2 + \frac{1}{\Omega^2h^2}\Big|\frac{\partial G^\star(t,s)}{\partial y}\Big|^2\Big), \quad -1 \le y \le 1, \quad s \ge 0. \tag{8.65}$$

In Fig. 8, we plot the isoclines for the dimensionless specific viscous dissipation δ_V^* and the dimensionless specific incompatibility dissipation δ_I^*, as defined by

$$\delta_V^*(y,s) := \Big|\frac{\partial v^*(t,s)}{\partial y}\Big|^2 \qquad \text{and} \qquad \delta_I^*(y,s) := \frac{1}{\Omega^2h^2}\Big|\frac{\partial G^*(t,s)}{\partial y}\Big|^2, \quad -1 \le y \le 1, \quad s \ge 0. \tag{8.66}$$

Consistent with these definitions, we then see that the dimensionless specific dissipation δ^* is related to the specific dissipation δ through

$$\delta^* = \frac{h^2\delta}{\nu\bar{v}^2} = \delta_V^* + \delta_I^*. \tag{8.67}$$

It is apparent in Fig. 8 that the isoclines for δ_V^* which correspond to low dissipation are tending to converge at the center of the channel $y = 0$ at $s \approx 0.2$, which correlates well not only with the time corresponding to the peak of v^* in Fig. 7, but also with the very low value of the corresponding isocline for $\delta_I^* \approx 0.01$. As s increases, the isoclines for δ_I^* slightly rise and fall in a central portion of the channel which contains an elliptically shaped isocline. Correspondingly, low dimensionless specific viscous dissipation is maintained in this portion while a noticeable growth of δ_V^* is rapidly diffused toward the boundaries. It is within the elliptical shaped region on the plot of the dimensionless specific incompatibility dissipation δ_I^* that we see that v^* undulates below its steady state value on Fig. 7. Thus, it appears that the transport of incompatibility into this region and the related increase in its dissipation play an important part in the adjustments that the velocity profile undergoes shortly after it reaches its peak value. It is clear from Fig. 8 that as s increases, δ_V^* and δ_I^* are both mostly present near the walls of the channel. However, there are subtle differences in the formation and persistence of these two boundary layer dissipation zones that play a part in the formation of the dimensionless velocity profile v^*, especially in the central portion of the channel. A point of interest is that Fig. 8 shows a distinct thin valley on the dimensionless specific incompatibility dissipation surface δ_I^* that forms early during the transition process to steady state, and it contains a zero isocline which may tend to regulate the adjustments that take place between the two forms of dissipation in the

interior of the channel as they seek a combined steady state of minimal dimensionless specific dissipation δ^*. This isocline separates the strong dissipative effect of the boundary from the weaker, but active, dimensionless specific incompatibility dissipation δ_I^* that is present in the interior of the channel, and that is actively compensating with the dimensionless specific viscous dissipation δ_V^* to flatten the velocity profile. Contrary to the isoclines for δ_I^*, the isoclines for δ_V^* in Fig. 8 are not bounded in the interior of the flow domain by a zero isocline that would promote interior adjustments apart from the boundary effect; $\delta_V^* = 0$ at the midline $y = 0$ of the flow region.

9. Discussion

This work is driven by the idea that during a flow the stretching and/or the shearing of fluid material filaments can sustain only a limited magnitude before the distortion rate $\boldsymbol{L}$, which determines the instantaneous smooth local geometric temporal change in the local arrangement of material particles, develops an incompatible component $\boldsymbol{\Lambda}$. When this occurs, $\boldsymbol{L}$, which is faithfully determined as the spatial gradient of the velocity $\boldsymbol{v}$, develops a component $\boldsymbol{\Lambda}$ which is not determined as the gradient of a vector field and, therefore, is incompatible. To characterize this incompatibility, we introduce the incompatibility $\boldsymbol{G} = -\operatorname{curl}\boldsymbol{\Lambda}$, being zero when $\boldsymbol{\Lambda}$ is a gradient and otherwise nominally non-zero. Thus, from the mechanics point of view, the two main fields that describe the fluid motion are $\boldsymbol{v}$ and $\boldsymbol{G}$, and we develop a physical theory for the balance laws which govern these fields.

The classical balance laws of mass, momentum, and moment of momentum for a material region $\mathcal{P}_t$ form an important part of the system of governing equations, and they, of course, introduce the fundamental unknown fields of specific mass density and the Cauchy stress tensor. We restrict attention to homogeneous and incompressible fluids, so that the mass density ϱ is constant and the velocity $\boldsymbol{v}$ is solenoidal.

Consistent with the role of the incompatibility $\boldsymbol{G}$ as an additional independent kinematical descriptor, we propose a balance law for the incompatibility $\boldsymbol{G}$ which balances the total rate of change of $\boldsymbol{G}$ in a material region $\mathcal{P}_t$ against the advective and diffusive transfer through its boundary together with a possible volumetric external rate of supply of incompatibility. This balance law requires the introduction of an unknown incompatibility diffusion flux $\boldsymbol{J}$, a third order tensor, which accounts for the surfacial diffusive transfer of incompatibility on $\partial\mathcal{P}_t$ and which, from a mechanics point of view, ultimately will require a constitutive relation expressed in terms of the fundamental kinematical descriptors $\boldsymbol{v}$ and $\boldsymbol{G}$. This balance law includes the possibility of an a priori specified volumetric external rate of supply. We show how this balance law may be recast equivalently as a surfacial balance law for an arbitrary material surface including the advective and diffusive transfer which associates with its edge. Fundamentally, a surfacial balance law expressing incompatibility for arbitrary material surfaces is to be expected because it follows from Stokes' theorem that the integral of $\boldsymbol{Gm}$ over a material surface whose oriented normal is $\boldsymbol{m}$ will vanish if $\boldsymbol{\Lambda}$ is a gradient — otherwise, when the incompatibility tensor $\boldsymbol{G}$ is nominally non-zero on that material surface, it is expected to generate incompatibility in time according to advective and diffusive transfer and external flux contribution.

An additional element of the governing balance equations is the balance of energy for a material region $\mathcal{P}_t$. For this, the rate of change of the internal energy plus the two kinetic energies, one due to the velocity $\boldsymbol{v}$ and the other due the incompatibility $\boldsymbol{G}$, of the region are balanced against the classical contributions associated with the power expended by external mechanical actions and with the energy transfers that accompany the flux and external radiative supply of heat to the region plus nonclassical contributions associated with the energy transfers that accompany the flux and external supply of incompatibility to the region. The expression for the energy transfers associated with incompatibility requires the introduction of a tensor $\boldsymbol{\Pi}$ which serves as a chemical potential for incompatibility and which is conjugate to both the surfacial incompatible diffusion flux and the external rate of supply of incompatibility.

The second law of thermodynamics in the form of the Clausius–Duhem inequality serves to identify the general dissipation inequality that is necessary for any acceptable constitutive theory and thermodynamic process. We then restrict our theory to isothermal processes, and propose a natural elementary constitutive structure for the Cauchy stress $\boldsymbol{T}$, the tensorial chemical potential $\boldsymbol{\Pi}$ for incompatibility, and the incompatibility diffusion flux $\boldsymbol{J}$ in terms of the descriptor fields $\boldsymbol{v}$ and $\boldsymbol{G}$. The constitutive relation for $\boldsymbol{J}$ introduces the diffusivity $\kappa > 0$ associated with the transport of incompatibility. A novel aspect of the Cauchy stress is that, aside from the non-constitutive constraint reaction part, there are two additional terms; one corresponds to the usual viscosity contribution related to the velocity $\boldsymbol{v}$, and the other is an incompatibility stress due to the incompatibility $\boldsymbol{G}$. This latter novel stress term not only contributes to the total shear stress but also accounts for a normal stress effect due to incompatibility. This structure, together with the balance laws of momentum, moment of momentum and incompatibility tensor field leads to the two final mixed system (5.1) and (5.2) of governing equations for $\boldsymbol{v}$ and $\boldsymbol{G}$: (i) The flow equation (5.1) represents a generalized version of the Navier–Stokes equation which contains the additional divergence of an incompatibility stress tensor field; (ii) The evolution equation (5.2) for the incompatibility tensor field. For this theory, the dissipation reduces to the sum of two positive terms, one being of the usual form, quadratic in the stretching tensor and containing the kinematic viscosity $\nu > 0$, and the other being quadratic in the gradient $\operatorname{grad}\boldsymbol{G}$ of the incompatibility tensor $\boldsymbol{G}$ and containing the diffusivity κ associated with the transport of incompatibility.

After a discussion of boundary conditions for $\boldsymbol{v}$ and $\boldsymbol{G}$ in Section 6, wherein we express that incompatibility enters a flow domain through its fixed boundary when a given critical wall shear stress is exceeded, we analyze in Sections 7.1–7.4 the classical problem of steady plane Poiseuille flow. We find that if the constant pressure gradient that drives the flow is below a certain level there is no incompatibility generated ($\boldsymbol{G} = \boldsymbol{0}$) and the velocity $\boldsymbol{v}$ has the classical parabolic profile. Above this level, at which the critical wall shear stress is exceeded, the flow becomes incompatible with $\boldsymbol{G} \neq \boldsymbol{0}$. In Section 7.5, we discuss physical considerations that dictate the size of Ωh, which should be small if incompatibility plays a minor role but large otherwise. In Section 7.6, we display the results of our analysis in dimensionless graphical form beginning with the observation that the incompatibility $\boldsymbol{G}$ shows its greatest

effect near the channel walls, tending to blunt the velocity field from its parabolic form. Other quantities fixed, this blunting is shown to be more pronounced the greater is the kinematic viscosity ν relative to the diffusivity κ associated with the transport of incompatibility. Correspondingly, for this scenario the quantity of flow rate is reduced, meaning that as incompatibility increases a larger pressure drop is required to maintain a given flow rate. For incompatible flow, the shear stress has two additive components, one due to the effect of viscosity and the other due to the effect of incompatibility, both being odd about the centerline of the flow domain. For large kinematic viscosity ν relative to diffusivity κ, that part of the shear stress due to viscous effects nearly vanishes outside of boundary layers near the walls and that part of the magnitude of the shear stress due to incompatibility exhibits absolute maxima near the walls. In addition, there is a significant streamwise normal stress effect that is due solely to incompatibility. Finally, we show that the dissipation for this Poiseuille flow is generally concentrated near the channel walls, the concentration becoming more pronounced for large ν relative to κ.

In Section 8 we study the dynamical transition of Poiseuille channel flow from rest to steady state, driven by the initial application of a pressure drop at a generic section of the channel which is thereafter held fixed. After setting up the related dynamical problem, we first show, in Sections 8.1 and 8.2, how the square integral norms of $\boldsymbol{v}$ and $\boldsymbol{G}$ exponentially limit to the steady fully developed forms as given in Section 7. The exponential decay rate that we find depends upon $\nu \min\{1, \kappa/\nu\}$, so the overall transition process is expected to be governed by the weaker of the two forms of diffusive transport. Then, in Section 8.3 we mostly concentrate on numerical results which illustrate in some detail how the velocity $\boldsymbol{v}$ and the incompatibility $\boldsymbol{G}$ are structured by diffusion and dissipation in the channel during the transition process. As the flow starts, there is a precursor laminar flow that develops until a particular time at which the wall shear stress becomes equal to an a priori given cut-off value at which incompatibility forms at the walls of the channel and begins to diffuse inward. The velocity profile at that critical time is obtained in Section 8.3.1 and it serves as an initial condition for determining, in Section 8.3.2, the velocity and incompatibility fields as time progresses. The numerical results are presented graphically and, as we discuss, the physical effects of diffusion and dissipation are found to be important synergistic elements in the formation process.

Certain features of the solutions of the steady and transient problems considered in Sections 7 and 8 resemble results from established theories for laminar flows of non-Newtonian fluids and turbulent flows of incompressible Newtonian fluids. These similarities are suggestive of connections that we find intriguing and plan to pursue in future works.

Acknowledgments

We are grateful to Luis Espath for providing crucial advice and assistance toward obtaining our numerical results and for help with plotting Fig. 7 and to Adel Sarmiento for his help with plotting Fig. 8. E.F. gratefully acknowledges support from the Okinawa Institute of Science and Technology Graduate University, Japan with subsidy funding from the Cabinet Office, Government of Japan.

Appendix A

All fields considered below are assumed to be as smooth as necessary to ensure the existence of indicated derivatives.

A.1. Vector and tensor identities

In addition to vectors, we consider second- and third-order tensors. Given a vector $\boldsymbol{a}$, the second-order tensor $\boldsymbol{a}\times$ is defined such that, for any vector $\boldsymbol{b}$,

$$(\boldsymbol{a}\times)\boldsymbol{b} = \boldsymbol{a}\times\boldsymbol{b}. \tag{A.1}$$

Since, by (A.1), the definition of the transpose of a second-order tensor, and the properties of the cross-product of two vectors, we have

$$\boldsymbol{c}\cdot((\boldsymbol{a}\times)^{\top}\boldsymbol{b}) = \boldsymbol{b}\cdot((\boldsymbol{a}\times)\boldsymbol{c}) = \boldsymbol{b}\cdot(\boldsymbol{a}\times\boldsymbol{c}) = -\boldsymbol{b}\cdot(\boldsymbol{c}\times\boldsymbol{a}) = -\boldsymbol{c}\cdot(\boldsymbol{a}\times\boldsymbol{b}) = -\boldsymbol{c}\cdot((\boldsymbol{a}\times)\boldsymbol{b}) \tag{A.2}$$

for every pair of vectors $\boldsymbol{b}$ and $\boldsymbol{c}$, then it follows that $\boldsymbol{a}\times$ must be skew:

$$(\boldsymbol{a}\times)^{\top} = -\boldsymbol{a}\times. \tag{A.3}$$

Thus, using (A.1) we have

$$(\boldsymbol{c}\times)(\boldsymbol{a}\times)\boldsymbol{b} = (\boldsymbol{c}\times)(\boldsymbol{a}\times\boldsymbol{b}) = \boldsymbol{c}\times(\boldsymbol{a}\times\boldsymbol{b}) = ((\boldsymbol{a}\otimes\boldsymbol{c}) - \boldsymbol{1}(\boldsymbol{a}\cdot\boldsymbol{c}))\boldsymbol{b}, \tag{A.4}$$

and applying (A.3) we obtain

$$(\boldsymbol{c}\times)^{\top}(\boldsymbol{a}\times) = -(\boldsymbol{c}\times)(\boldsymbol{a}\times) = (\boldsymbol{a}\otimes\boldsymbol{c}) - \boldsymbol{1}(\boldsymbol{a}\cdot\boldsymbol{c}) \qquad \Longrightarrow \qquad (\boldsymbol{c}\times)\cdot(\boldsymbol{a}\times) = 2\boldsymbol{a}\cdot\boldsymbol{c}. \tag{A.5}$$

To every second-order tensor $\boldsymbol{A}$, there thus corresponds a vector $\boldsymbol{a}$, called the axial vector of $\boldsymbol{A}$, defined such that

$$\boldsymbol{A} - \boldsymbol{A}^{\top} = \boldsymbol{a}\times. \tag{A.6}$$

In particular, given vectors $\boldsymbol{a}$ and $\boldsymbol{b}$, it follows that

$$\boldsymbol{a}\otimes\boldsymbol{b} - \boldsymbol{b}\otimes\boldsymbol{a} = (\boldsymbol{b}\times\boldsymbol{a})\times, \tag{A.7}$$

which, with (A.5) and (A.3), shows that

$$(\boldsymbol{c}\times)\cdot(\boldsymbol{a}\otimes\boldsymbol{b})=\boldsymbol{c}\cdot(\boldsymbol{b}\times\boldsymbol{a}). \tag{A.8}$$

Moreover, a second-order tensor $\boldsymbol{A}$ with axial vector $\boldsymbol{a}$ can be expressed as the sum,

$$\boldsymbol{A}=\operatorname{sym}(\boldsymbol{A}-\tfrac{1}{3}(\operatorname{tr}\boldsymbol{A})\boldsymbol{1})+\tfrac{1}{3}(\operatorname{tr}\boldsymbol{A})\boldsymbol{1}+\tfrac{1}{2}\boldsymbol{a}\times, \tag{A.9}$$

of a traceless symmetric component $\operatorname{sym}(\boldsymbol{A}-\frac{1}{3}(\operatorname{tr}\boldsymbol{A})\boldsymbol{1})$, a spherical component $\frac{1}{3}(\operatorname{tr}\boldsymbol{A})\boldsymbol{1}$, and a skew component $\frac{1}{2}\boldsymbol{a}\times$.

Given a vector $\boldsymbol{a}$ and a second-order tensor $\boldsymbol{B}$, $\boldsymbol{a}\otimes\boldsymbol{B}$ and $\boldsymbol{B}\otimes\boldsymbol{a}$ are the third-order tensors defined such that, for any vector $\boldsymbol{c}$,

$$(\boldsymbol{a}\otimes\boldsymbol{B})\boldsymbol{c}=\boldsymbol{a}\otimes(\boldsymbol{B}\boldsymbol{c})\qquad\text{and}\qquad(\boldsymbol{B}\otimes\boldsymbol{a})\boldsymbol{c}=(\boldsymbol{a}\cdot\boldsymbol{c})\boldsymbol{B}. \tag{A.10}$$

Moreover, given a third-order tensor $\boldsymbol{C}$, $\boldsymbol{C}\boldsymbol{a}$ is the second-order tensor defined such that, for any second-order tensor $\boldsymbol{B}$,

$$(\boldsymbol{C}\boldsymbol{a})\cdot\boldsymbol{B}=\boldsymbol{C}\cdot(\boldsymbol{B}\otimes\boldsymbol{a}), \tag{A.11}$$

$\boldsymbol{C}[\boldsymbol{B}]$ is the vector defined such that, for any vector $\boldsymbol{a}$,

$$(\boldsymbol{C}[\boldsymbol{B}])\cdot\boldsymbol{a}=\boldsymbol{C}\cdot(\boldsymbol{a}\otimes\boldsymbol{B}), \tag{A.12}$$

and $\boldsymbol{C}^t$ is the third-order tensor defined such that, for any pair of vectors $\boldsymbol{a}$ and $\boldsymbol{b}$,

$$(\boldsymbol{C}^t\boldsymbol{a})\boldsymbol{b}=(\boldsymbol{C}\boldsymbol{b})\boldsymbol{a}, \tag{A.13}$$

with the consequence that

$$\boldsymbol{C}^t[\boldsymbol{A}]=\boldsymbol{C}[\boldsymbol{A}^\top] \tag{A.14}$$

for any second-order tensor $\boldsymbol{A}$.

Given a vector $\boldsymbol{a}$ and a second-order tensor $\boldsymbol{B}$, $\boldsymbol{a}\times\boldsymbol{B}$ and $\boldsymbol{B}\times\boldsymbol{a}$ denote the second-order tensors defined through

$$\boldsymbol{a}\times\boldsymbol{B}=(\boldsymbol{a}\times)\boldsymbol{B}\qquad\text{and}\qquad\boldsymbol{B}\times\boldsymbol{a}=\boldsymbol{B}(\boldsymbol{a}\times), \tag{A.15}$$

and by analogy to the definition (A.1) of the skew tensor $\boldsymbol{a}\times$ determined by a vector $\boldsymbol{a}$, $\boldsymbol{A}\times$ is the third-order tensor defined such that, for every vector $\boldsymbol{b}$,

$$(\boldsymbol{A}\times)\boldsymbol{b}=\boldsymbol{A}\times\boldsymbol{b}. \tag{A.16}$$

In particular, choosing $\boldsymbol{B}=\boldsymbol{1}$ in (A.15) gives $\boldsymbol{a}\times\boldsymbol{1}=(\boldsymbol{a}\times)\boldsymbol{1}=\boldsymbol{a}\times$ and $\boldsymbol{1}\times\boldsymbol{a}=\boldsymbol{1}(\boldsymbol{a}\times)=\boldsymbol{a}\times$, and with (A.16) we have

$$\boldsymbol{a}\times\boldsymbol{1}=\boldsymbol{1}\times\boldsymbol{a}=(\boldsymbol{1}\times)\boldsymbol{a}=\boldsymbol{a}\times. \tag{A.17}$$

Now, referring to (A.1), and letting $\{\boldsymbol{\imath}_1,\boldsymbol{\imath}_2,\boldsymbol{\imath}_3\}$ denote a right handed orthonormal basis for three-dimensional Euclidean vector space $\mathbb{V}^3$, we see that $(\boldsymbol{\imath}_k\times)\boldsymbol{\imath}_j=\boldsymbol{\imath}_k\times\boldsymbol{\imath}_j$, so $\boldsymbol{\imath}_i\cdot(\boldsymbol{\imath}_k\times)\boldsymbol{\imath}_j=-\epsilon_{ijk}$, and we may then write $(\boldsymbol{\imath}_k\times)=-\epsilon_{ijk}\boldsymbol{\imath}_i\otimes\boldsymbol{\imath}_j$. Consequently, with the aid of (A.17) we have $((\boldsymbol{1}\times)\boldsymbol{\imath}_k)\boldsymbol{\imath}_j\cdot\boldsymbol{\imath}_i=-\epsilon_{ijk}$ which yields the representation

$$\boldsymbol{1}\times=-\epsilon_{ijk}\boldsymbol{\imath}_i\otimes\boldsymbol{\imath}_j\otimes\boldsymbol{\imath}_k. \tag{A.18}$$

In addition, to determine $(\boldsymbol{a}\times)\times$ we first observe, from $(\text{A.17})_3$, (A.16) and $(\text{A.15})_2$ that $((\boldsymbol{a}\times)\times)\boldsymbol{b}=(\boldsymbol{a}\times)\times\boldsymbol{b}=(\boldsymbol{a}\times)(\boldsymbol{b}\times)=((\boldsymbol{1}\times)\boldsymbol{a})(\boldsymbol{b}\times)$. Thus,

$$((\boldsymbol{a}\times)\times)\boldsymbol{\imath}_k=((\boldsymbol{1}\times)\boldsymbol{a})(\boldsymbol{\imath}_k\times)=((\boldsymbol{1}\times)\boldsymbol{a})(-\epsilon_{rsk}\boldsymbol{\imath}_r\otimes\boldsymbol{\imath}_s), \tag{A.19}$$

and we find that

$$(((\boldsymbol{a}\times)\times)\boldsymbol{\imath}_k)\boldsymbol{\imath}_j\cdot\boldsymbol{\imath}_i=-\epsilon_{rjk}((\boldsymbol{1}\times)\boldsymbol{a})\boldsymbol{\imath}_r\cdot\boldsymbol{\imath}_i=-\epsilon_{rjk}a_m((\boldsymbol{1}\times)\boldsymbol{\imath}_m)\boldsymbol{\imath}_r\cdot\boldsymbol{\imath}_i=\epsilon_{rjk}\epsilon_{irm}a_m=(\delta_{ik}\delta_{mj}-\delta_{ij}\delta_{mk})a_m\delta_{ik}a_j-\delta_{ij}a_k, \tag{A.20}$$

which establishes the representation

$$(\boldsymbol{a}\times)\times=\boldsymbol{\imath}_i\otimes\boldsymbol{a}\otimes\boldsymbol{\imath}_i-\boldsymbol{\imath}_i\otimes\boldsymbol{\imath}_i\otimes\boldsymbol{a}. \tag{A.21}$$

Since $(\boldsymbol{c}\otimes\boldsymbol{d})\boldsymbol{A}=\boldsymbol{c}\otimes(\boldsymbol{A}^\top\boldsymbol{d})$ for any second-order tensor $\boldsymbol{A}$ and any pair of vectors $\boldsymbol{c}$ and $\boldsymbol{d}$, choosing $\boldsymbol{B}=\boldsymbol{c}\otimes\boldsymbol{d}$ in $(\text{A.15})_2$ and invoking (A.3) shows that

$$(\boldsymbol{c}\otimes\boldsymbol{d})\times\boldsymbol{a}=(\boldsymbol{c}\otimes\boldsymbol{d})(\boldsymbol{a}\times)=\boldsymbol{c}\otimes((\boldsymbol{a}\times)^\top\boldsymbol{d})=-\boldsymbol{c}\otimes(\boldsymbol{a}\times\boldsymbol{d})=\boldsymbol{c}\otimes((\boldsymbol{d}\times)\boldsymbol{a})=(\boldsymbol{c}\otimes(\boldsymbol{d}\times))\boldsymbol{a} \tag{A.22}$$

for any vector $\boldsymbol{a}$, from which, with the aid of (A.16) it follows that

$$(\boldsymbol{c}\otimes\boldsymbol{d})\times=\boldsymbol{c}\otimes(\boldsymbol{d}\times) \tag{A.23}$$

for any pair of vectors $\boldsymbol{c}$ and $\boldsymbol{d}$.

Now, setting $\boldsymbol{C}=\boldsymbol{1}\times$ in (A.11) and using (A.17) we see that

$$(\boldsymbol{1}\times)\cdot(\boldsymbol{B}\otimes\boldsymbol{a})=((\boldsymbol{1}\times)\boldsymbol{a})\cdot\boldsymbol{B}=(\boldsymbol{a}\times)\cdot\boldsymbol{B}, \tag{A.24}$$

from which it follows that

$$(\boldsymbol{1}\times)\cdot(\boldsymbol{B}\otimes\boldsymbol{a})=0\qquad\text{if}\qquad\boldsymbol{B}=\boldsymbol{B}^\top. \tag{A.25}$$

A.2. Differential identities

Let $\boldsymbol{f}$ be a vector field. Then, its gradient $\operatorname{grad}\boldsymbol{f}$ is a second-order tensor field and, thus, by (A.9), admits a decomposition of the form

$$\operatorname{grad}\boldsymbol{f} = \operatorname{sym}(\operatorname{grad}\boldsymbol{f} - \tfrac{1}{3}(\operatorname{tr}(\operatorname{grad}\boldsymbol{f}))\boldsymbol{1}) + \tfrac{1}{3}(\operatorname{tr}(\operatorname{grad}\boldsymbol{f}))\boldsymbol{1} + \operatorname{skw}(\operatorname{grad}\boldsymbol{f}). \tag{A.26}$$

The divergence and curl of $\boldsymbol{f}$ are the scalar and vector fields, $\operatorname{div}\boldsymbol{f}$ and $\operatorname{curl}\boldsymbol{f}$, defined by

$$\operatorname{div}\boldsymbol{f} = \operatorname{tr}(\operatorname{grad}\boldsymbol{f}) \qquad \text{and} \qquad (\operatorname{curl}\boldsymbol{f})\times = 2\operatorname{skw}(\operatorname{grad}\boldsymbol{f}), \tag{A.27}$$

with the consequence that (A.26) becomes

$$\operatorname{grad}\boldsymbol{f} = \operatorname{sym}(\operatorname{grad}\boldsymbol{f} - \tfrac{1}{3}(\operatorname{div}\boldsymbol{f})\boldsymbol{1}) + \tfrac{1}{3}(\operatorname{div}\boldsymbol{f})\boldsymbol{1} + \tfrac{1}{2}(\operatorname{curl}\boldsymbol{f})\times. \tag{A.28}$$

Since the first two terms on the right-hand side of (A.28) are symmetric, on computing the scalar product with a skew tensor $\boldsymbol{g}\times$ on both sides of (A.28) and using the identity (A.5), it follows that

$$\boldsymbol{g}\cdot\operatorname{curl}\boldsymbol{f} = (\boldsymbol{g}\times)\cdot\operatorname{grad}\boldsymbol{f} \tag{A.29}$$

for any vectorial quantity $\boldsymbol{g}$. If, in particular, $\boldsymbol{f}$ is of the form $\boldsymbol{f} = \zeta\boldsymbol{a}$, with $\boldsymbol{a}$ a constant vector, then, since, by (A.29) and (A.8),

$$\boldsymbol{g}\cdot\operatorname{curl}(\zeta\boldsymbol{a}) = (\boldsymbol{g}\times)\cdot\operatorname{grad}(\zeta\boldsymbol{a}) = (\boldsymbol{g}\times)\cdot(\boldsymbol{a}\otimes\operatorname{grad}\zeta) = \boldsymbol{g}\cdot((\operatorname{grad}\zeta)\times\boldsymbol{a}) \tag{A.30}$$

for any choice of $\boldsymbol{g}$, it follows that

$$\operatorname{curl}(\zeta\boldsymbol{a}) = (\operatorname{grad}\zeta)\times\boldsymbol{a} \tag{A.31}$$

for any constant vector $\boldsymbol{a}$.

Next, let $\boldsymbol{F}$ be a second-order tensor field. Then, since the gradient $\operatorname{grad}\boldsymbol{F}$ is a third-order tensor field, it is convenient to introduce a constant vector $\boldsymbol{a}$ and to consider the gradient of the vector field $\boldsymbol{F}^{\top}\boldsymbol{a}$. On appealing to (A.27) with $\boldsymbol{f} = \boldsymbol{F}^{\top}\boldsymbol{a}$, the divergence and curl of $\boldsymbol{F}$, $\operatorname{div}\boldsymbol{F}$ and $\operatorname{curl}\boldsymbol{F}$, are herein identified as the vector and second-order tensor fields defined such that

$$\boldsymbol{a}\cdot\operatorname{div}\boldsymbol{F} = \operatorname{div}(\boldsymbol{F}^{\top}\boldsymbol{a}) \qquad \text{and} \qquad (\operatorname{curl}\boldsymbol{F})^{\top}\boldsymbol{a} = \operatorname{curl}(\boldsymbol{F}^{\top}\boldsymbol{a}) \tag{A.32}$$

for any constant vector $\boldsymbol{a}$. Let ζ be a scalar field. Then, by (A.31) and $(A.32)_2$, we see that

$$(\operatorname{curl}(\zeta\boldsymbol{1}))^{\top}\boldsymbol{a} = \operatorname{curl}(\zeta\boldsymbol{1}^{\top}\boldsymbol{a}) = \operatorname{curl}(\zeta\boldsymbol{a}) = (\operatorname{grad}\zeta)\times\boldsymbol{a}, \tag{A.33}$$

for any constant vector $\boldsymbol{a}$, from which, with (A.1), it follows that

$$\operatorname{curl}(\zeta\boldsymbol{1}) = -(\operatorname{grad}\zeta)\times. \tag{A.34}$$

Similarly, by (A.1), (A.31), and $(A.32)_2$,

$$(\operatorname{curl}(\zeta\boldsymbol{B}))^{\top}\boldsymbol{a} = \operatorname{curl}(\zeta\boldsymbol{B}^{\top}\boldsymbol{a}) = (\operatorname{grad}\zeta)\times(\boldsymbol{B}^{\top}\boldsymbol{a}) = ((\operatorname{grad}\zeta)\times)\boldsymbol{B}^{\top}\boldsymbol{a} \tag{A.35}$$

for any constant vector $\boldsymbol{a}$ and any constant second-order tensor $\boldsymbol{B}$, from which it follows, using (A.3) and $(A.15)_2$, that

$$\operatorname{curl}(\zeta\boldsymbol{B}) = -\boldsymbol{B}((\operatorname{grad}\zeta)\times) = -(\boldsymbol{B}\times)\operatorname{grad}\zeta = -\boldsymbol{B}\times\operatorname{grad}\zeta \tag{A.36}$$

for any constant second-order tensor $\boldsymbol{B}$. Also, by (A.8), $(A.27)_1$, $(A.32)_1$, and the definition of the trace of a second-order tensor, we see that

$$\boldsymbol{a}\cdot\operatorname{curl}\boldsymbol{f} = (\boldsymbol{a}\times)\cdot\operatorname{grad}\boldsymbol{f} = \operatorname{tr}((\boldsymbol{a}\times)^{\top}\operatorname{grad}\boldsymbol{f}) = -\operatorname{tr}((\boldsymbol{a}\times)\operatorname{grad}\boldsymbol{f}) = -\operatorname{tr}(\operatorname{grad}(\boldsymbol{a}\times\boldsymbol{f})) = -\operatorname{div}((\boldsymbol{f}\times)^{\top}\boldsymbol{a}) = -\boldsymbol{a}\cdot\operatorname{div}(\boldsymbol{f}\times) \tag{A.37}$$

for any constant vector $\boldsymbol{a}$, and it follows that $\operatorname{curl}\boldsymbol{f}$ can be obtained alternatively from the divergence of the associated skew tensor field $\boldsymbol{f}\times$ through the identity

$$\operatorname{curl}\boldsymbol{f} = -\operatorname{div}(\boldsymbol{f}\times). \tag{A.38}$$

Furthermore, using (A.9), $(A.32)_2$, and (A.29) we see that

$$\boldsymbol{a}\cdot(\operatorname{curl}\boldsymbol{F})\boldsymbol{g} = \boldsymbol{g}\cdot\operatorname{curl}(\boldsymbol{F}^{\top}\boldsymbol{a}) = (\boldsymbol{g}\times)\cdot\operatorname{grad}(\boldsymbol{F}^{\top}\boldsymbol{a}) = (\operatorname{grad}\boldsymbol{F})\cdot(\boldsymbol{a}\otimes(\boldsymbol{g}\times)) = \boldsymbol{a}\cdot((\operatorname{grad}\boldsymbol{F})[\boldsymbol{g}\times]) \tag{A.39}$$

for any constant vector $\boldsymbol{a}$, and it follows that

$$(\operatorname{curl}\boldsymbol{F})\boldsymbol{g} = (\operatorname{grad}\boldsymbol{F})[\boldsymbol{g}\times] \tag{A.40}$$

for any vectorial quantity $\boldsymbol{g}$. Additionally, on noticing from (A.32) that

$$\boldsymbol{a}\cdot\operatorname{div}\operatorname{curl}\boldsymbol{F} = \operatorname{div}((\operatorname{curl}\boldsymbol{F})^{\top}\boldsymbol{a}) = \operatorname{div}\operatorname{curl}(\boldsymbol{F}^{\top}\boldsymbol{a}) \tag{A.41}$$

for any constant vector $\boldsymbol{a}$ and recalling that $\operatorname{div}\operatorname{curl}\boldsymbol{f} = 0$ for any vector field $\boldsymbol{f}$, it follows that

$$\operatorname{div}\operatorname{curl}\boldsymbol{F} = \boldsymbol{0}. \tag{A.42}$$

Next, given vector and tensor fields $\boldsymbol{g}$ and $\boldsymbol{F}$, it follows from (A.12), $(A.32)_2$ and (A.3) that

$$\begin{aligned}(\operatorname{curl}(\boldsymbol{F}\times\boldsymbol{g}))^{\top}\boldsymbol{a} &= \operatorname{curl}((\boldsymbol{F}\times\boldsymbol{g})^{\top}\boldsymbol{a})\\ &= \operatorname{curl}((\boldsymbol{F}(\boldsymbol{g}\times))^{\top}\boldsymbol{a})\\ &= -\operatorname{curl}((\boldsymbol{g}\times)\boldsymbol{F}^{\top}\boldsymbol{a})\\ &= \operatorname{curl}((\boldsymbol{F}^{\top}\boldsymbol{a})\times\boldsymbol{g})\\ &= (\operatorname{grad}(\boldsymbol{F}^{\top}\boldsymbol{a})-(\operatorname{div}(\boldsymbol{F}^{\top}\boldsymbol{a}))\boldsymbol{1})\boldsymbol{g}-(\operatorname{grad}\boldsymbol{g}-(\operatorname{div}\boldsymbol{g})\boldsymbol{1})\boldsymbol{F}^{\top}\boldsymbol{a}\\ &= ((\operatorname{grad}\boldsymbol{F})\boldsymbol{g}-(\operatorname{div}\boldsymbol{F})\otimes\boldsymbol{g}-\boldsymbol{F}(\operatorname{grad}\boldsymbol{g})^{\top}+(\operatorname{div}\boldsymbol{g})\boldsymbol{F})^{\top}\boldsymbol{a},\end{aligned}\tag{A.43}$$

for any constant vector $\boldsymbol{a}$ and, consequently, that

$$\operatorname{curl}(\boldsymbol{F}\times\boldsymbol{g})=\operatorname{curl}(\boldsymbol{F}(\boldsymbol{g}\times))=(\operatorname{grad}\boldsymbol{F})\boldsymbol{g}-(\operatorname{div}\boldsymbol{F})\otimes\boldsymbol{g}-\boldsymbol{F}(\operatorname{grad}\boldsymbol{g})^{\top}+(\operatorname{div}\boldsymbol{g})\boldsymbol{F}.\tag{A.44}$$

Furthermore, from $(A.32)_2$, for any constant vector $\boldsymbol{a}$,

$$\begin{aligned}(\operatorname{curl}\operatorname{curl}\boldsymbol{F})^{\top}\boldsymbol{a} &= \operatorname{curl}((\operatorname{curl}\boldsymbol{F})^{\top}\boldsymbol{a})\\ &= \operatorname{curl}\operatorname{curl}(\boldsymbol{F}^{\top}\boldsymbol{a})\\ &= \operatorname{grad}\operatorname{div}(\boldsymbol{F}^{\top}\boldsymbol{a})-\Delta(\boldsymbol{F}^{\top}\boldsymbol{a})\\ &= \operatorname{grad}(\boldsymbol{a}\cdot\operatorname{div}\boldsymbol{F})-(\Delta\boldsymbol{F})^{\top}\boldsymbol{a}\\ &= (\operatorname{grad}\operatorname{div}\boldsymbol{F}-\Delta\boldsymbol{F})^{\top}\boldsymbol{a},\end{aligned}\tag{A.45}$$

where Δ denotes the Laplacian, and, thus, that

$$\operatorname{curl}\operatorname{curl}\boldsymbol{F}=\operatorname{grad}\operatorname{div}\boldsymbol{F}-\Delta\boldsymbol{F}.\tag{A.46}$$

By (A.12), (A.23), $(A.32)_2$ and (A.40),

$$\begin{aligned}((\boldsymbol{a}\otimes\boldsymbol{b})\times)\cdot\operatorname{grad}\boldsymbol{F} &= ((\boldsymbol{a}\otimes(\boldsymbol{b}\times)))\cdot\operatorname{grad}\boldsymbol{F}\\ &= ((\operatorname{grad}\boldsymbol{F})[\boldsymbol{b}\times])\cdot\boldsymbol{a}\\ &= ((\operatorname{curl}\boldsymbol{F})\boldsymbol{b})\cdot\boldsymbol{a},\\ &= \boldsymbol{b}\cdot((\operatorname{curl}\boldsymbol{F})^{\top}\boldsymbol{a})\\ &= (\boldsymbol{a}\otimes\boldsymbol{b})\cdot\operatorname{curl}\boldsymbol{F},\end{aligned}\tag{A.47}$$

from which it follows that

$$((\boldsymbol{a}\otimes\boldsymbol{b})\times)\cdot\operatorname{grad}\boldsymbol{F}=(\boldsymbol{a}\otimes\boldsymbol{b})\cdot\operatorname{curl}\boldsymbol{F}\tag{A.48}$$

for any pair of vectors $\boldsymbol{a}$ and $\boldsymbol{b}$. Thus, since any second-order tensor can be represented as a linear combination of second-order tensors of the general form $\boldsymbol{a}\otimes\boldsymbol{b}$, the requirement that $(A.32)_2$ hold for any vector $\boldsymbol{a}$ implies that

$$\boldsymbol{A}\cdot\operatorname{curl}\boldsymbol{F}=(\boldsymbol{A}\times)\cdot\operatorname{grad}\boldsymbol{F}\tag{A.49}$$

holds for any second-order tensor $\boldsymbol{A}$. Conversely, on setting $\boldsymbol{A}=\boldsymbol{a}\otimes\boldsymbol{b}$ in the requirement that (A.49) hold for all $\boldsymbol{A}$ of the form $\boldsymbol{A}=\boldsymbol{a}\otimes\boldsymbol{b}$, with $\boldsymbol{a}$ and $\boldsymbol{b}$ being arbitrarily chosen vectors, we see using (A.23) that (A.48) is equivalently

$$((\boldsymbol{a}\otimes(\boldsymbol{b}\times)))\cdot\operatorname{grad}\boldsymbol{F}=\boldsymbol{a}\cdot(\operatorname{curl}\boldsymbol{F})\boldsymbol{b},\tag{A.50}$$

which, according to (A.39), is equivalently

$$\boldsymbol{b}\cdot\operatorname{curl}(\boldsymbol{F}^{\top}\boldsymbol{a})=\boldsymbol{a}\cdot(\operatorname{curl}\boldsymbol{F})\boldsymbol{b}=\boldsymbol{b}\cdot(\operatorname{curl}\boldsymbol{F})^{\top}\boldsymbol{a},\tag{A.51}$$

and implies that $(A.32)_2$ must hold for all $\boldsymbol{a}$. Imposing (A.49) for all second-order tensors $\boldsymbol{A}$ thus provides an equivalent alternative to imposing $(A.32)_2$ for all vectors $\boldsymbol{a}$. In particular, on choosing $\boldsymbol{A}=\boldsymbol{1}$ in (A.49), it follows that $\operatorname{tr}(\operatorname{curl}\boldsymbol{F})=\boldsymbol{1}\cdot\operatorname{curl}\boldsymbol{F}=(\boldsymbol{1}\times)\cdot\operatorname{grad}\boldsymbol{F}$ and, with (A.18), that

$$\operatorname{tr}(\operatorname{curl}\boldsymbol{F})=0\qquad\text{if}\qquad\boldsymbol{F}=\boldsymbol{F}^{\top}.\tag{A.52}$$

Finally, from the relation $(\boldsymbol{a}\times)\cdot\operatorname{curl}\boldsymbol{F}=\boldsymbol{a}\cdot(\operatorname{div}(\boldsymbol{F}^{\top})-\operatorname{grad}\operatorname{tr}\boldsymbol{F})$, which holds for any constant vector $\boldsymbol{a}$ as a consequence of (A.21) and (A.49), it follows from (A.42) on choosing $\boldsymbol{A}=\boldsymbol{a}\times$ that

$$(\boldsymbol{a}\times)\cdot\operatorname{curl}((\operatorname{curl}\boldsymbol{F})^{\top})=\boldsymbol{a}\cdot(\operatorname{div}\operatorname{curl}\boldsymbol{F}-\operatorname{grad}\operatorname{tr}(\operatorname{curl}\boldsymbol{F}))=-\boldsymbol{a}\cdot\operatorname{grad}\operatorname{tr}(\operatorname{curl}\boldsymbol{F})\tag{A.53}$$

for any vector $\boldsymbol{a}$ and, in view of (A.52) and noting that $\boldsymbol{a}\times$ is skew, that

$$\operatorname{curl}((\operatorname{curl}\boldsymbol{F})^{\top})=(\operatorname{curl}((\operatorname{curl}\boldsymbol{F})^{\top}))^{\top}\qquad\text{if}\qquad\boldsymbol{F}=\boldsymbol{F}^{\top}.\tag{A.54}$$

A.3. Material time rate

We use a superposed dot to denote the material time rate. In particular, for a scalar field α,

$$\dot{\alpha} = \frac{\partial \alpha}{\partial t} + (\operatorname{grad} \alpha) \cdot \boldsymbol{v}. \tag{A.55}$$

The material time derivatives $\dot{\boldsymbol{\varphi}}$ and $\dot{\boldsymbol{\Sigma}}$ of vector and second-order tensor fields $\boldsymbol{f}$ and $\boldsymbol{F}$ are, thus, given by

$$\dot{\boldsymbol{\varphi}} = \frac{\partial \boldsymbol{f}}{\partial t} + (\operatorname{grad} \boldsymbol{f})\boldsymbol{v} \qquad \text{and} \qquad \dot{\boldsymbol{F}} = \frac{\partial \boldsymbol{F}}{\partial t} + (\operatorname{grad} \boldsymbol{F})\boldsymbol{v}, \tag{A.56}$$

where the vector field $(\operatorname{grad} \boldsymbol{f})\boldsymbol{v}$ satisfies

$$\boldsymbol{c} \cdot ((\operatorname{grad} \boldsymbol{f})\boldsymbol{v}) = \boldsymbol{v} \cdot \operatorname{grad}(\boldsymbol{f} \cdot \boldsymbol{c}) \tag{A.57}$$

for any constant vector $\boldsymbol{c}$ and, similarly, $(\operatorname{grad} \boldsymbol{F})\boldsymbol{v}$ is the second-order tensor field which satisfies

$$(\boldsymbol{a} \otimes \boldsymbol{c}) \cdot ((\operatorname{grad} \boldsymbol{F})\boldsymbol{v}) = \boldsymbol{v} \cdot \operatorname{grad}(\boldsymbol{a} \cdot \boldsymbol{F}\boldsymbol{c}) \tag{A.58}$$

for any pair of constant vectors $\boldsymbol{a}$ and $\boldsymbol{c}$.

A.4. Select representations in terms of rectangular Cartesian components

Relative to a fixed right-handed orthonormal basis $\{\boldsymbol{\imath}_1, \boldsymbol{\imath}_2, \boldsymbol{\imath}_3\}$, the second- and third-order tensors $\boldsymbol{a}\times$ and $\boldsymbol{A}\times$ defined through (A.1) and $(A.15)_2$ admit representations of the form

$$\boldsymbol{a}\times = \epsilon_{ikj} a_k \boldsymbol{\imath}_i \otimes \boldsymbol{\imath}_j, \qquad \text{and} \qquad \boldsymbol{A}\times = A_{ip}\epsilon_{jpk} \boldsymbol{\imath}_i \otimes \boldsymbol{\imath}_j \otimes \boldsymbol{\imath}_k, \tag{A.59}$$

where $a_i = \boldsymbol{a} \cdot \boldsymbol{\imath}_i$, $A_{ij} = \boldsymbol{\imath}_i \cdot \boldsymbol{A}\boldsymbol{\imath}_j$, and the standard summation convention applies. Representations for the special cases $\boldsymbol{\imath}_k\times$ and $\boldsymbol{1}\times$, as well as for $(\boldsymbol{a}\times)\times$ were presented in (A.17)–(A.21) and were used in Appendices A and B.

Also, the gradient $\operatorname{grad} \boldsymbol{f}$ of a vector field $\boldsymbol{f}$ admits the representation

$$\operatorname{grad} \boldsymbol{f} = f_{i,j} \boldsymbol{\imath}_i \otimes \boldsymbol{\imath}_j. \tag{A.60}$$

Thus, from (A.27), the divergence and curl, $\operatorname{div} \boldsymbol{f}$ and $\operatorname{curl} \boldsymbol{f}$, of $\boldsymbol{f}$ admit representations of the form

$$\operatorname{div} \boldsymbol{f} = f_{i,i} \qquad \text{and} \qquad \operatorname{curl} \boldsymbol{f} = \epsilon_{ijk} f_{k,j} \boldsymbol{\imath}_i, \tag{A.61}$$

while, from (A.32), the divergence and curl, $\operatorname{div} \boldsymbol{F}$ and $\operatorname{curl} \boldsymbol{F}$, of a second-order tensor field $\boldsymbol{F}$ admit representations of the form

$$\operatorname{div} \boldsymbol{F} = F_{ij,j} \boldsymbol{\imath}_i \qquad \text{and} \qquad \operatorname{curl} \boldsymbol{F} = \epsilon_{jrs} F_{is,r} \boldsymbol{\imath}_i \otimes \boldsymbol{\imath}_j. \tag{A.62}$$

by (A.46), the double curl, $\operatorname{curl}\operatorname{curl} \boldsymbol{F}$, of $\boldsymbol{F}$ admits the representation

$$\operatorname{curl}\operatorname{curl} \boldsymbol{F} = (F_{ik,kj} - F_{ij,kk}) \boldsymbol{\imath}_i \otimes \boldsymbol{\imath}_j. \tag{A.63}$$

Finally, the material time derivatives $\dot{\boldsymbol{f}}$ and $\dot{\boldsymbol{F}}$ of vector and second-order tensor fields $\boldsymbol{f}$ and $\boldsymbol{F}$ admit the representations

$$\dot{\boldsymbol{f}} = \left(\frac{\partial f_i}{\partial t} + f_{i,j} v_j \right) \boldsymbol{\imath}_i \qquad \text{and} \qquad \dot{\boldsymbol{F}} = \left(\frac{\partial F_{ij}}{\partial t} + F_{ij,k} v_k \right) \boldsymbol{\imath}_i \otimes \boldsymbol{\imath}_j. \tag{A.64}$$

Appendix B. Supplementary data

Supplementary material related to this article can be found online at https://doi.org/10.1016/j.ijengsci.2021.103540.

References

Abe, H., Kawamura, H., & Choi, H. (2004). Very large-scale structures and their effects on the wall shear-stress fluctuations in a turbulent channel flow up to $\mathrm{Re}_\tau = 600$. *Journal of Fluids Engineering*, *126*, 835–843.

Abe, H., Kawamura, H., & Matsuo, Y. (2001). Direct numerical simulation of a fully developed turbulent channel flow with respect to the Reynolds number dependence. *Journal of Fluids Engineering*, *123*, 382–393.

Acharya, A., & Fosdick, R. (2019). Some preliminary observations on a defect Navier–Stokes system. *Comptes Rendus Mécanique*, *347*, 677–684.

Akyildiz, F. T., & Jones, R. S. (1993). The generation of steady flow in a rectangular duct. *Rheologica Acta*, *32*, 499–504.

Bernardini, M., Pirozzoli, S., & Orlandi, P. (2014). Velocity statistics in turbulent channel flow up to $\mathrm{Re}_\tau = 4000$. *Journal of Fluid Mechanics*, *742*, 171–191.

Bowen, R. M. (1989). *Introduction to continuum mechanics for engineers*. New York and London: Plenum Press.

Cesàro, E. (1906). Sulle formole del Volterra fondamentali nella teoria delle distorsioni elastiche. *Nuovo Cimento*, *12*, 143–154.

Chong, J. S., & Franks, R. G. E. (1970a). Time-dependent flow of quasi-linear viscoelastic fluids. *Journal of Applied Polymer Science*, *14*, 1639–1650.

Chong, J. S., & Franks, R. G. E. (1970b). Time-dependent flow of quasi-linear viscoelastic fluids. *Journal of Applied Polymer Science*, *14*, 17–34.

Del Alamo, J. C., Jiménez, J., Zandonade, P., & Moser, R. D. (2004). Scaling of the energy spectra of turbulent channels. *Journal of Fluid Mechanics*, *500*, 135–144.

Deltete, R. (1999). *The historical development of energetics. Die geschichtlichen entwicklung der energetik*. Dordrecht: Kluwer, (trans. Helm, G., Veit & Comp., Leipzig, 1898).

Deltete, R. J. (2008). Wilhelm ostwald's energetics 3: Energetic theory and applications, part II. *Foundations of Chemistry*, *10*, 187–221.

Fielder, R., & Thomas, R. H. (1967). The unsteady motion of a lamina in an elastic-viscous liquid. *Rheologica Acta*, *6*, 306–311.

Fong, C. F. C. M. (1972). Unsteady flow of a finite linear viscoelastic fluid. *Journal of Applied Mathematics and Mechanics (ZAMM)*, *83*, 241–243.
Fosdick, R. (2016). A generalized continuum theory with internal corner and surface contact interactions. *Continuum Mechanics and Thermodynamics*, (28), 275–292.
Fosdick, R., & Royer-Carfagni, G. (2005). A Stokes theorem for second-order tensor fields and its implications in continuum mechanics. *International Journal of Non-Linear Mechanics*, *40*, 381–386.
Fosdick, R., & Royer-Carfagni, G. (2020). Hadamard's conditions of compatibility from Cesaro's line-integral representation. *International Journal of Engineering Science*, *146*, 1–12.
Griffiths, P. T. (2020). Non-Newtonian channel flow—exact solutions. *IMA Journal of Applied Mathematics*, *85*, 263–279.
Hoyas, S., & Jiménez, J. (2003). Scaling of the velocity fluctuations in turbulent channels up to $\mathrm{Re}_\tau = 2003$. *Physics of Fluids*, *25*, 011702–1–4.
Jammer, M. (1961). *Concepts of mass in classical and modern physics*. Cambridge: Harvard University Press.
Kim, J., Moin, P., & Moser, R. (1987). Turbulence statistics in fully developed channel flow at low Reynolds number. *Journal of Fluid Mechanics*, *177*, 133–166.
Lee, M., & Moser, R. D. (2015). Direct numerical simulation of turbulent channel flow up to $\mathrm{Re}_\tau \approx 5200$. *Journal of Fluid Mechanics*, *774*, 395–415.
Lozano-Durán, A., & Jiménez, J. (2014). Effect of the computational domain on direct simulations of turbulent channels up to $\mathrm{Re}_\tau = 4200$. *Physics of Fluids*, *26*, Article 011702.
Matsuhisa, S., & Bird, R. B. (1965). Analytical and numerical solutions for laminar flow of the non-Newtonian Ellis fluid. *AIChE Journal*, *11*, 588–595.
Monty, J. P., & Chong, M. S. (2009). Turbulent channel flow: comparison of streamwise velocity data from experiments and direct numerical simulation. *Journal of Fluid Mechanics*, *633*, 461–474.
Oliveira, P. J. (2002). An exact solution for tube and slit flow of a FENE-P fluid. *Acta Mechanica*, *158*, 157–167.
Oliveira, P. J., & Pinho, F. T. (1999). Analytical solution for fully developed channel and pipe flow of Phan-Thien–Tanner fluids. *Journal of Fluid Mechanics*, *387*, 271–280.
Rotem, Z., & Shinnar, R. (1961). Non-Newtonian flow between parallel boundaries in linear movements. *Chemical Engineering Science*, *15*, 130–143.
Saramito, P. (2016). *Complex fluids*. Switzerland: Springer International Publishing.
Schechter, R. S. (1961). On the steady flow of a non-Newtonian fluid in cylinder ducts. *AIChE Journal*, *7*, 445–448.
Schultz, M. P., & Flack, K. A. (2013). Reynolds-number scaling of turbulent channel flow. *Physics of Fluids*, *25*, 023104–1–13.
Siline, M., & Leonov, A. I. (2001). On flows of viscoelastic liquids in long channels and dies. *International Journal of Engineering Science*, *39*, 415–437.
Waters, N. D., & King, M. J. (1970). Unsteady flow of an elastico-viscous fluid. *Rheologica Acta*, *9*, 345–355.
White, J. L. (1981). Laminar shear flow of plastic viscoelastic fluids. *Rheologica Acta*, *20*, 381–389.
Yoo, J. Y., & Choi, H. Ch. (1989). On the steady simple shear flows of the one-mode Giesekus fluid. *Rheologica Acta*, *28*, 13–24.